

Design, Simulation, and Analysis of a PV Power and Reverse Osmosis System for a House in Iran

by

© **Seyed Mohammad Mousavi**

A thesis submitted to the School of Graduate Studies in partial fulfillment of
the requirements for the degree of

Master of Engineering

**Faculty of Engineering and Applied Science
Memorial University of Newfoundland**

May 2022

St. John's

Newfoundland and Labrador

Canada

Abstract

Electricity demand is increasing and new energy resources are required, especially environment-friendly resources like PV systems. On the other hand, water scarcity is another growing issue in the modern world, and the availability of potable water is a concern. Therefore, designing a system to address both problems in one solution is needed. In this thesis, a photovoltaic (PV) power system and reverse osmosis (RO) system were designed, simulated, and analyzed for a rural house in Tehran, Iran. Water system configuration in the house was investigated, RO system components were merged into the system, and a new design was proposed. RO load and house load were calculated, and different hybrid renewable energy systems (HRES) were introduced. Optimization results with HOMER Pro software suggested that the PV battery RO system had several advantages over other systems. Moreover, the software offered optimum low cost system sizing. Then the PV and RO system dynamic model was introduced to check the behaviour of the system. This part was conducted in two phases; in the first phase, a transfer function-based model for a small-scale RO unit was introduced, and the model precisely mimicked the system's behaviour for different inputs. In the second phase, components of the PV system were simulated in MATLAB/Simulink, and it was proved that the proposed electrical system powers the loads with a fixed and stable voltage and frequency in all the conditions. Finally, three different maximum power point tracking (MPPT) techniques were designed and simulated for the PV system and shown that the fuzzy logic (FL) controller offers better results.

Acknowledgment

First of all, I would like to express my sincere gratitude to my supervisor, Prof. M. Tariq Iqbal, for his valuable guidance, continuous support, and belief in me. He was beside me in every step of this research, and I appreciate his instruction, patience, motivation, enthusiasm, and wealth of knowledge.

Next, I would like to thank Elecomp Fadak Security Systems Company for partially funding this research, which enabled me to start this research and helped me to continue this graduate study.

Moreover, I like to thank the School of Graduate Studies (SGS) and Faculty of Engineering and Applied Science, Memorial University, for providing a conducive environment to carry out this research.

Last but foremost, my heartfelt acknowledgement goes to my family and friends. They encouraged me through my studies and supported me emotionally every day of this journey. I am thankful for having you beside me.

Table of Contents

Abstract	i
Acknowledgment	ii
Table of Contents	iii
List of Figures	vi
List of Tables	ix
List of Abbreviations	x
Chapter 1. Introduction and Literature Review	1
1.1 Introduction.....	1
1.2 Background	3
1.2.1 Renewable Resources in Iran.....	3
1.2.2 Renewable Energy Systems	4
1.2.3 Water Resources in Iran.....	6
1.2.4 Water Desalination Systems	8
1.3 Literature Review	10
1.3.1 PVRO System Design.....	10
1.3.2 System Optimization and Cost Analysis	11
1.3.3 Dynamic Modelling and System Simulation	13
1.3.4 MPPT Control Techniques for PV System.....	15
1.4 Motivations	16
1.5 Research Objectives	17
1.6 Thesis Organization.....	18
References.....	20
Chapter 2. Optimum Sizing Comparison of Stand-alone Hybrid PV Systems for a Rural House in Iran Equipped with a RO Water Desalination System	25
Abstract.....	26
2.1 Introduction.....	27
2.2 Material and Methods.....	30
2.2.1 Characteristics of the Selected Site	31
2.2.2 Water System Configuration.....	32

2.2.3	Load Demand Data.....	33
2.2.4	Solar Radiation.....	36
2.2.5	System Components.....	37
2.2.6	Economic Analysis.....	40
2.3	Designing Hybrid PV Systems with HOMER Pro.....	41
2.3.1	Photovoltaic System with Battery Storage.....	43
2.3.2	Photovoltaic System with Battery Storage and Gas Generator.....	46
2.4	Results and Discussion.....	50
2.5	Conclusions.....	56
	Limitations and Future Works.....	57
	References.....	57
Chapter 3.	Design and Dynamic Modelling of a Hybrid PV-Battery System for a House with an RO Water Desalination Unit in Iran	63
	Abstract.....	64
	Nomenclature.....	65
3.1	Introduction.....	66
3.2	Site Specifications and System Configuration.....	70
3.2.1	Site Location.....	70
3.2.2	Solar Energy Source.....	72
3.2.3	Water System Configuration and RO Load.....	73
3.2.4	Electrical system configuration and the house load.....	76
3.3	Optimum Sizing of the PVRO System in HOMER Pro.....	77
3.4	Dynamic Modelling of Small-scale RO unit.....	80
3.4.1	RO Unit Modelling (Transfer Function-Based).....	80
3.4.2	Simulation and Result.....	82
3.5	Electrical Dynamic Modelling and Simulation of the Proposed PV System in MATLAB/Simulink.....	83
3.5.1	PV Arrays.....	84
3.5.2	Non-Inverting Buck-Boost Converter.....	86
3.5.3	Battery System.....	88
3.5.4	MPPT Controller.....	90
3.5.5	CCCV Battery Charge Controller.....	91
3.5.6	Inverter.....	94

3.5.7 Inverter Voltage Controller	95
3.5.8 Transformer	97
3.5.9 Load Model	98
3.6 Simulation Results and Discussion	99
3.7 Conclusion	106
Acknowledgement	107
References	108
Chapter 4. MPPT Techniques Comparison for a Small-Scale PVRO System in Iran	114
Abstract	115
4.1 Introduction	116
4.2 PVRO System Configuration	118
4.2.1 Load and System Sizing	118
4.2.2 Non-Inverting Buck-Boost Converter	121
4.2.3 System Diagram	122
4.3 Perturb and Observe (P&O) Method	123
4.4 Incremental Conductance (InC) Method	126
4.5 Fuzzy Logic (FL) Method	128
4.5.1 Fuzzification	130
4.5.2 Rule-based Inference Engine	130
4.5.3 Defuzzification	132
4.6 Results and Discussion	133
4.7 Conclusion	136
Acknowledgement	137
References	137
Chapter 5. Conclusions and Future Works	140
5.1 Conclusions	140
5.2 Future Works	144
5.3 List of Publications	146

List of Figures

Figure 1.1. Solar energy resources in Iran [7].....	5
Figure 1.2. Groundwater depletion during 2002-2015 in Iran [12].....	7
Figure 2.1. Reverse osmosis unit.....	33
Figure 2.2. Water system configuration.....	34
Figure 2.3. Monthly solar radiation and clearness index in Sinak village	37
Figure 2.4. PV-Battery system configuration in HOMER Pro.....	44
Figure 2.5. Power balance of PV-Battery system in a specific period of time	45
Figure 2.6. Surface plot of sensitivity analysis for PV-battery system.....	46
Figure 2.7. PV-Battery-Generator system configuration in HOMER Pro.....	47
Figure 2.8. The power balance of PV-Battery-Generator system in a specific period	49
Figure 2.9. Surface plot of sensitivity analysis for PV-battery-generator system.....	50
Figure 2.10. Cost comparison between PV-battery system and PV-battery-generator system	52
Figure 2.11. Impact of House Load and Average radiation fluctuation on NPC in PV- battery system.....	53
Figure 2.12. Impact of House Load and Average radiation fluctuation on NPC in PV- battery-generator system.....	54
Figure 3.1. Different views of the selected house in Sinak village	71
Figure 3.2. Well water system elements in the house.....	72
Figure 3.3. Monthly solar radiation, temperature, and clearness index in Sinak village	73
Figure 3.4. The proposed water system configuration for selected site.....	74
Figure 3.5. PV-battery-RO system in HOMER Pro	78
Figure 3.6. Electrical specifications and size of the proposed system by HOMER Pro	79
Figure 3.7. General diagram of a reverse osmosis plant.....	81
Figure 3.8. RO unit parameters: (a) input pressure (b) output flow rate	83
Figure 3.9. General block diagram of the proposed PV battery system	84
Figure 3.10. Single diode model of a PV module	85

Figure 3.11. Non-inverting buck boost converter topology	87
Figure 3.12. P&O MPPT technique principle	90
Figure 3.13. P&O method flowchart	92
Figure 3.14. Lead-acid battery charging profile in CCCV charging method.....	93
Figure 3.15. Voltage and current controller in CCCV charging method.....	94
Figure 3.16. Single-phase H-bridge inverter topology	95
Figure 3.17. Inverter voltage controller	96
Figure 3.18. Load model for the PVRO system in MATLAB/Simulink	99
Figure 3.19. MATLAB/Simulink model for the proposed PV-battery system.....	102
Figure 3.20. Solar Irradiance applied to PV arrays (w/m^2).....	103
Figure 3.21. Temperature applied to the PV arrays ($^{\circ}C$)	103
Figure 3.22. PV arrays output voltage	103
Figure 3.23. PV arrays output current.....	103
Figure 3.24. PV arrays output power.....	104
Figure 3.25. DC link voltage.....	104
Figure 3.26. Output AC voltage	104
Figure 3.27. Output AC current.....	104
Figure 3.28. Battery bank state of charge (SOC)	105
Figure 3.29. Battery bank current	105
Figure 3.30. Battery bank voltage.....	105
Figure 4.1. PVRO system schematic in HOMER Pro	120
Figure 4.2. System sizing and electrical specification for the PVRO system proposed by HOMER Pro.....	120
Figure 4.3. Non-inverting buck-boost (NIBB) converter topology.....	121
Figure 4.4. Proposed PV system diagram implemented in MATLAB/Simulink.....	123
Figure 4.5. Typical P-V curve of a PV panel with MPP and various regions.....	124
Figure 4.6. Perturb and Observe (P&O) MPPT controller flowchart.....	125
Figure 4.7. Perturb and Observe (P&O) MPPT controller in Simulink.....	125
Figure 4.8. Incremental Conductance (InC) MPPT controller flowchart	127
Figure 4.9. Incremental Conductance (InC) MPPT controller in Simulink.....	128
Figure 4.10. Fuzzy Logic (FL) MPPT controller flowchart.....	129

Figure 4.11. Membership functions for inputs E and ΔE , and output ΔD in FL controller	131
Figure 4.12. FL Controller Rule Surface	132
Figure 4.13. Fuzzy Logic (FL) MPPT controller in Simulink	133
Figure 4.14. Simulation results for P&O, InC, and FL MPPT controller	134

List of Tables

Table 2.1. Different appliances in the house with their daily energy consumption	35
Table 2.2. Deferrable load characteristics.....	36
Table 2.3. Technical and economic information of the components in the system	39
Table 2.4. Cost summary of PV-Battery system	45
Table 2.5. Cost summary of PV-Battery-Generator system.....	49
Table 2.6. Energy-related comparison details	51
Table 2.7. Features comparison of proposed scenario with other systems	55
Table 3.1. Daily energy consumption of various appliances in the house.....	77
Table 3.2. NIBB converter operation modes.....	87
Table 3.3. Switching modes and output voltage in the inverter	95
Table 4.1. FL Controller Rule Table.....	131
Table 4.2. Average Power and Power Efficiency of MPPT Techniques	132
Table 4.3. Time Details for Proposed MPPT techniques.....	136

List of Abbreviations

RO	Reverse Osmosis
PVRO	Photovoltaic Reverse Osmosis
RES	Renewable Energy System
HRES	Hybrid Renewable Energy system
WHO	World Health Organization
IDA	International Desalination Association
GHG	Greenhouse Gas
TDS	Total Dissolved Solids
HOMER	Hybrid Optimization of Multiple Energy Resources
SOC	State Of Charge
MPPT	Maximum Power Point Tracking
PWM	Pulse Width Modulation
SPWM	Sinusoidal Pulse Width Modulation
P&O	Perturb and Observe
InC	Incremental Conductance
FL	Fuzzy Logic
FLC	Fuzzy Logic Controller
CC	Cycle Charging
LF	Load Following
NPC	Net Present Cost
COE	Cost Of Energy
O&M	Operation and Maintenance
GPD	Gallon Per Day
GPM	Gallon Per Minute
CCCV	Constant Current Constant Voltage
NIBB	Non-Inverting Buck Boost
SCADA	Supervisory Control and Data Acquisition

Chapter 1. Introduction and Literature Review

1.1 Introduction

Electricity has become a crucial commodity due to development in different sections like industry and agriculture during the past century. Importance of the energy and electricity is increasing because it is predicted that the global population will increase from 7.7 billion to 9 billion in 2040. The International Energy Agency (IEA) 2020 annual report indicates the world's energy consumption will increase by 19% by the end of 2040. Scientists are concerned about future energy demand because fossil fuel resources currently supply 80% of the total energy. More greenhouse gas (GHG) emissions result from burning non-environmental friendly resources such as coal, oil, and natural gas [1].

The proper replacement for fossil fuel resources, which increase climate change, is renewable energies. Based on the report mentioned above, renewable resources overtake coal in 2025, and by 2030, 40% of the global electricity will be generated by hydro, solar PV, wind, bioenergy, geothermal, and marine power [1]. Renewable energy sources (RES) have become popular because of numerous advantageous like less emission, cost reduction over time, and sustainability. Solar PV systems have the highest growth rate among all renewable systems due to the advent of new cheaper PV cell production technologies. Moreover, storage units like batteries and hydrogen storage can add reliability to a PV system, making it appropriate for various applications [2].

Water scarcity is as critical as the energy crisis in the modern world because over-consumption of potable water leads to 74% of natural disasters like droughts and floods

between 2001 and 2018. Moreover, it is predicted that global water demand increases by 20% to 30% per year by 2050 due to population growth. Nowadays, 1.42 billion people, including 450 million children, live in high water scarcity regions. Only 3% percent of global water is fresh water and decreasing mainly because of climate change. The agriculture section uses 70% of this fresh water, while 700 children daily die worldwide from diarrhea relevant to unsafe water [3].

Water desalination is a good solution to provide future fresh water from different sources such as lake water, well water, or seawater. Desalination is a process of removing inappropriate or even toxic contaminants from brackish water like salt, manganese, iron, fluoride, phosphate, nitrate, and calcium. An old method to purify water used from the late of 1950th is the indirect method, which is based on the water evaporation process. During the past decades, advent of direct desalination methods, known as membrane methods, improved output water quality. The reverse osmosis (RO) system, which works based on the principles of osmosis, injects pressurized brackish water into the semi-permeable membrane to trap the unwanted ingredients and purify water [4].

Rural houses mostly suffer from a lack of electricity grid connection, and they use conventional fossil fuel-driven generators to meet the electrical demands. As a result, a renewable system like PV can power the house with environmentally friendly energy. On the other hand, the well water quality in rural areas is not acceptable and can cause irreparable diseases, especially in children. A PV system can meet the required electricity for a desalination system to provide purified water. This system can be designed, simulated, and analyzed to power a rural house in Iran equipped with an RO desalination system. The

system is designed in an optimized manner that is cost-effective and dynamically analyzed. Moreover, numerous control methods can be investigated to increase the efficiency of the system.

1.2 Background

A PV-powered house with an RO system consists of two different systems: A PV system and a RO system. Numerous factors should be considered in designing such a renewable system like resources availability and systems' knowledge [5]. Sufficient backgrounds regarding PV systems and RO systems are presented separately in the following four sections.

1.2.1 Renewable Resources in Iran

Iran is the fourth country in oil reservoirs and the second country in natural gas reservoirs globally. Despite these large fossil fuel resources, the government has numerous plans to develop renewable energy systems. Firstly, they want to reduce CO₂ emissions by increasing renewable power generation. On the other hand, most power plants and transmission lines are old and need to be replaced or regularly repaired to maintain operation. Nevertheless, the main reason for the renewable energy interest is long term energy security, which can be achieved by decreasing the dependency of the electrical grid on fossil fuels. Iran has undeniable renewable energy potential in which 14% of the electricity was generated by hydropower between 1950 to 2000. Because of several droughts in the country, the interest in solar, wind and geothermal has been increased. SUNA, the renewable energy organization in Iran, states that 30000 MW wind power

capacity exists in the country, and 15 wind farms, including Manjil and Rudbar, are installed. Moreover, Stanford University reported that 14 locations in Iran have the potential for geothermal energy productions and 13 geothermal wells already exist in Meshkin Shahr area [6].

With 300 clear sunny days and an annual average of 2200 kWh/m² solar radiation, as shown in Figure 1.1 [7], Iran has tremendous potential for solar power generation. Installation of PV panels with 10% efficiency only on the 1% of the Iran total areas, which is 1,600,000 km², can generate 9 million MWh of energy. More than 2800 yearly actual radiation hours convinced governments in Iran to build solar plants in various locations such as Shiraz, Tehran, Semnan, Taleghan, Yazd, and Khorasan. PV plant installations in Iran have had an accelerating rate in which between 2001 to 2007, the installed capacity increased 8.9% annually, and it is expected the total PV capacity will reach 139,298 MW in 2030. As well as the largest solar plant in Mallard, thousands of small-scale PV systems are installed in the country and most of those installations are grid-connected [8]. However, there is little interest in small-scale PV systems because the government has subsidized petrol for decades.

1.2.2 Renewable Energy Systems

Renewable energy system (RES) has various components and configurations. A RES can be stand-alone or grid-connected in small-scale or large plant applications. A single

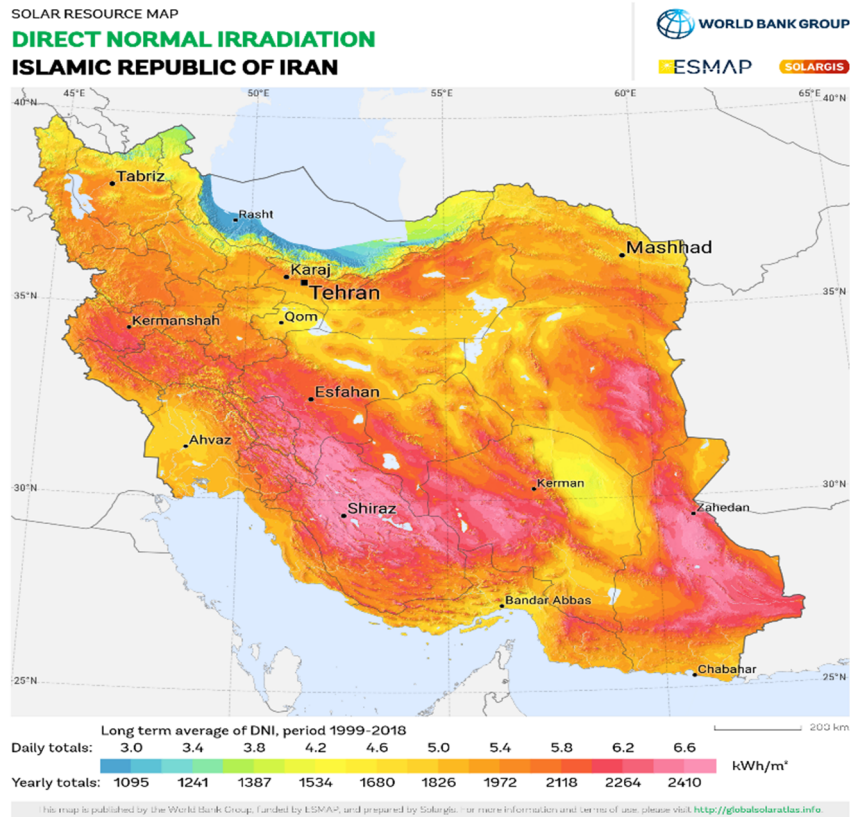


Figure 1.1. Solar energy resources in Iran [7]

technology base system comprises one of the following in small-scale applications: wind turbine, solar technologies like PV panel, micro-hydro turbine, and biomass technology. Selecting an appropriate technology is highly dependent on the location. Wind turbines and PV panels are suitable for plane or high-elevated areas, while micro-hydro and biomass are appropriate for hilly locations. Moreover, PV panels are the best option for residential applications. A hybrid renewable energy system (HRES), a system with two or more components of renewable technologies, storage systems, or conventional energy generators, is recommended by scientists for remote regions because of its high reliability. Three different possible configurations exist to connect different components in HRES together: DC coupled configuration, AC coupled configuration, and Hybrid DC-AC

coupled configuration. In HRES systems, storage options include battery storage, supercapacitor, hydrogen storage, flywheel energy storage, and compressed air energy storage [9].

Although a solar power system can be a thermal energy technology for direct water heating, indirect applications such as generating electricity by concentrated solar power (CSP) or photovoltaic (PV) panels have become more popular. Generally, A PV system comprises PV panels, input filter, DC-DC converter, DC link, DC-AC inverter, and output filter. PV power plants are all grid-connected to power the electrical grid. In residential applications, the PV system can be grid-connected or stand-alone. Although grid-connected systems have a higher contribution in global installations, stand-alone PV systems are proper solutions for remote areas. Finally, the Pico PV systems (<10 watts) are stand-alone systems that have experienced rapid developments in the past decades [10].

1.2.3 Water Resources in Iran

Renewable water sources in Iran dropped from 3,935 m³ per person in 1979 to 1732 m³ per person in 2017. This number is close to the yearly threshold of water requirements for each person, which is 1700 m³, and below this number, the country will suffer from water stress. The total average available potable water in Iran is 137 km³ currently, which has been decreased during the past four decades because of the following reasons: (1) A large number of major rivers in Iran are hydrologically closed; (2) Lakes such as Urmia lake has lost most of their areas and volumes; (3) Increasing droughts, climate change, and overall temperature [11].

The main parts of the fresh water in Iran, around 60%, are in groundwater resources. Researchers prove that huge human water withdrawal is a vital factor for groundwater depletion in conjunction with environmental and hydrological factors mentioned above that can trigger water stress. They believe that the rate of uptake freshwater is three times greater than the rate of recharge water from nature, and it causes 77% of groundwater resources to experience extreme depletion. Figure 1.2 depicts groundwater depletion from 2002 to 2015 in Iran [12].

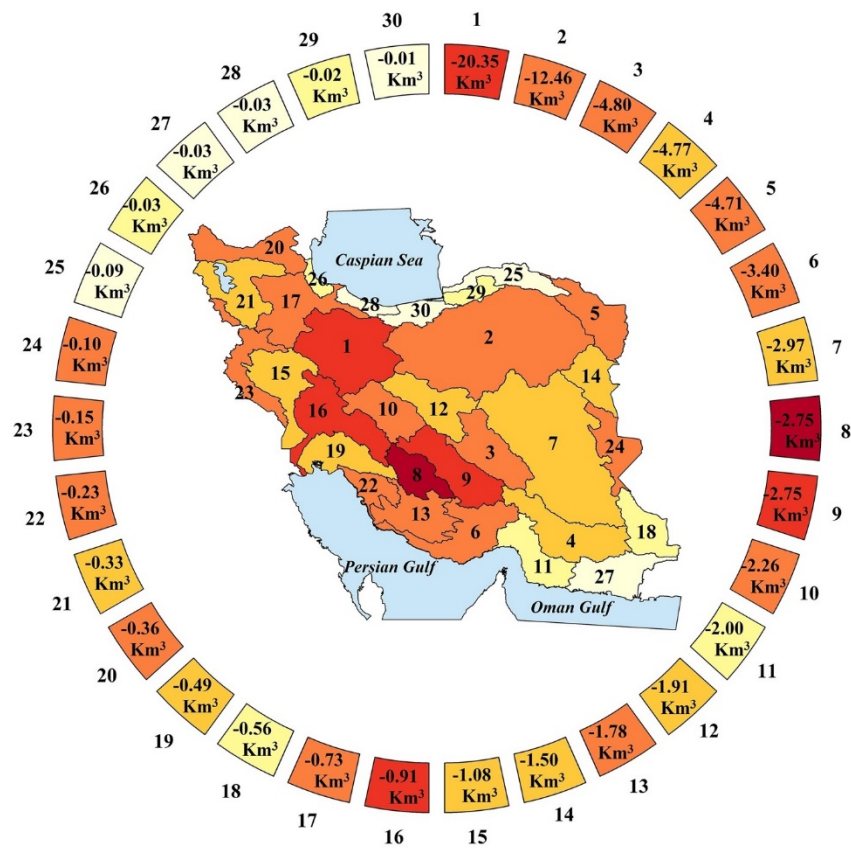


Figure 1.2. Groundwater depletion during 2002-2015 in Iran [12]

With three main saltwater resources, including the Caspian Sea, Persian Gulf, and Sea of Oman, Iran has a good potential to provide fresh water from seawater by desalination

process. The first desalination plant was installed in 1960 in Khark Island in Iran. Afterward, 15 community-based desalination plants were installed in different regions such as Chabahar, Bandar Abbas, Bushehr, Zahedan, and Qeshm Island. Small-scale desalination systems can improve the future water scarcity in Iran as equal to large plants by desalinating brackish well waters in remote areas [13].

1.2.4 Water Desalination Systems

According to the world health organization (WHO) reports, the maximum limit of the total dissolved solids (TDS) and salt should be less than 500 ppm for fresh or drinking water. Less than 5% of the freshwater resources are in this range, and subsequently, desalination is required. Sailors firstly used water desalination in the sixteenth century, where they purified seawater for drinking purposes, and during the past century, the use of desalination equipment has increased rapidly. According to the International Desalination Association (IDA), a total of 5 million m³/day available desalinated water in 1980 increased to approximately 100 million m³/day in 2020 by means of 18,500 desalination plants in 183 countries. Among all regions, Middle East, North America, and Asia have the largest capacities by 53%, 17%, and 11% of global capacity, respectively [14, 15].

Water desalination methods are divided into two main categories:

- **Membrane desalination:** In this category, a semi-permeable membrane is used to trap contaminants from forced water. Three different driving forces are used, including pressure, electrical potential difference, and concentration difference. Reverse osmosis (RO) and forward osmosis (FO) methods work by pressurized

water and concentration difference driving force, respectively. Electrodialysis (ED) and electrodialysis reversal (EDR) methods work based on electrical potential differences. Moreover, the Nanofiltration (NF) method is another method in this category by high removal diatomic ions ability. Any combination of these methods can be considered as a hybrid method like NF-FO.

- **Thermal desalination:** all methods in this category are based on water evaporation and distillation. Thermal desalination is appropriate for high salty water, and as a result, they have been used in the Middle East in large desalination plants. The multi-stage flash (MSF) method, which includes 15-28 levels or stages, heats the water with various pressure and temperature. The multi-effect desalination (MED) method normally contains 8 to 16 stages and uses latent heat in each stage to evaporate water. In the vapour compression (VC) method, the water vapour will apply to the evaporator, and preheating is required. Regarding the heat source, mechanical vapour compression (MVC) uses electrical energy, and thermal vapour compression (TVC) uses high-pressure steam.

The RO method has become tremendously popular in the last two decades because of improved membrane technology and the recovery energy system. The most important advantage of the RO method is less capital investment and operation cost compare with other methods. Moreover, the RO method has less destructive environmental effects. Based on the IDA report in 2014, 65% of the global desalination capacity was produced by the RO method [14, 16].

1.3 Literature Review

1.3.1 PVRO System Design

In the RO method, the water desalination process is highly energy-consuming and needs an electricity source to pressurize injected water to the membrane. The first available source is fossil fuel to power a RO system. Not only do fossil fuel resources generate tremendous emissions and are not environmentally friendly, but it is also costly to consider them for producing freshwater. PV panels have been used in RO systems for three decades due to remarkable progress in panel materials. PVRO systems have the major share of renewable desalination systems and numerous research conducted in both community-base and small-scale systems. Designing such a system depends on the system's location, water requirement, system components and configuration. Alghoul et al. [17] designed and implemented a small-scale PVRO system for Malaysian conditions. Their system consists of 2 kW PV panels, 600 W RO load, four membranes in a two-stage configuration, and a battery bank. Although the system was designed to purify input water with a TDS level less than 2000 ppm, it produces output potable water with TDS level less than 50 ppm when the input water TDS level is less than 5000 ppm. The proposed system could produce 5.1 m³ fresh water per day by 10 hours daily operation. Moreover, the battery autonomy in the system was 22 and 24 hours in daytime and nighttime, respectively, which indicated that temperature affected the battery operation in the daytime.

A small-scale PV-driven RO system was designed by Banat et al. for a village in Jordan [18]. Their system has a daily capacity of 0.5 m³ and consists of 1533 Wp panels, DC-DC converter, 24, 230 Ah battery, 746 W softener unit, 60 W intake pump, and 57.6 W RO

unit. They prove that real specific energy consumption depends on the recovery percentage and the recovery percentage is temperature-dependent from 29% to 41%. Gorjian et al. [19] designed and implemented a small-scale stand-alone photovoltaic-thermal (PVT) system for a RO desalination unit in Tehran, Iran, with 83.7% efficiency. The system comprises a 60 W PV module, 30 Ah battery, two 180 W DC-DC converters, DC circulation pump, and DC RO pump. In this innovative hybrid configuration, the researchers evaluated the water quality parameters like THD and pH, and they prove that temperature has positive effects on the system performance and productivity.

1.3.2 System Optimization and Cost Analysis

Numerous factors affect the system configuration in designing a renewable energy system like a PVRO system for a house. Renewable energy sources in the selected site, types of storage in the system, size and type of the loads, environmental factors, efficiency, reliability, size and cost of the components, overall system cost, and maintenance cost are among these factors. As a result, system optimization and cost analysis is an important first step in system designing. Optimization methods can be divided into three main categories: (1) Classical optimization algorithms: linear programming model (LPM), non-linear programming (NLP), and dynamic programming (DP). (2) Simulation and optimization software: HOMER software, HYBRID2 software, HOGA software, RETScreen software, HYBRIDS software, and PVsyst software. (3) Modern optimization algorithms: deterministic algorithm and probabilistic algorithm [20]. Saleem et al. [21] developed PVRO systems for three different cities of Pakistan, including Lahore, Hasil Pur, and Faisalabad. They used IMSDesign software to calculate the required membrane to produce

output water with 295.44, 237.69, and 241.98 TDS in those cities from 1495, 2190, and 241.98 TDS input water. The software proposed that all designed systems working 10 hours/day could produce 0.8 m³ daily potable water, and the required energy for the systems in each city is 60, 95, and 311 kWh per month, respectively. PVsyst software was used to calculate the required PV panels and the software suggested 9, 15, and 40 255 W PV panels for mentioned cities. Finally, the authors presented a cost analysis for each city separately.

Optimization helps researchers to merge various sources in one system to achieve the most cost and energy effective configuration. Mostafaeipour et al. [22] investigated three stand-alone hybrid renewable energy systems for a water desalination system in Iran. They performed the optimization based on the life cycle cost and loss of power supply probability factors. The first system is a hybrid photovoltaic – wind – hydrogen - RO system; the second is hybrid wind – hydrogen - RO system; and the third is hybrid photovoltaic – hydrogen - RO system. They used artificial bee swarm optimization (ABSO) to set the loss of power supply probability of less than 10%. The results show that the third system was the most cost-effective while the first and second systems are in the other ranks. In another research, Mostafaeipour et al. [23] did the techno-economic analysis for PVRO systems in nine different districts of Bushehr province in Iran. HOMER software was used for system optimization and cost analysis for all regions. They stated that Delvar and Deylam ports' systems required annual energy of 72,336 kWh and 47,915 kWh, respectively. Based on the software results, PVRO systems of these two ports can produce 148 m³ to 228 m³ daily freshwater with a cost of 1.96 to 3.02 \$/m³. Finally, it is predicted

that the designed system in Deylam is a promising hybrid system while the price of desalinated water is lower than exciting potable city water.

1.3.3 Dynamic Modelling and System Simulation

The next vital step in system designing is checking the dynamic of the system. Dynamic modelling for renewable energy systems helps designers predict the system's behaviour to any changes in the input parameters. Moreover, it can mimic the system's response in any turbulences in the system. As much as the researchers learn about the system's dynamic, they can better control the system. In other words, system optimization provides an overview of the system components, but the dynamic modelling presents more details on the components and how they interact with each other. As mentioned above, the PVRO system comprises two systems and subsequently dynamic models for both system is required. For system simulation, various software can be considered which can support PV systems and RO systems separately. However, MATLAB/Simulink can be used for dynamic simulation of both systems

Riverol et al. [24] explained that four different parameters could be controlled in an RO system: feed water pressure, feed water PH, freshwater conductivity, and flow rate. They stated that the potable water flow rate and conductivity could be controlled by controlling the manipulated parameters of pressure and PH. They proposed a model based on the parameters estimation, real data from the system, and a zero-poles discrete model. The transfer function-based model in this study is valid in certain ranges of input and output parameters. Three different groups of RO dynamic models were described in [25] by Gambier et al.: irreversible thermodynamic model, porous model, and homogenous or non-

porous membrane model. They demonstrated that although numerous linear transfer function-based models can present the RO system, their model based on the physical laws and simulation in MATLAB/Simulink shows promising results. Balance equation for energy, concentration, mass, and momentum is used for extracting a lumped parameter dynamic model.

PV system electrical dynamic simulation mainly consists of PV arrays, DC-DC converter, battery storage, DC load, DC-AC converter, AC load, and control units. Jiang et al. [26] designed, simulated, and analyzed a hybrid PV system for a rural house in China. Their proposed system consists of 65 kWh/day primary load, 1.4 kWh/day deferrable load, 13 kW PV arrays, 20 batteries, 15 kW inverter, and a diesel generator. The authors used simplified incremental conductance maximum power point tracking (MPPT) controller for the DC-DC converter and a PID controller for the DC-AC converter. Finally, it is proved that the system works properly in the following three different conditions: (1) maximum load with a dip of solar irradiance and 50% battery SOC; (2) average load with increasing solar irradiance and 50% SOC; (3) average load with maximum solar irradiation and 99.3% SOC.

A stand-alone PV-battery system dynamic model was simulated and analyzed with MATLAB/Simulink in [27] by Jayalakshmi et al. Three different loads including three-phase squirrel-cage induction motor, three-phase resistive load, and DC load powered by the PV panels to check the system's performance. Control units, including incremental conductance MPPT controller, PI controller for buck-boost converter, and constant voltage-constant frequency controller for inverter, were explained in detail. The authors

showed that the designed system could deliver the power in constant DC bus voltage of 780 volts and three different load combinations: variable DC and AC loads, constant AC and variable DC load, and constant DC and AC loads. Lawrence et al. [28] designed and simulated a stand-alone hybrid PV system for a rural house in Nigeria. Their system comprises PV panels, boost converter, incremental conductance MPPT controller, battery storage, transformer, single-phase PWM inverter, and constant voltage inverter controller. They showed the designed system could deliver the power in a constant voltage of 220 volts and a constant frequency of 60 Hz under various environmental conditions.

1.3.4 MPPT Control Techniques for PV System

One of the important steps after designing a system, especially a renewable energy system, is to increase the system's efficiency. It is achievable by adding a controller to the system, improving the existing controller, or replacing by a new controller to check the performance. A major drawback in the PV systems is that their output produced energy change continuously by variation in input environmental factors such as radiation and temperature. As a result, a controller is needed to force the panels to work in their maximum power point, known as maximum power point tracking (MPPT) control system. MPPT control techniques can be categorized into two main groups; (1) traditional techniques like perturb and observe (P&O), incremental conductance (InC), fractional short circuit current and fractional open-circuit voltage; (2) artificial intelligence techniques like fuzzy logic controller (FLC), particle swarm optimization method, and neural networks. Sadek et al. [29] designed a PV battery system with a conventional P&O MPPT controller and simulated it in MATLAB software. Afterward, they replaced the controller with a P&O-

based FLC controller to increase delivered energy to combined DC and AC loads. The authors proved that the proposed FLC controller had better performance in rising time, steady-state error, and settling time.

Three different MPPT controllers, including P&O, incremental conductance, and FLC, were presented in [30] by Selman et al. for controlling a PV system with a DC-DC boost converter. They carefully designed and implemented the controller in Simulink and described how they work. The comparison was made in two categories: (1) controllers' performance with irradiance variation; (2) controllers' performance with temperature variation. In both categories, it is shown that the FL controller has better efficiency with lower oscillation. Bendib et al. [31] compared the P&O and FLC MPPT controller results in a PV system with a DC-DC buck converter to evaluate the system's efficiency. The FLC controller in this research comprises three components. The fuzzification component firstly has to convert real data from the panel to fuzzy variables. The inference engine with membership functions and fuzzy rules can perform the MPPT concept and generate fuzzy outputs. The defuzzification component will transfer fuzzy data to the appropriate duty cycle for the converter. The author claimed that the FLC controller had better efficiency while following rapid changes in irradiance and temperature.

1.4 Motivations

Powering the isolated houses in rural areas is a tremendous concern, especially that the trends are to design an emission-free and environmentally friendly system. As a renewable energy system, a stand-alone PV battery system is an option widely spread worldwide. In

rural areas, providing potable water for the inhabitants is another concern, especially nowadays when most countries are experiencing severe freshwater shortages. Water desalination is a growing method to meet water requirements. Among available desalination systems, RO systems are promising options. Powering a house with an isolated PV system needs a remarkable area on the ground level or the rooftop for panel installation to meet the electricity requirement. Moreover, water desalination with an RO system is energy-intensive, and a PV system for a small-scale unit is not cost-effective. Although designing separate renewable energy systems for both purposes is inefficient, designing a PV system to power a house and a reverse osmosis system simultaneously is an excellent solution. Therefore, this research aims to design a PV battery system for a rural house equipped with a RO system in Iran. With system design, optimization, cost analysis, dynamic modelling, and system control for better efficiency, generating the required electricity and potable water for the house is possible.

1.5 Research Objectives

According to the motivations stated, the key objectives of this research are listed following, and they are successfully achieved within the study:

1. To investigate the current water system in the house and design a new water system configuration with RO system components. The new water system will be considered a deferrable load, and in conjunction with the regular house load, the designed renewable system will power both of them.

2. To design and simulate two different isolated hybrid renewable energy systems with optimization software and check the advantages and disadvantages of each system. The cost analysis will evaluate the possibility of the selected system.
3. To present a dynamic model for the reverse osmosis system based on the transfer function model and check the behaviour of the RO system to input parameter's variation.
4. To completely model the PV system, all other components like converter and inverter, and deferrable load in MATLAB/Simulink and check the system's dynamic behaviour. The system's responses will be checked in a wide range of environmental changes and internal system states.
5. To propose and simulate different MPPT control techniques for the PV system to compare and select the most appropriate control technique to increase the system's efficiency.

1.6 Thesis Organization

The thesis is prepared in manuscript style format, and a summary of each chapter is presented following:

Chapter 2 presents the optimization of stand-alone PV systems for a rural house and small-scale RO system in Tehran, Iran. Water system configuration and related components are explained in this chapter. Two different loads are defined, and the electrical system is optimized in the HOMER software to select the best option. PV battery system and PV battery-gas-generator system are two offered scenarios compared in various

aspects. Cost analysis, sensitivity analysis, size of the components, and dispatch control strategies are discussed in this chapter. The work on this chapter meets objectives 1 and 2. This paper is accepted in the Jordan Journal of Electrical Engineering (JJEE), and it will be published in the next available issue of the journal.

Chapter 3 presents the design, simulation, and analysis of the dynamic model for the proposed system. All the components' sizes from the previous chapter are considered to design the system in MATLAB/Simulink. Firstly, a dynamic analysis of the small-scale RO system is presented based on a transfer function model to check the system's responses according to various inputs. Then, a complete electrical dynamic model consisting of a series of components to transfer energy from PV to the loads is described. The behaviour of the system is checked in four different conditions, and it is depicted that the system is working properly under various changes in parameters. The work on this chapter meets objectives 3 and 4. This paper is accepted in the European Journal of Electrical Engineering and Computer Science (EJECE), and it will be published in the next issue of the journal.

Chapter 4 presents three different MPPT techniques for the designed system in the previous chapter to increase efficiency and improve the system's performance. All techniques are designed, simulated and analyzed in MATLAB/Simulink software, and the results are compared. Proposed MPPT controllers for the PV system in this chapter, P&O, InC method, and FLC, will evaluate the effects of changes in the environmental factors. The work on this chapter meets objective 5. This paper has been accepted and presented at the IEEE 12th annual Information Technology, Electronics and Mobile Communication Conference (IEMCON), Vancouver, BC, Canada, October 2021.

Chapter 5 presents key research findings in the thesis, conclusion, recommendation, and future works.

References

- [1] Iea, “World Energy Outlook 2020 – Analysis,” IEA, 13-Oct-2020. [Online]. Available: <https://www.iea.org/reports/world-energy-outlook-2020>. [Accessed: 09-Sep-2021].
- [2] M. Madziga, A. Rahil, and R. Mansoor, “Comparison between Three Off-Grid Hybrid Systems (Solar Photovoltaic, Diesel Generator and Battery Storage System) for Electrification for Gwakwani Village, South Africa,” *Environments*, vol. 5, no. 5, p. 57, May 2018, doi: 10.3390/environments5050057.
- [3] Unicef.org, 2021. [Online]. Available: <https://www.unicef.org/media/95241/file/water-security-for-all.pdf>. [Accessed: 09-Sep- 2021].
- [4] M. A. | 05/27/2020, T. E. | 06/02/2021, L. E. | 03/26/2021, and M. A. | 05/14/2021, “What is Desalination?,” IDE Technologies. [Online]. Available: https://www.ide-tech.com/en/solutions/desalination/what-is-desalination/?data=item_1. [Accessed: 09-Sep-2021].
- [5] S. M. Shalaby, “Reverse osmosis desalination powered by photovoltaic and solar Rankine cycle power systems: A review,” *Renewable and Sustainable Energy Reviews*, vol. 73, pp. 789–797, Jun. 2017, doi: 10.1016/j.rser.2017.01.170.

- [6] “Renewable Energy Potential of Iran,” ERI. [Online]. Available: <https://www.eurasian-research.org/publication/renewable-energy-potential-of-iran/>. [Accessed: 09-Sep-2021].
- [7] “Solar resource maps of Iran,” Solargis. [Online]. Available: <https://solargis.com/maps-and-gis-data/download/iran>. [Accessed: 09-Sep-2021].
- [8] G. Najafi, B. Ghobadian, R. Mamat, T. Yusaf, and W. H. Azmi, “Solar energy in Iran: Current state and outlook,” *Renewable and Sustainable Energy Reviews*, vol. 49, pp. 931–942, Sep. 2015, doi: 10.1016/j.rser.2015.04.056.
- [9] A. Chauhan and R. P. Saini, “A review on Integrated Renewable Energy System based power generation for stand-alone applications: Configurations, storage options, sizing methodologies and control,” *Renewable and Sustainable Energy Reviews*, vol. 38, pp. 99–120, Oct. 2014, doi: 10.1016/j.rser.2014.05.079.
- [10] M. Malinowski, J. I. Leon and H. Abu-Rub, "Solar Photovoltaic and Thermal Energy Systems: Current Technology and Future Trends," in *Proceedings of the IEEE*, vol. 105, no. 11, pp. 2132-2146, Nov. 2017, doi: 10.1109/JPROC.2017.2690343.
- [11] S. Ashraf, A. Nazemi, and A. AghaKouchak, “Anthropogenic drought dominates groundwater depletion in Iran,” *Sci Rep*, vol. 11, no. 1, p. 9135, Dec. 2021, doi: 10.1038/s41598-021-88522-y.
- [12] D. Reed, *Water, security and U.S. foreign policy*. London: Taylor and Francis, 2017. Accessed: Sep. 09, 2021. [Online]. Available: <http://search.ebscohost.com/login.aspx?direct=true&scope=site&db=nlebk&db=nlabk&AN=1544142>

- [13] S. Gorjian and B. Ghobadian, "Solar desalination: A sustainable solution to water crisis in Iran," *Renewable and Sustainable Energy Reviews*, vol. 48, pp. 571–584, Aug. 2015, doi: 10.1016/j.rser.2015.04.009.
- [14] "Home," *Idadesal*, 07-Sep-1970. [Online]. Available: <https://idadesal.org/>. [Accessed: 09-Sep-2021].
- [15] M. A. M. Khan, S. Rehman, and F. A. Al-Sulaiman, "A hybrid renewable energy system as a potential energy source for water desalination using reverse osmosis: A review," *Renewable and Sustainable Energy Reviews*, vol. 97, pp. 456–477, Dec. 2018, doi: 10.1016/j.rser.2018.08.049.
- [16] F. Esmailion, "Hybrid renewable energy systems for desalination," *Appl Water Sci*, vol. 10, no. 3, p. 84, Mar. 2020, doi: 10.1007/s13201-020-1168-5.
- [17] M. A. Alghoul et al., "Design and experimental performance of brackish water reverse osmosis desalination unit powered by 2 kW photovoltaic system," *Renewable Energy*, vol. 93, pp. 101–114, Aug. 2016, doi: 10.1016/j.renene.2016.02.015.
- [18] F. Banat, H. Qiblawey, and Q. A.- Nasser, "Design and Operation of Small-Scale Photovoltaic-Driven Reverse Osmosis (PV-RO) Desalination Plant for Water Supply in Rural Areas," *CWEEE*, vol. 01, no. 03, pp. 31–36, 2012, doi: 10.4236/cweee.2012.13004.
- [19] S. Gorjian, B. Ghobadian, F. J. Jamshidian, H. Sharon, and S. Saadi, "Performance evaluation and economics of a locally-made stand-alone hybrid photovoltaic-thermal brackish water reverse osmosis unit," *Cleaner Engineering and Technology*, vol. 2, p. 1-12, Jun. 2021, doi: 10.1016/j.clet.2021.100078.

- [20] M. Akorede, A. Oladeji, B. Ariyo, I. Omeiza, and M. Marzband, "Review of Researches on Techno-Economic Analysis and Environmental Impact of Hybrid Energy Systems," *JJEE*, vol. 6, no. 2, p. 78, 2020, doi: 10.5455/jjee.204-1589458540.
- [21] M. W. Saleem, A. Abbas, M. Asim, G. M. Uddin, T. N. Chaudhary, and A. Ullah, "Design and cost estimation of solar powered reverse osmosis desalination system," *Advances in Mechanical Engineering*, vol. 13, no. 6, pp. 1-11, Jun. 2021, doi: 10.1177/16878140211029090.
- [22] A. Maleki, F. Pourfayaz, and M. H. Ahmadi, "Design of a cost-effective wind/photovoltaic/hydrogen energy system for supplying a desalination unit by a heuristic approach," *Solar Energy*, vol. 139, pp. 666–675, Dec. 2016, doi: 10.1016/j.solener.2016.09.028.
- [23] A. Mostafaeipour, M. Qolipour, M. Rezaei, and E. Babae-Tirkolae, "Investigation of off-grid photovoltaic systems for a reverse osmosis desalination system: A case study," *Desalination*, vol. 454, pp. 91–103, Mar. 2019, doi: 10.1016/j.desal.2018.03.007.
- [24] C. Riverol and V. Pilipovik, "Mathematical Modeling of Perfect Decoupled Control System and Its Application: A Reverse Osmosis Desalination Industrial-Scale Unit," *Journal of Automated Methods and Management in Chemistry*, vol. 2005, no. 2, pp. 50–54, 2005, doi: 10.1155/JAMMC.2005.50.
- [25] A. Gambier, A. Krasnik and E. Badreddin, "Dynamic Modeling of a Simple Reverse Osmosis Desalination Plant for Advanced Control Purposes," 2007 American Control Conference, 2007, pp. 4854-4859, doi: 10.1109/ACC.2007.4283019.

- [26] B. Jiang and M. T. Iqbal, "Dynamic Modeling and Simulation of an Isolated Hybrid Power System in a Rural Area of China," *Journal of Solar Energy*, vol. 2018, pp. 1–13, Jun. 2018, doi: 10.1155/2018/5409069.
- [27] N. S. Jayalakshmi, D. N. Gaonkar, A. Patil and S. A. RAZA, "Dynamic modeling and performance study of a stand-alone photovoltaic system with battery supplying dynamic load," *International Journal of Renewable Energy Research*, vol. 4, no. 3, pp. 635-640, 2014.
- [28] L. O. Aghenta and M. T. Iqbal, "Design and Dynamic Modelling of a Hybrid Power System for a House in Nigeria," *International Journal of Photoenergy*, vol. 2019, pp. 1–13, Apr. 2019, doi: 10.1155/2019/6501785.
- [29] S. M. Sadek, F. H. Fahmy, A. E.-S. A. Nafeh, and M. A. El-Magd, "Fuzzy P & O Maximum Power Point Tracking Algorithm for a Stand-Alone Photovoltaic System Feeding Hybrid Loads," *SGRE*, vol. 05, no. 02, pp. 19–30, 2014, doi: 10.4236/sgre.2014.52003.
- [30] N. Hussein Selman and J. R. Mahmood "Comparison Between Perturb & Observe, Incremental Conductance and Fuzzy Logic MPPT Techniques at Different Weather Conditions," *IJRSET*, vol. 5, no. 7, pp. 12556–12569, Jul. 2016, doi: 10.15680/IJRSET.2016.0507069.
- [31] B. Bendib, F. Krim, H. Belmili, M. F. Almi, and S. Boulouma, "Advanced Fuzzy MPPT Controller for a Stand-alone PV System," *Energy Procedia*, vol. 50, pp. 383–392, 2014, doi: 10.1016/j.egypro.2014.06.046.

Chapter 2.

Optimum Sizing Comparison of Stand-alone Hybrid PV Systems for a Rural House in Iran Equipped with a RO Water Desalination System

Mohammad Mousavi¹, M. Tariq Iqbal²

^{1,2}Electrical and Computer Engineering Department, Faculty of Engineering and Applied
Science, Memorial University of Newfoundland, St. John's, Canada

A version of the manuscript in this chapter has been accepted as a journal paper in the Jordan Journal of Electrical Engineering (JJEE). As the primary author in this paper, Mohammad Mousavi carried out the research under the supervision of M. Tariq Iqbal as the co-author. The MEng candidate performed the literature review and was involved in method selection, system designs, calculations, simulation, and data analysis. Moreover, he prepared the first draft of the paper. The co-author supervised the research by actualization the research ideas, reviewing and correcting the manuscript.

Abstract

Energy and water crisis affects every aspect of modern human life, and addressing both in one solution is a growing trend. Merging Hybrid Renewable Energy Systems (HRES) and water desalination system that provides potable water from brackish water in one system is a promising solution. In this study, the optimization of stand-alone hybrid PV systems for powering a house equipped with a Reverse Osmosis (RO) water desalination system in Sinak village, Tehran, Iran, is discussed. RO system configuration, regular house load and RO deferrable load, solar radiation capability, and HRES components have been analyzed in the first part. The next part is about optimization, cost analysis, and sensitivity analysis of two scenarios, including a photovoltaic system with battery storage and a photovoltaic system with battery storage and gas generator in HOMER Pro software. Moreover, different dispatch strategies for controlling the systems like cycle charging (CC) and load following (LF) are described. In the last part, a comparison between scenarios shows that a hybrid PV-battery-RO system is more energy-effective, environmentally friendly, and has less control complexity, while fewer sensitivity variables affect the system's cost. Net present cost (NPC) and cost of electricity (COE) in this system are 10,245 US\$ and 0.31 US\$/kWh, respectively, with zero carbon emission.

Keywords — Hybrid Renewable Energy Systems (HRES), PV system, Reverse Osmosis (RO) water desalination, HOMER Pro software, Techno-economic analysis, sensitivity analysis.

2.1 Introduction

Climate change is a probable consequence of the overexploitation of fossil fuel-driven energy, and greenhouse gas (GHG) emission, as an immediate result of this fossil fuel burning, has a remarkable adverse effect on environmental pollution. The first solution for the global warming issue is reducing GHG emissions by considering clean energy sources [1]. Hybrid renewable energy systems (HRES) have become popular recently because of their promising advantages over conventional energy sources, like cost reduction over time, fewer emissions, higher reliability, better stability, more efficiency, and desirable performance. The main objective of designing a hybrid renewable energy system is to merge two or more renewable and non-renewable energy sources in one system to meet the energy requirements. [2]

Energy is a crucial commodity in the modern world, and water is essential for human life. About 97% of the water resources globally are saltwater, including seawater, groundwater, and oceans' water. As a result, only 3% of the global water is in the form of freshwater. Moreover, only 10% of this potable water is accessible for household applications. Nowadays, water scarcity is the most significant human issue due to increasing water demand. [3] A water desalination system is a terrific method to resolve this water crisis. Desalination is the process of removing salt from the sea or brackish water to make it pure for drinking. There are numerous water desalination methods, and the central problem for these methods is the high level of energy consumption. However, the Reverse Osmosis (RO) method is a popular method because of its low energy consumption, low-priced technology, and wide accessibility [4].

Energy management and optimization increase the efficiency of any hybrid renewable energy system (HRES). Akorede et al. [5] proposed a critical review on optimization approaches of HRES. This study suggests that cost analysis, system reliability, and environmental considerations are the main factors that affect the optimization results. They introduced three main categories for optimization methods: classical optimization algorithms, simulation and optimization software such as HOMER, HYBRID2, HOGA, RETScreen, and HYBRIDS, and modern optimization algorithms. As the feasibility of a renewable system with one component is not realistic, system optimization helps researchers merge numerous renewable sources such as solar and wind into one system. For example, [2] and [6] introduce an appropriate hybrid design for existing infrastructure, accurate cost analysis, and control methods. Various methods have been introduced in research for optimization. Peng et al. [7] investigate an HRES combined with a water desalination system for a remote area in Iran. Their proposed system consists of a wind turbine, photovoltaic (PV) arrays, batteries, and a RO desalination unit. They used numerous optimization methods like bee swarm, particle swarm, simulated annealing, harmony search, chaotic search, and Tabu search algorithm for optimization. The research approves that HRES reduces system costs and increases system reliability in general.

Maleki et al. [8] analyzed various possibilities for bringing hydrogen energy storage to the hybrid system for water desalination of stand-alone sites in Iran. They proposed three hybrid systems and used Artificial Bee Swarm Optimization (ABSO) method in this study. They proved that PV-hydrogen-RO is the most cost-effective energy system in comparison with PV-wind-hydrogen-RO and wind-hydrogen-RO. Mostafaiepour et al. [9] investigated

off-grid PV systems to power a RO desalination system in different districts of Boushehr province in Iran. They used HOMER Pro software and Excel software to analyze technical and economic aspects of the systems. Their proposed PVRO desalination system includes a reverse osmosis membrane, high-pressure pump, motor, batteries, converter, and PV arrays.

Numerous studies analyze the system's techno-economic aspects as far as small-scale photovoltaic-driven reverse osmosis water desalination system is concerned. Da Silva et al. [10] investigated techno-economic aspects of a small-scale PVRO system in Brazil. They predict that the designed system with 26 to 33 m² PV panel can provide 250 people's freshwater consumption for two days at a cost from 1.44 to 1.65 \$/m³. Two small-scale PVRO systems are suggested by Hajji et al. [11] to provide 20 m³/day desalinated water in the south of Morocco. The first option consists of a 36 m³/day RO unit, 23 kW PV panel, and 50.5 kWh battery storage with a lower initial investment cost of approximately 93,400 US\$. On the other hand, the second one generates water with a lower cost of 1.6 US\$/m³ in the system with a 72 m³/day RO unit, 32 kW PV panel, and 38.5 kWh battery bank.

Different power resources can power the desalination system. El-Ghonemy [12] analyzed four power supply systems for a small-scale RO unit, including PV module-battery-inverter system, PV module-battery-inverter-diesel generator system, diesel generator system, and local national grid electricity. The author showed that cost of energy (COE) for the first, second and last system is 0.46, 0.25, and 0.1 \$/kWh. Iran has a good potential for solar energy, as it is located in the earth's sunbelt. Moreover, the water crisis in Iran has worsened because the total per capita annual water has been decreased [13].

Based on these two facts, a hybrid renewable energy system (HRES) that includes a photovoltaic panel that feeds reverse osmosis (RO) water desalination is a promising solution. This study compares two stand-alone hybrid PV systems for a rural house in Iran equipped with a RO water desalination system. Two scenarios are:

- Photovoltaic system with Battery storage
- Photovoltaic system with Battery storage and Gas generator

In this paper, there are three main parts. Firstly, site characteristics such as load calculation, solar radiation, system configuration and design methods are presented. Secondly, the design results and simulating of two scenarios are completed in HOMER Pro software, and techno-economic analysis of the proposed scenarios is described. Finally, results, discussion, and comparison about possible scenarios are made.

2.2 Material and Methods

Appropriate design of a hybrid renewable energy system is achievable when every aspect of the system has been analyzed. Different energy sources and demands in the system bring more complexity to the design, and every parameter should be considered. The following framework has been considered in this paper for an accurate evaluation of the system:

- characteristics of the selected site
- water system configuration
- load demand data
- solar radiation

- system components
- economic analysis

2.2.1 Characteristics of the Selected Site

Iran, located in an arid and semi-arid region, is among the top water-stressed countries and suffers water shortages in various industrial, agricultural, and domestic sections because of uneven deducted rainfall patterns [13]. Tehran, the capital of Iran, is located in the north of the country and faces severe population migration and pollution in the last few years. Sinak village, as the selected location for this study, is a village in Lavasanat District, Shemiranat County, Tehran Province, Iran (35°51'06.1"N 51°41'14.3"E).

The selected house for this study is a village house, which has two characteristics: firstly, like most of the houses in rural areas, there is no electrical grid to power the house, and as a result, the only option for these houses is a traditional stand-alone system for electrical source, which is costly and produces noise and pollution. Secondly, the selected site's water source is well water, containing high amounts of harmful ingredients and contaminants. Atefeh et al. [14] investigated the Lavasane–E Kochak district's underground drinking water quality. They proved that the average total dissolved solids (TDS) parameter in this region is around 600 ppm.

Four people live in that house, and their major sources of electricity consumption are lighting, running electrical appliances, and water pumping. People use natural gas for cooking and heating in Iran because of its availability, and as a result, electricity

consumption is relatively low. Because of the Iranian houses' low energy consumption rate, the photovoltaic panel is a promising component in the hybrid renewable energy system.

2.2.2 Water System Configuration

Based on the house's current system configuration, the well brackish water is pumped by a submersible pump, and it goes to the above-ground tank. A jet pump will then increase the tank's water pressure, and then it goes to the house. The submersible pump in this house is located at a depth of 25 meters from the ground surface. It has three stainless steel impellers, which can pump water to the maximum height of 38 meters. The above-ground tank has 1000 liter capacity, located on the rooftop with three meters height from the ground. The jet pump in this house has a 2-pole electric induction motor for continuous operations, and the stator is made with low-loss laminated electric sheet steel.

The reverse osmosis (RO) system is designed based on the existing water configuration for the house. Based on the site survey, the daily average of 1500 litres of water consumption is the best fit for this four-person house. The RO system will only provide desalinated water for drinking and cooking, around 100 litres per day. The reverse osmosis unit mainly consists of a semipermeable membrane that traps minerals while the high-pressure water is injected into it. [15] ISpring RCC7P-AK is a selected RO unit that includes a pressure pump, and multiple stage filtration consists of reverse osmosis (RO) technology which removes various contaminants. The presence of GAC and CTO filters helps the system to remove chemicals effectively. The capacity of this small RO unit is 75 gallons per day and is depicted in Figure 2.1 [16]



Figure 2.1. Reverse osmosis unit

The water system configuration of the selected house with the reverse osmosis system is shown in Figure 2.2. In this system, pumped water from the well is used for the house's general water consumption and desalination system. The iSpring T32M 3.2 gallon pressurized storage tank is located after the RO membrane to increase the system's performance.

2.2.3 Load Demand Data

This study's hybrid renewable energy system is designed to power both the house and the desalination system. As a result, load demand consists of two major parts: house energy consumption and reverse osmosis water desalination system energy consumption. House

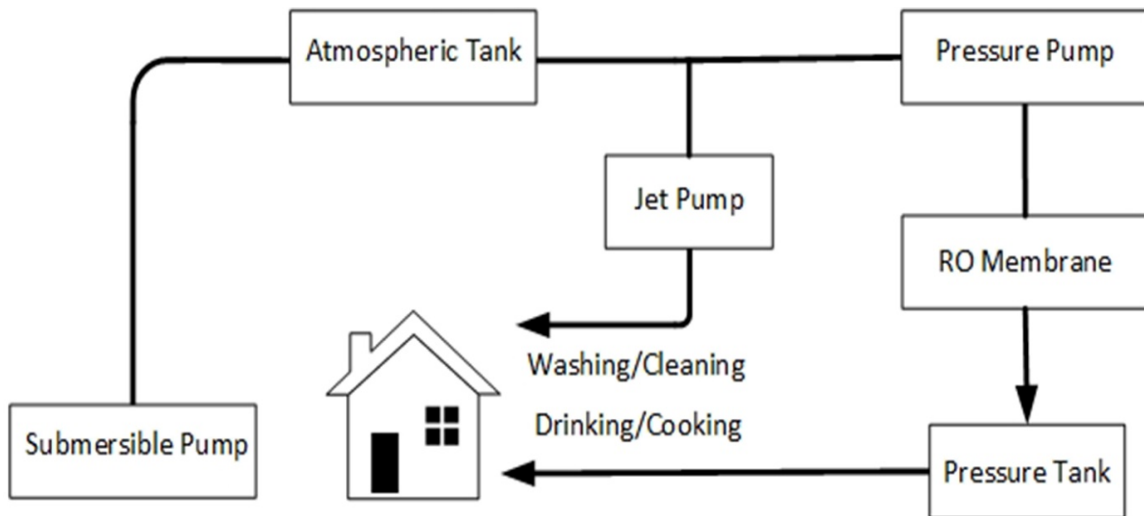


Figure 2.2. Water system configuration

load is a regular load that exists during a day, and HRES has to provide it. On the other hand, RO system load can be provided whenever excess energy exists in the system. In other words, the water desalination system can be considered as a deferrable load. A deferrable load requires a certain amount of electrical energy provided by the sources whenever excess energy exists in the system. [17]

Energy consumption of the rural house can be achieved from a metering system, or the total load can be calculated by listing the power consumption of household appliances. Since there is no metering system for the village house in this study, the second method is applicable. Table 2.1 shows a list of different house appliances by their wattage and energy consumption during a day. This table indicates that the regular daily load of the house is approximately 5.42 kWh/day.

Table 2.1. Different appliances in the house with their daily energy consumption

Household appliances	Rated watts (watt)	Timed used (hour)	Daily energy consumption (kWh)
Refrigerator	150	8	1.2
Microwave	900	0.3	0.27
Electric meat grinder	350	0.1	0.035
Blender	400	0.1	0.04
Cooker hood	140	0.4	0.056
Washing machine	200	0.3	0.06
Vacuum cleaner	900	0.2	0.18
Electric shaver	15	0.2	0.003
TV 42" LCD	120	3	0.36
Laptop	50	8	0.4
Home phone	6	24	0.144
Home internet router	10	24	0.24
Wall-mounted gas boiler	140	6	0.84
Light bulb - LED*6	72	2	0.144
Light bulb - Common*2	200	3	0.6
Light Bulb - LED*38	266	2	0.532
Extractor Fan*2	40	8	0.32

The energy required for the reverse osmosis system and the watering system of the house, known as the deferrable load in this study, consists of all the water systems' loads, including submersible pump, jet pump, and pressure pump load. The exact amount of energy consumption of the pumps is calculated to meet the house's water usage. The submersible pump has three stainless steel impeller which can pump water to the height of 38 meters, and its wattage is 1100 watts. The submersible pump needs to operate 30 minutes to pump 1500 litres of well water, which means 550 watts daily energy. The jet pump in this house is the Pentax PM45 peripheral turbine pump with a two-pole induction

motor. The motor's power rating is 470 watts, and it needs to operate one hour daily to provide water for washing and cleaning purposes. Finally, to have 110 litres (10% margin is considered) of desalinated water, the 60-watt pressure pump in the RO unit needs to operate daily for 9.2 hours, which means 550 watts daily energy. Table 2.2 presents the deferrable loads individually and the total load of the system. Based on the data in this table, the total deferrable load is for the system is 1.57 kWh/day, which the HRES should provide.

Table 2.2. Deferrable load characteristics

Deferrable load	Daily energy consumption (kWh)
Submersible pump load	0.55
Jet pump load	0.47
Pressure pump load	0.55
Total deferrable load	1.57

2.2.4 Solar Radiation

The selected site is in a rural area near Tehran city, located on a high elevation. There is significant solar irradiance in Sinak village because of its favourable location. Based on the database, which is downloaded from NASA's prediction of worldwide energy resources, the monthly radiation and clearness index graph is depicted in Figure 2.3. The

average annual solar irradiance in this region is 4.89 KWh/m²/day, while the irradiance's maximum and minimum exist in January and December, respectively.

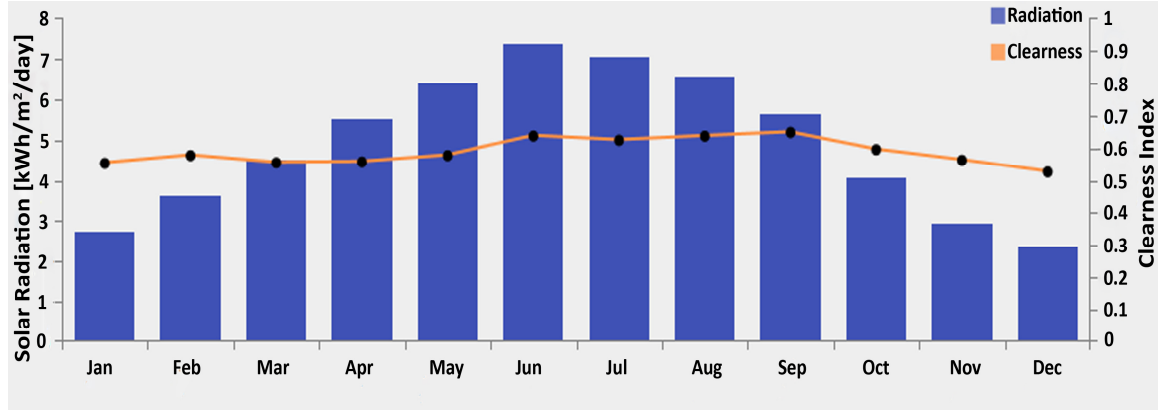


Figure 2.3. Monthly solar radiation and clearness index in Sinak village

2.2.5 System Components

2.2.5.1 PV Module

The PV panel in this study is a fixed tracking system module with significant efficiency of around 17.49%. The nominal maximum output power is 340 watts, and this power will be produced in DC format when the PV panel has exposed to the sunlight directly. As a result, the output power has a direct relation with temperature, which is described in Equation 2.1: [18]

$$P_{PV} = P_{PV, rated} \cdot f_{PV} \cdot \frac{G_T}{G_{T,STC}} \cdot [1 + \alpha_p (T_C - T_{C,STC})] \quad (2.1)$$

In this equation, $P_{PV, rated}$ is the nominal maximum output power of the PV panel, f_{PV} is the derating factor of PV panel, G_T is the actual solar irradiance, $G_{T,STC}$ is the solar radiation under standard test, α_p is the power temperature coefficient, T_C is the PV cell temperature, and $T_{C,STC}$ is the operating cell temperature of the PV panel under standard test condition.

2.2.5.2 Battery

The lead-acid battery is the selected battery for this study, and its maximum capacity is 254 Ah under the nominal voltage of 6 volts. The DC bus voltage is set to 48 volts in this study to reduce the DC bus current. The minimum state of charge (SOC) is 20% in the design, and the round trip efficiency is 85 %. Moreover, the total throughput of the battery is 914.30 kWh.

2.2.5.3 Gas Generator

A gas generator is responsible for supporting the loads in the second scenario. In the worst case, the gas generator can act as the house's primary energy source if the PV panels become disconnected from the system. Natural gas in Iran is cheap, whereas Iran's natural gas price is 0.1 \$/m³. The selected generator in this study has the capacity and lifetime of 1000 watts and 40000 hours, respectively, and it runs on natural gas.

2.2.5.4 Inverter

The inverter's main responsibility is to convert the solar panel's output power in DC format to the AC load. In the sizing of the inverter, it is noticeable that the rated power should be 20% more than the total wattage of the peak load, which is connected to the AC bus. As a result, a 4 kW solar inverter with 96% efficiency and 10 years of a lifetime is selected for this project.

The technical and economic information of the components is listed in Table 2.3. All the financial information in this list is per one item in the system.

Table 2.3. Technical and economic information of the components in the system

Component	Specification	Description
PV panel	Size	340 W
	Efficiency	17.49%
	Temperature Coefficient	0.41 %/° C
	Lifetime	25 years
	Tracking system	Fixed
	capital cost	\$400
	Replacement cost	\$300
	O&M cost	2.2 \$/year
Battery	Type	Lead-acid
	Nominal voltage	6 V
	Round Trip Efficiency	80%
	Maximum Capacity	254 Ah
	Nominal Capacity	1.52 KWh
	Throughput	914.3 KWh
	capital cost	\$200
	Replacement cost	\$175
Gas generator	O&M cost	1.75 \$/year
	Size	1 KW
	Lifetime	40000 h
	fuel cost	0.1 \$/m ³
	capital cost	\$400
	Replacement cost	\$300
Inverter	O&M cost	0.05 \$/op.hour
	Size	4 kW
	Efficiency	96%
	Lifetime	10 years
	capital cost	\$1000
	Replacement cost	\$750
	O&M cost	7.5 \$/year

2.2.6 Economic Analysis

Optimization in HOMER Pro software is based on various considerations, and one of them is an economic analysis between possible configurations. Net present cost (NPC) is the main factor in ranking the components' optimal economic configuration. NPC is all present costs of the system during the lifetime of the project and can be obtained from Equation 2.2 [19].

$$NPC = \frac{C_{annual,total}}{CRF(r, R_{project})} \quad (2.2)$$

$C_{annual,total}$ is the system annual total cost, r represents the annual interest rate, $R_{Project}$ is the project lifetime (year). In this equation, CRF is the capacity recovery factor and is achievable by the below equation. In this equation n is the number of years, and i is the discount rate [20].

$$CRF = \frac{i(1+i)^n}{(1+i)^n - 1} \quad (2.3)$$

Moreover, the other important factor in economic optimization in HOMER Pro software is the cost of electricity (COE), which the following equation can calculate: [20]

$$COE = \frac{\sum_{j=1}^n \frac{I_j + M_j + F_j}{(1+i)^j}}{\frac{E_j}{(1+i)^j}} \quad (2.4)$$

In Equation 2.4, I_j is the invested budget, M_j is the O&M expense, F_j is the fuel cost, and E_j is the generated electricity in one year.

2.3 Designing Hybrid PV Systems with HOMER Pro

Hybrid Optimization of Multiple Energy Resources (HOMER) software from the National Renewable Energy Laboratory (NREL) is an advanced software for simulating and optimizing microgrids by considering various energy sources, especially renewable energies such as solar and wind energy. Moreover, different system components can be applied to the grid-connected or stand-alone system. In designing a hybrid renewable energy system, various factors are considered. Type of the available renewable energy sources in the under-design system, type of the loads in the system, size of the components, environmental factors, components and overall system cost, maintenance cost, efficiency and reliability of the system are among the factors which affect system configuration. [21]

An optimization approach in HOMER Pro software for a stand-alone hybrid PV system with photovoltaic as the main component is based on the following major considerations: (1) Designed system is cost-effective. The HOMER software introduces the most cost-effective system mainly based on the net present cost and lowest cost of electricity. (2) The system has a high renewable fraction. Non-renewable sources exist in the software, such as gas generators, and the software approach is designing a system for injecting more renewable energies while meeting the required uninterrupted electricity. (3) Environmental factors are considered. Introducing renewable energy systems to the grid

produces more clean energy, and the HOMER software analyses proposed systems to reduce emissions.

In this paper, despite the other studies which design HRES as the source for a house or the RO unit, the system is double-purpose. In other words, designed electrical system power a house and RO desalination system simultaneously. The HOMER Pro software is used for the techno-economic analysis to optimize the system and introduce a feasible solution. In rural areas, except for the factors mentioned above, availability of the components and simplicity is another factor. Based on these facts, two possible scenarios for powering the system are considered in this paper, which are:

1. Photovoltaic system with battery storage: There is relatively high solar radiation in the selected site in this study because of its high elevation. Subsequently, a PV system is a reasonable renewable option for this system. Moreover, battery storage manufacturers in Iran can produce low-priced battery systems, with 25 years life span, compared to other storage technologies such as supercapacitors. As a result, the battery system is widely available. This configuration is 100% renewable without any emissions. In this system, the battery arrays store renewable energy to support the system when PV power production is not enough.
2. Photovoltaic system with the battery system and gas generator: One method to reduce renewable energy production and system cost is to inject fossil fuel-driven components into the HRES system. Although most research use diesel generators,

a gas generator is selected in this study because the distribution system brings natural gas through pipelines to houses in Iran at an extremely low price, even the rural ones. This hybrid system balances the system cost by decreasing PV panels and batteries while producing emissions. Both battery bank and gas generator, known as supporting components, actively meet the load demand with high efficiency when the main source cannot produce energy.

2.3.1 Photovoltaic System with Battery Storage

A PV system with battery storage has numerous advantages, including zero emissions, higher renewable fraction, eliminating operational noise, and system controllability. A photovoltaic system with battery storage is a widespread hybrid system in which the supporting storage system can cover power shortages in a green manner. As far as cost reduction is concerned, in countries with high fuel costs, eliminating conventional fossil fuel-driven resources can reduce the system cost. This scenario has a 100% renewable fraction with a 2.68 kW PV array size and a converter of 4 kW. Two kinds of daily loads are defined: the primary house load of 5.42 kWh with a 1.74 kW peak of load and a 1.57 kWh deferrable RO system load. The HOMER Pro software optimization result suggests 24 6-volt, 254 Ah batteries for this scenario with 8 batteries in each string. The battery system's total capacity is approximately 762 Ah, and the annual throughput is 1,579 kWh. DC bus voltage is 48 V, and battery system autonomy is 100 hours which means the system can operate more than 4 days without solar energy. The actual system configuration in HOMER software is shown in Figure 2.4.

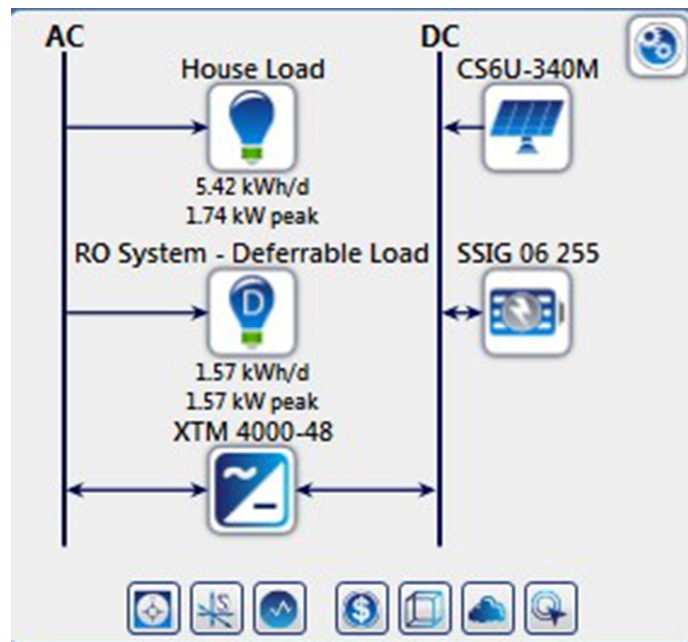


Figure 2.4. PV-Battery system configuration in HOMER Pro

Decision-making about how the resources in hybrid renewable energy systems serve the loads is critical because appropriate timing for switching on or off the components will affect system sizing. The control of resources in HRES is achievable by using two main dispatch control techniques in the software: cycle charging (CC) dispatch strategy and load following (LF) dispatch strategy. The dispatch Strategy for the system consists of battery storage is cycle charging (CC). As it is depicted in Figure 2.5, with this strategy, PV panels feed regular and deferrable higher priority, and excess energy will charge the battery. As the battery is the only backup system in this scenario, the arrays' size should be large enough to power the system in the absence of the solar system in the CC dispatch strategy. Table 2.4 projects the cost summary of the system. Based on this table, the net present cost

(NPC) during the project's lifetime is around \$10,245. Moreover, there is no CO2 emission, and the system is environmentally friendly.

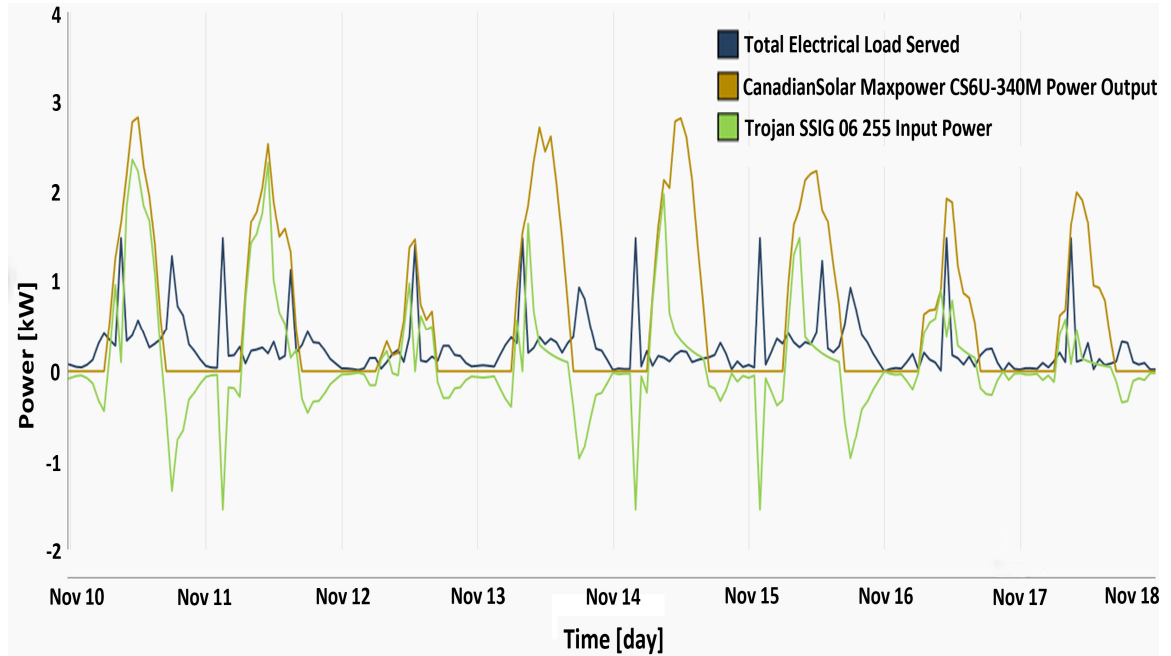


Figure 2.5. Power balance of PV-Battery system in a specific period of time

Table 2.4. Cost summary of PV-Battery system

Cost Summary	Capital	Replacement	O&M	Total
CanadianSolar MaxPower CS6U-340M	\$2,363.05	\$0.00	\$224.02	\$2,587.07
Trojan SSIG 06 255	\$4,800.00	\$1,898.29	\$542.96	\$7,039.41
Studer Xtender XTM 4000-48	\$370.40	\$245.42	\$35.91	\$618.46
System	\$7,533.45	\$2,143.71	\$802.89	\$10,244.93

In the techno-economic analysis of the hybrid renewable energy systems, sensitivity analysis is one method to check the system's robustness. Various inputs can affect the system's output, which is the cost of the system in this study. As far as the sensitivity

variables that are highly effective in the cost of the system in this scenario are concerned, variations in regular house load and solar radiation are considered to check the system's net present cost (NPC). For this analysis, each sensitivity variable is $\pm 10\%$ and $\pm 5\%$ of the normal amount of the variables, which is 4.878, 5.149, 5.42, 5.691, and 5.962 kWh/day for house load and 4.4032, 4.6478, 4.8925, 5.1371, and 5.3817 kWh/m²/day for average solar radiation. These variables can be defined in HOMER software, and the sensitivity analysis result is depicted in Figure 2.6. The results in the surface plot indicate that NPC is sensitive to house load and solar radiation variation equally and can be changed from \$9,885 to \$11,768.

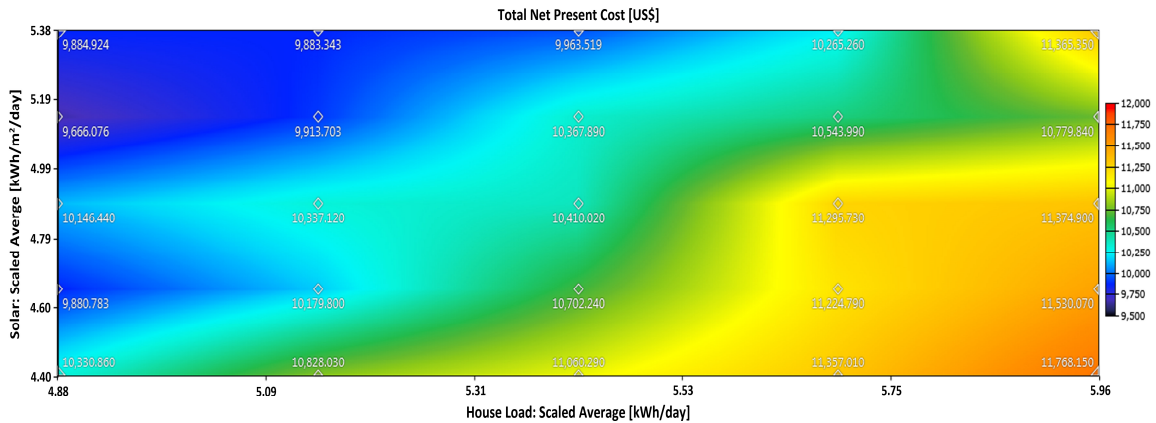


Figure 2.6. Surface plot of sensitivity analysis for PV-battery system

2.3.2 Photovoltaic System with Battery Storage and Gas Generator

Increasing the reliability of a hybrid renewable energy system is crucial in designing, which is achievable by adding more power source or storage components to the system to provide a power shortage of the renewable source. Although adding different components to the system will increase complexity, more factors for controlling the microgrid are

available. In this scenario, 1 kW gas generator and 8 batteries (1 string) with a total capacity of 254 Ah and 1.28 kW solar panels power the same load in the previous scenario simultaneously. The battery system's autonomy is 33.5 h, which indicates that the batteries can feed the loads for 1.4 days in lack of gas generator and PV panels. Moreover, the annual throughput of the battery strings is 760 kWh. Figure 2.7 depicts the actual configuration for this scenario in HOMER software.

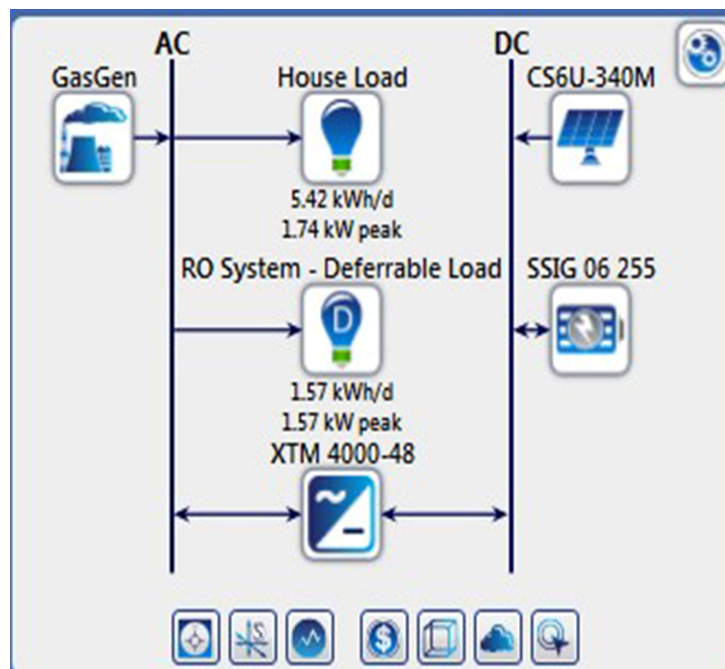


Figure 2.7. PV-Battery-Generator system configuration in HOMER Pro

The controlling process in this scenario is more complicated than the previous scenario. As a result, the load following (LF) dispatch strategy in this configuration has been applied to the system. In load following dispatch, the generator produces power to serve the regular load, and renewable sources feed deferrable load and battery storage. It means deferrable

load and batteries have a lower priority for the gas generator. The power balance between components in the system is depicted in Figure 2.8, and system operation in LF strategy follow below steps: [2, 22]

- $P_{PV} = P_{Load}$: PV feed the load, the battery does not discharge, the gas generator is off
- $P_{PV} > P_{Load}$: PV feed the load, PV charge the battery, if required, the gas generator is off
- $P_{PV} < P_{Load}$:
 - $SOC = SOC_{min}$: generator serves the primary load, PV feed deferrable load and charge battery.
 - $SOC > SOC_{min}$: cost of producing energy for generator and battery is calculated
 - ✓ $C_{battery} > C_{generator}$: Battery will serve the load
 - ✓ $C_{battery} < C_{generator}$: Generator will serve the load

The cost summary of the system is depicted in Table 2.5. Decreasing the initial capital cost to \$3,260 and net present cost (NPC) to \$6,460 are the main advantages of having a gas generator in the system configuration. However, producing CO₂ emissions by burning 399 m³ natural gas and decreasing renewable fraction to 58.1% are the main drawbacks of this scenario. The gas generator in this scenario adds extra cost to the system because of fuel cost, which is \$515.

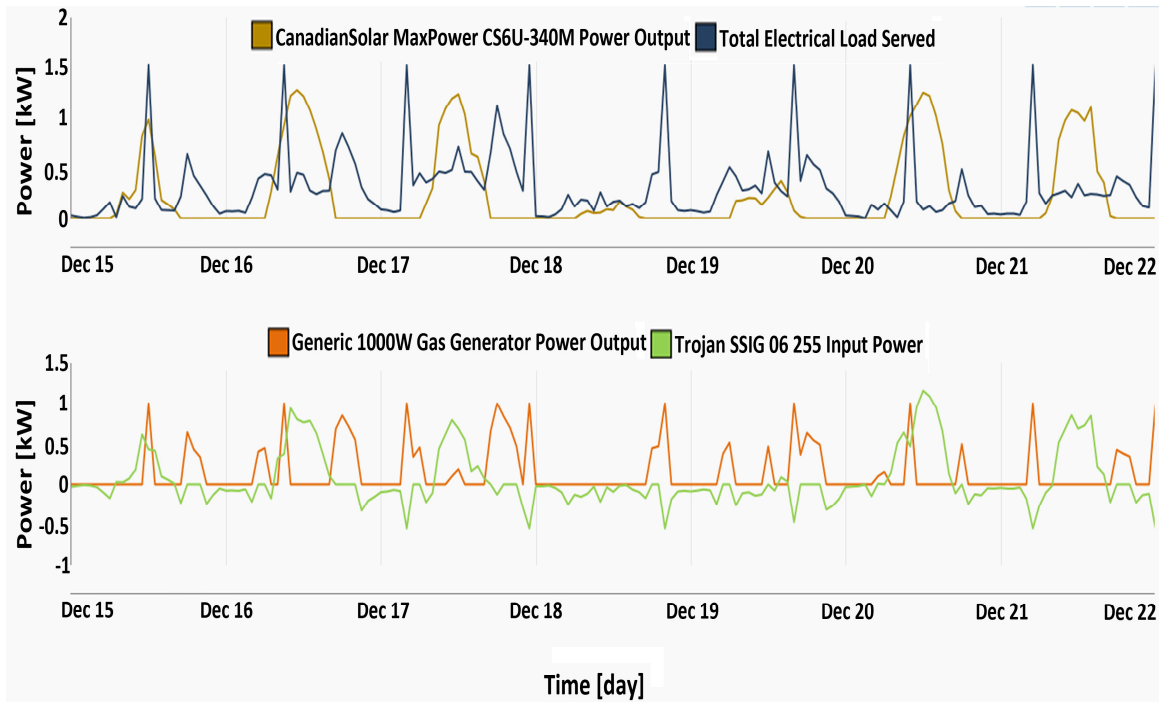


Figure 2.8. The power balance of PV-Battery-Generator system in a specific period

Table 2.5. Cost summary of PV-Battery-Generator system

Cost Summary	Capital	Replacement	O&M	Fuel	Total
CanadianSolar MaxPower CS6U-340M	\$1,127.16	\$0.00	\$106.86	\$0.00	\$1,234.02
Generic 1000W Gas Generator	\$400.00	\$82.98	\$1,149.90	\$515.38	\$2,084.44
Trojan SSIG 06 255	\$1,600.00	\$1,274.13	\$180.99	\$0.00	\$2,920.67
Studer Xtender XTM 4000-48	\$132.54	\$87.82	\$12.85	\$0.00	\$221.30
System	\$3,259.70	\$1,444.92	\$1,450.60	\$515.38	\$6,460.43

The sensitivity analysis method for the PV system with battery storage and gas generator is the same as the previous scenario. Two main sensitivity variables are regular house load and solar radiation, which are $\pm 10\%$ and $\pm 5\%$ of the normal amount of the variables. As the system's inputs vary from 4.878 to 5.962 kWh/day and 4.4032 to 5.3817

kWh/m²/day in five equal steps, the NPC has been changed from \$5,970 to \$6,947. The surface plot in Figure 2.9 depicts sensitivity analysis for this scenario. Although house load variation and solar radiation variation affect the NPC equally, the variation in natural gas price is another sensitive variable discussed in the next section.

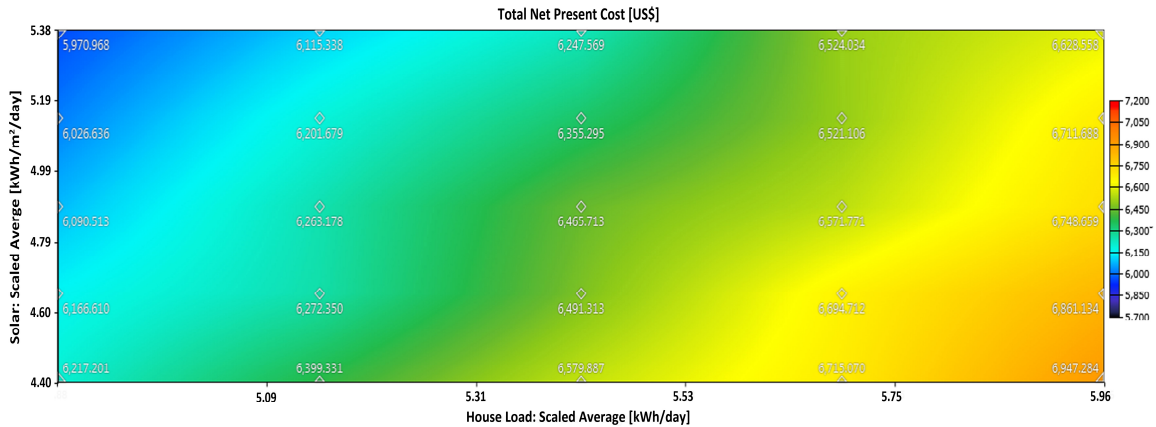


Figure 2.9. Surface plot of sensitivity analysis for PV-battery-generator system

2.4 Results and Discussion

The hybrid renewable energy system for a rural house equipped with reverse osmosis (RO) water desalination system needs precise initial analysis to achieve appropriate configuration. This analysis is essential for two reasons: firstly, the electrical system is stand-alone in rural areas, and the renewable system has to produce uninterrupted electricity for primary house load. Secondly, the water desalination system provides essential water for drinking and cooking, and as a result, the power of the RO system should be guaranteed. Different factors should be considered for configuration selection, such as cost analysis, control methods of the system, system complexity, and environmental factors.

Comparison in this study is made in the three categories of energy, cost, and sensitivity analysis. Energy-related comparison details are presented in Table 2.6. Based on these results, the advantages of both battery and generator in the system are fewer PV panels from 8 to 4, 66.6% reduction in the number of batteries. On the other hand, there are more drawbacks to the system by adding the gas generator. The renewable fraction of the first scenario is 100%, which means it produces clean energy. In the second scenario, yearly fuel consumption is 399 m³, while in the first one is zero. Battery autonomy in the first scenario is more than the second one, which means the system can operate longer without other resources. In the PV-Battery-generator system, there is carbon emission, and the controlling system is load-following which means more complexity in the system. Moreover, as far as installation is concerned, new installation consideration for the generator is required while PV panels and batteries are in the system, and extra components easily can be added to the system. From the energy perspective of the system, the PV-battery system is a reasonable solution.

Table 2.6. Energy-related comparison details

	PV-Battery	PV-Battery-Generator
PV	2.68 kW	1.28 kW
Generator	0	1.068 kW
Battery Numbers	24	8
Converter	4 kW	4 kW
Renewable fraction	100%	58.1%
Fuel	0	399 m ³ /year
Autonomy	100 h	33.5 h
Excess electricity	1,665 kWh/year	511 kWh/year
Unmet Load	1.08 kWh/year	1.57 kWh/year

CO2 Emission	0	770 kg/year
Dispatch	CC	LF

The cost comparison between the PV-battery system and PV-battery-generator system is depicted in Figure 2.10. NPC, initial capital cost, replacement cost, and COE for the system with the generator are lower around \$6,460, \$3,260, \$1,445, and \$0.2, respectively, because the natural gas cost is remarkably low in Iran. However, the system with a gas generator has higher O&M cost and fuel cost, causing the system cost in the long term.

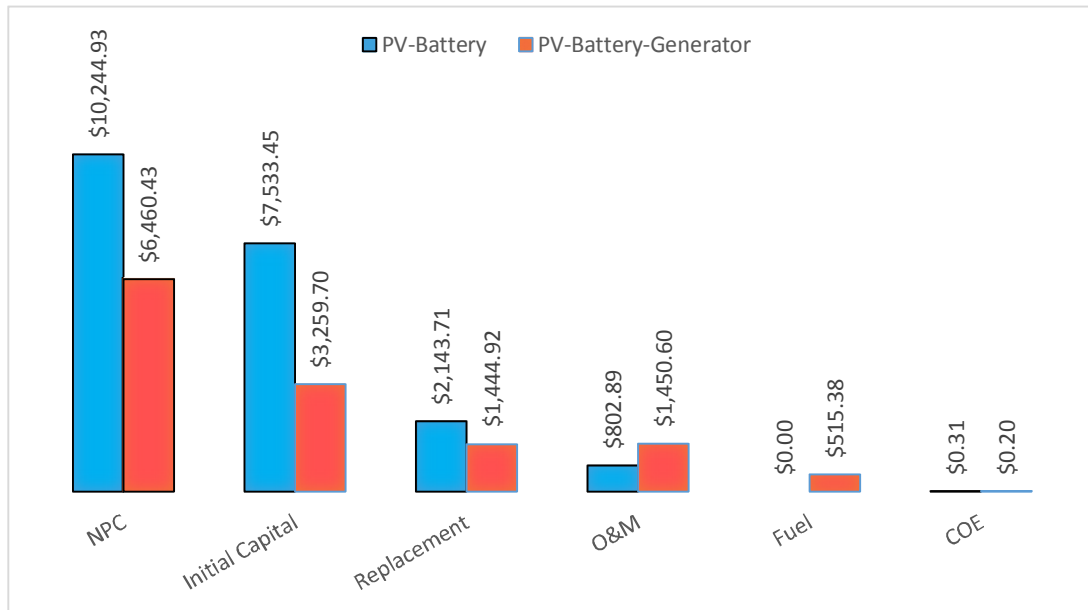


Figure 2.10. Cost comparison between PV-battery system and PV-battery-generator system

Sensitivity analysis in this study indicates that both scenarios are sensitive to the house load variation and solar radiation variation. Figure 2.11 and Figure 2.12 show the line charts for both scenarios. In these charts, NPC is depicted based on the percentages of variations in each sensitivity variable when others are fixed to zero variation. PV-battery

system NPC is fluctuating -2.5% to 9.2% and 6.2% to -4.2% by -10% to 10% variation in house load and solar radiation respectively. Moreover PV-battery-generator system NPC is fluctuating -5.8% to 4.3% and 1.7% to -3.3% by the same variation. However, in the second scenario, another sensitivity variable affects NPC, which is natural gas price. In Iran, natural gas price is fluctuating rapidly, and subsequently, the cost of the system is fluctuating. As Fig. 12 indicates, NPC varies from -3.3% to 1.6%, with similar percentages of fluctuation in gas price. In other words, the PV system with a generator is more sensitive with three variables.

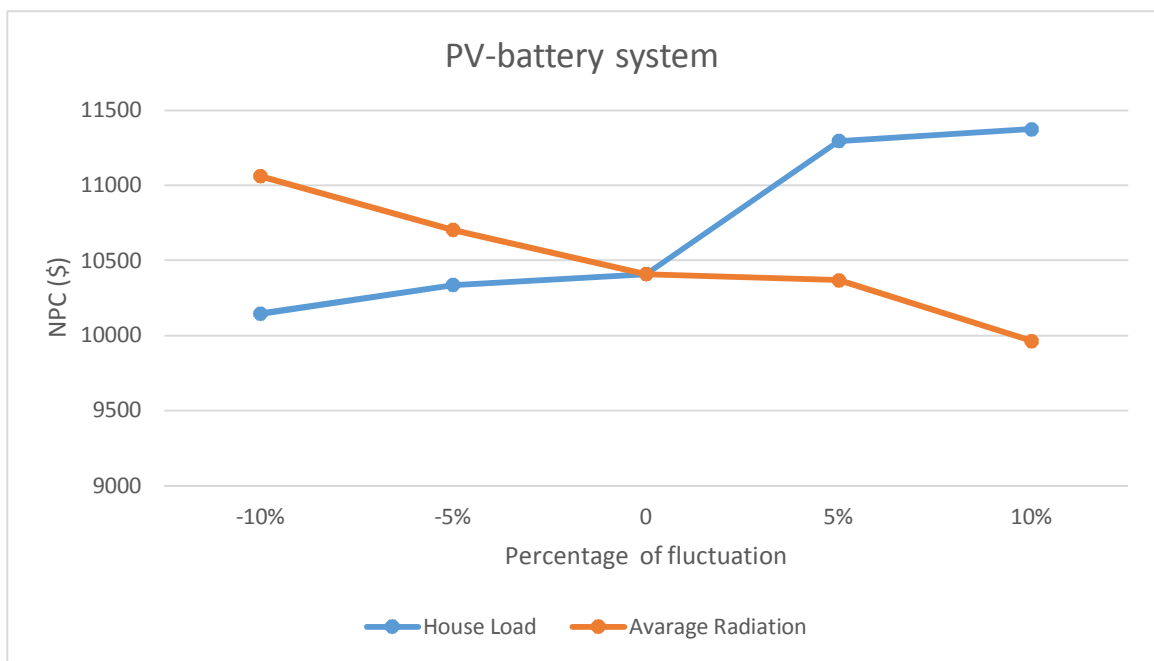


Figure 2.11. Impact of House Load and Average radiation fluctuation on NPC in PV-battery system

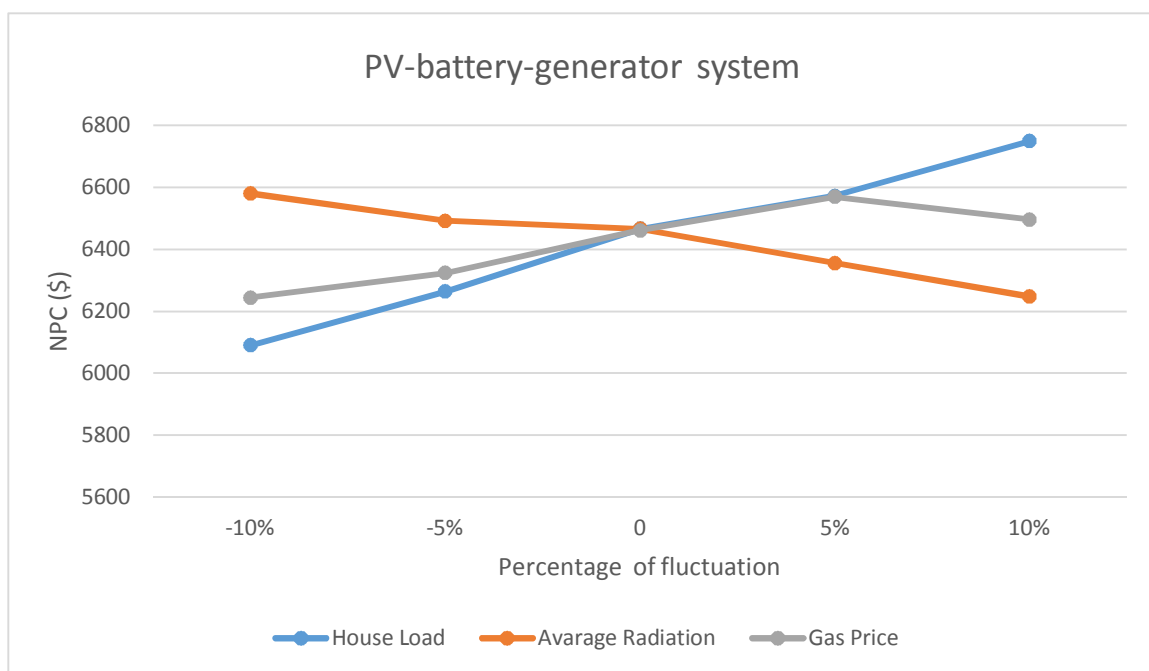


Figure 2.12. Impact of House Load and Average radiation fluctuation on NPC in PV-battery-generator system

A list of research about small-scale RO systems in Iran is presented in Table 2.7 to compare the present study result. Different locations such as Khorasan, Davarzan, and Kish Island are selected to design a RO system with PV panels, wind turbines, hydrogen storage, battery bank storage, diesel generator, and water storage tank. The designed PV-battery-RO system in this study is a double purpose system that can power a house and water desalination system with zero GHG emissions. HOMER Pro software is used for optimization as a precise, easy to use, and flexible method for future changes. The designed system is cost-effective in which net present cost (NPC) and cost of electricity (COE) in the system are \$10,245 and 0.31 \$/kWh, respectively. Moreover, sensitivity analysis confirms that fewer sensitivity variables cause less sensitivity for the PV-battery-RO system in this study.

Table 2.7. Features comparison of proposed scenario with other systems

Authors	System	Location	Optimization Method	Features
Maleki et al. [7]	PV-wind-hydrogen storage-RO	Davarzan, Iran	artificial bee swarm optimization	Large-scale system GHG emission-free Cost-effective and reliable system Sensitivity analysis check
Peng et al. [6]	PV-wind-Battery-RO	Khorasan, Iran	Hybrid Nineteen evolutionary algorithms	Medium-scale system minimizing HRES life cycle cost high reliability Complex optimization method
Esfahani et al. [23]	PV-Water storage tank-RO	Kish Island, Iran	Pinch analysis and genetic algorithm	Small-scale system Large water storage tank Zero required outsourced water Total annual cost of 13,652 \$/year.
Wu et al. [24]	PV-Battery-diesel generator-RO	Khorasan, Iran	Tabu search	Small-scale system GHG emission in the system Cost-effective optimization NPC: \$28,130 , COE: 0.5975 \$/kWh
This study	PV-Battery-RO	Tehran, Iran	HOMER Pro software	Small-scale system Double purposes electrical system GHG emission-free Sensitivity analysis check Cost-effective optimization NPC: \$10,245 , COE: 0.31 \$/kWh

2.5 Conclusions

Hybrid renewable energy systems are among the wide-ranging solutions nowadays for addressing the water scarcity in rural areas. A reverse osmosis water desalination system powered by a small-scale hybrid PV system is the best option for this purpose. In this study, the selected rural house in Iran was precisely surveyed, and two types of daily loads were defined: 5.42 kWh/day primary house load and 1.57 kWh/day deferrable RO load. HRES components are introduced in detail based on the site information. This study suggested two major scenarios for powering the loads to optimization and comparison: (1) Photovoltaic system with battery storage, and (2) Photovoltaic system with battery storage and gas generator. Moreover, two different dispatch strategies, including cycle charging (CC) and load following (LF), were described.

Both scenarios are simulated and optimized in the HOMER Pro software to achieve the most cost-effective solutions. Based on the software's optimization data, although the system with both battery and gas generator has less NPC and initial capital cost around \$6,460 and \$3,260, this scenario use LF dispatch strategy and has yearly 399 m³ natural gas consumption, which cause carbon emission. On the other hand, the PV-Battery-RO system, as a selected scenario in this paper, has fewer O&M costs and zero fuel costs. This system is environmentally friendly with zero carbon emission, has more autonomy by 100 hours working without an electricity source, and has less control complexity due to CC dispatch strategy and fewer components in the system.

The proposed small-scale stand-alone PV-battery system in this study is a double-purpose system that can simultaneously power a rural house and RO system. Cost analysis results with HOMER Pro software indicate that net present cost (NPC) and cost of electricity (COE) in this system are \$10,245 and 0.31 \$/kWh, respectively, which are comparatively lower than designs in other research. Moreover, sensitivity analysis indicates that although both presented scenarios are affected by variation in house load and solar radiation, the PV-battery system is less sensitive because of fewer sensitivity variables than other systems.

Limitations and Future Works

This study proposed different ideas about powering a rural house equipped with the RO system by the hybrid renewable energy systems based on cost analysis optimization. The price of components is fluctuating in Iran, and subsequently, the cost analysis will be affected. Experimental control unit for controlling different aspects of the system, such as the deferrable load and RO unit, is challenging. As a result, a SCADA system for monitoring the critical parameters in the system can be future work. Moreover, as a future study, dynamic simulation of the electrical system can analyze the behaviour of the designed system in various conditions.

References

- [1] N. Wood and K. Roelich, "Tensions, capabilities, and justice in climate change mitigation of fossil fuels," *Energy Research & Social Science*, vol. 52, pp. 114–122, Jun. 2019, doi: 10.1016/j.erss.2019.02.014.

- [2] M. Madziga, A. Rahil, and R. Mansoor, "Comparison between Three Off-Grid Hybrid Systems (Solar Photovoltaic, Diesel Generator and Battery Storage System) for Electrification for Gwakwani Village, South Africa," *Environments*, vol. 5, no. 5, p. 57, May 2018, doi: 10.3390/environments5050057.
- [3] M. A. M. Khan, S. Rehman, and F. A. Al-Sulaiman, "A hybrid renewable energy system as a potential energy source for water desalination using reverse osmosis: A review," *Renewable and Sustainable Energy Reviews*, vol. 97, pp. 456–477, Dec. 2018, doi: 10.1016/j.rser.2018.08.049.
- [4] M. Bdour, Z. Dalala, M. Al-Addous, A. Kharabsheh, and H. Khzouz, "Mapping RO-Water Desalination System Powered by Standalone PV System for the Optimum Pressure and Energy Saving," *Applied Sciences*, vol. 10, no. 6, p. 2161, Mar. 2020, doi: 10.3390/app10062161.
- [5] M. Akorede, A. Oladeji, B. Ariyo, I. Omeiza, and M. Marzband, "Review of Researches on Techno-Economic Analysis and Environmental Impact of Hybrid Energy Systems," *JJEE*, vol. 6, no. 2, p. 78, 2020, doi: 10.5455/jjee.204-1589458540.
- [6] M. Hossain, S. Mekhilef, and L. Olatomiwa, "Performance evaluation of a stand-alone PV-wind-diesel-battery hybrid system feasible for a large resort center in South China Sea, Malaysia," *Sustainable Cities and Society*, vol. 28, pp. 358–366, Jan. 2017, doi: 10.1016/j.scs.2016.10.008.
- [7] W. Peng, A. Maleki, M. A. Rosen, and P. Azarikhah, "Optimization of a hybrid system for solar-wind-based water desalination by reverse osmosis: Comparison of

- approaches,” *Desalination*, vol. 442, pp. 16–31, Sep. 2018, doi: 10.1016/j.desal.2018.03.021.
- [8] A. Maleki, F. Pourfayaz, and M. H. Ahmadi, “Design of a cost-effective wind/photovoltaic/hydrogen energy system for supplying a desalination unit by a heuristic approach,” *Solar Energy*, vol. 139, pp. 666–675, Dec. 2016, doi: 10.1016/j.solener.2016.09.028.
- [9] A. Mostafaeipour, M. Qolipour, M. Rezaei, and E. Babae-Tirkolaee, “Investigation of off-grid photovoltaic systems for a reverse osmosis desalination system: A case study,” *Desalination*, vol. 454, pp. 91–103, Mar. 2019, doi: 10.1016/j.desal.2018.03.007.
- [10] G. D. Pimentel da Silva and M. H. Sharqawy, “Techno-economic analysis of low impact solar brackish water desalination system in the Brazilian Semiarid region,” *Journal of Cleaner Production*, vol. 248, p. 119255, Mar. 2020, doi: 10.1016/j.jclepro.2019.119255.
- [11] S. Hajji, A. Bentamy, N. Mbodji and A. Hajji, "Design and cost optimization of small-scale PV-powered reverse osmosis desalination (case study)," 32nd European Photovoltaic Solar Energy Conference and Exhibit, Jun 2016, pp. 2796-2802, doi: 10.4229/EUPVSEC20162016-6AV.6.9.
- [12] A.M.K. El-Ghonemy, " Small capacity solar-powered desalination units: analysis to inform decision making," *IOSR Journal of Mechanical and Civil Engineering (IOSRJMCE)*, vol. 6, Issue 3 Ver. IV, pp. 114-126, 2016, doi: 10.9790/7388060304114126.

- [13] S. Gorjian and B. Ghobadian, "Solar desalination: A sustainable solution to water crisis in Iran," *Renewable and Sustainable Energy Reviews*, vol. 48, pp. 571–584, Aug. 2015, doi: 10.1016/j.rser.2015.04.009.
- [14] M. Atefeh, L. Taghavi, M. Khani, A. Bayati and M. Sayadi, "Investigation of the quality of drinking water wells in lavasan-e kouchak district," *Environmental Science and Technology*, vol. 18, pp. 53-66, 2016.
- [15] E. Ahmadi, B. McLellan, B. Mohammadi-Ivatloo, and T. Tezuka, "The Role of Renewable Energy Resources in Sustainability of Water Desalination as a Potential Fresh-Water Source: An Updated Review," *Sustainability*, vol. 12, no. 13, p. 5233, Jun. 2020, doi: 10.3390/su12135233.
- [16] iSpring RCC7P-AK Under Sink 6-Stage Reverse Osmosis Drinking Filtration System and Water Softener with Alkaline Remineralization, and Pump. [Online]. Available: <https://www.123filter.com/ac/ispring-6-stage-superb-taste-boosted-performance-under-sink-reverse-osmosis-drinking-water-filtration-with-alkaline-remineralization-rcc7p-ak>. [Accessed: 16-Sep-2021].
- [17] A. Papavasiliou and S. S. Oren, "Supplying renewable energy to deferrable loads: Algorithms and economic analysis," *IEEE PES General Meeting*, 2010, pp. 1-8, doi: 10.1109/PES.2010.5589405.
- [18] T. Salameh, M. A. Abdelkareem, A. G. Olabi, E. T. Sayed, M. Al-Chaderchi, and H. Rezk, "Integrated standalone hybrid solar PV, fuel cell and diesel generator power system for battery or supercapacitor storage systems in Khorfakkan, United Arab

- Emirates,” *International Journal of Hydrogen Energy*, vol. 46, no. 8, pp. 6014–6027, Jan. 2021, doi: 10.1016/j.ijhydene.2020.08.153.
- [19] Y. Alharthi, M. Siddiki, and G. Chaudhry, “Resource Assessment and Techno-Economic Analysis of a Grid-Connected Solar PV-Wind Hybrid System for Different Locations in Saudi Arabia,” *Sustainability*, vol. 10, no. 10, p. 3690, Oct. 2018, doi: 10.3390/su10103690.
- [20] S. Das, A. Ray, and S. De, “Optimum combination of renewable resources to meet local power demand in distributed generation: A case study for a remote place of India,” *Energy*, vol. 209, p. 118473, Jul.2020, doi: 10.1016/j.energy.2020.118473.
- [21] L. O. Aghenta and M. T. Iqbal, “Design and Dynamic Modelling of a Hybrid Power System for a House in Nigeria,” *International Journal of Photoenergy*, vol. 2019, pp. 1–13, Apr. 2019, doi: 10.1155/2019/6501785.
- [22] A. Aziz, M. Tajuddin, M. Adzman, M. Ramli, and S. Mekhilef, “Energy Management and Optimization of a PV/Diesel/Battery Hybrid Energy System Using a Combined Dispatch Strategy,” *Sustainability*, vol. 11, no. 3, p. 683, Jan. 2019, doi: 10.3390/su11030683.
- [23] I. Janghorban Esfahani and C. Yoo, “An optimization algorithm-based pinch analysis and GA for an off-grid batteryless photovoltaic-powered reverse osmosis desalination system,” *Renewable Energy*, vol. 91, pp. 233–248, Jun. 2016, doi: 10.1016/j.renene.2016.01.049.
- [24] B. Wu, A. Maleki, F. Pourfayaz, and M. A. Rosen, “Optimal design of stand-alone reverse osmosis desalination driven by a photovoltaic and diesel generator hybrid

system,” *Solar Energy*, vol. 163, pp. 91–103, Mar. 2018, doi:
10.1016/j.solener.2018.01.016.

Chapter 3.

Design and Dynamic Modelling of a Hybrid PV-Battery System for a House with an RO Water Desalination Unit in Iran

Mohammad Mousavi¹, M. Tariq Iqbal²

^{1,2}Electrical and Computer Engineering Department, Faculty of Engineering and Applied
Science, Memorial University of Newfoundland, St. John's, Canada

A version of the manuscript in this chapter has been accepted as a journal paper in the European Journal of Electrical Engineering and Computer Science (EJECE). As the primary author in this paper, Mohammad Mousavi carried out the research under the supervision of M. Tariq Iqbal as the co-author. The MEng candidate performed the literature review and was involved in system selection, designs, calculations, simulation, and data analysis. Moreover, he prepared the first draft of the paper. The co-author supervised the research by actualization the research ideas, reviewing and correcting the manuscript.

Abstract

Energy crisis and power shortage are major concerns in Iran nowadays, where people experience several blackouts during the day. On the other hand, potable water scarcity is another trend in Iran. In this study, the design and dynamic modelling of a stand-alone hybrid PV-Battery-RO system are discussed for a house in Sinak village, Tehran, Iran. Site characteristics are analyzed in the first part to estimate the house load and deferrable RO load. In the second part, the system has been modelled in HOMER pro software to determine the size of the photovoltaic panels and battery. Moreover, complete electrical details of the system such as system autonomy, unmet load and excess energy have been described. In the third part, dynamic modelling of the small-scale RO unit based on a transfer function is described. The introduced transfer function correctly simulates the system's output flow rate in response to input water pressure variations. Electrical dynamic modelling of the PV- battery system has been designed in MATLAB/Simulink. The results prove that introduced model can simulate the system's behavior in four conditions: normal operating conditions, zero irradiance conditions, maximum irradiance conditions, and net-zero energy conditions. The battery supports the system, and PV arrays power the loads with a fixed and stable voltage and frequency in all the conditions.

Keywords — Dynamic modelling, HOMER Pro, PV-battery system, Renewable energy, RO system

Nomenclature

P	Feed water pressure
F	Output water flow rate
C	Output water conductivity
I_{ph}	Light generated power
I_d	Diode current
I_0	Diode saturation current
V_d	Diode voltage
V_T	Thermal voltage equivalent
A	Diode ideality factor
K	Boltzmann constant
T	Cell temperature
q	Electron charge
N_{cell}	Number of cells in a PV module
V_{pv}	PV output voltage
I_{pv}	PV output current
P_{pv}	PV output power
D	Switch duty cycle
K_{batt}	Polarization constant
Q	Maximum battery capacity
it	Extracted capacity in battery
i^*	Low frequency current dynamic
V_{dc}	DC bus voltage
G	Switch gate signal
m_a	Amplitude modulation index
m_f	Frequency modulation index
SOC	State of charge

3.1 Introduction

Fossil fuel consumption has increased in the past decades proportional to population growth and required energy for industries. Nowadays, 66% of electricity generation and 81% of the world's energy are based on fossil fuel-driven resources, which produce greenhouse gas emissions (GHG) and subsequently increase global warming. Moreover, the sustainability of fossil fuels is not possible as it is predicted that oil, natural gas, and coal resources will last for approximately 40, 60, 200 years, respectively [1]. The best solution to address these problems is renewable energy sources, mainly solar and wind energies, producing sustainable energy. A typical renewable energy system, which can be stand-alone or grid-connected, consists of renewable technology like a wind turbine or photovoltaic panel, storage elements, and conventional generators. Due to numerous advantages of renewable energy systems like stability, and being environmentally friendly, it is expected that they generate 25% of the world's electricity in 2040 [2].

Water scarcity is as important as the energy crisis in modern societies because only 3% of the world water is potable water, and 97% is ocean water or non-accessible fresh water. Based on the World Health Organization (WHO) standards, the Total Dissolved Solids (TDS) should be less than 500 ppm for drinking water. For most regions globally, especially in the rural areas, the TDS is not in the acceptable range, which can cause illnesses and immunity system problems in children [3]. A promising solution to the water scarcity problem is water desalination, which is the process of removing salt and other inappropriate ingredients from the ocean or well water and produces fresh water. Among various water desalination methods, Reverse Osmosis (RO) method is more popular in

small-scale systems due to low energy consumption and cheaper technology. The RO process mainly consists of injecting pressurized water into a membrane to trap unwanted ingredients [4].

With a total area of about 1,600,000 m² and 300 clear sunny days in a year, Iran is among countries with the promising potential to harvesting solar energy. Iran is located between the latitude of 25 to 40 degrees north and has average solar radiation of 2200 kilowatts hours per square meter. Only 1% of the land with 10% solar system efficiency can produce 90 million MWh daily energy in Iran. The largest solar power plant in Iran is in Mallard, Tehran, and other small-scale solar systems are located in Shiraz, Semnan, Taleghan, Yazd, and Khorasan [5]. Iran, which is ranked as the 17th most populated country, is among 10 top water-stressed countries globally. Water stress in Iran is because of population growth and uneven rainfall pattern with an average of 250 mm, which is less than one-third of the global average. Renewable water resources in Iran were less than 1700 cubic meters per person per year in 2017 and decreasing rapidly. As a result, because of the availability of solar energy, generating electricity by a Photovoltaic (PV) system to produce fresh water by the RO desalination method can reduce stress on various sections in Iran [6].

Banat et al. [7] designed a small-scale PVRO desalination plant for a village in the northern part of Jordan. Their system consists of 30 PV panels, 2 panels in series and 15 strings in parallel, with the capacity of 1.623 kW power, two batteries with the specification of 230 Ah 12 Volts, charge regulator, softener, pumps and RO unit. They proved that this system has a capacity of 0.5 m³/day to meet the village's potable water requirement.

Feasibility and cost analysis of off-grid PVRO systems for 9 different districts of Bushehr in Iran is presented in [8] by Mostafaeipour et al.. They used HOMER and Excel software to analyze the systems, and results showed that electricity production of the PV system for Delvar and Deylam ports is 72,336 and 47,915 kWh per year, respectively. Moreover, the daily maximum of 228 m³ and minimum of 148 m³ of potable water can be produced for these two ports in a reasonable cost manner.

A small-scale PVRO system can produce desalinated water for a village or a group of houses because PV panels produce enough energy to power a small-scale RO system. In a different configuration, the PV panels can power a small-scale RO unit and the house. Haratian et al. [9] investigated a PV- battery off-grid system for a laboratory in Khomeinishahr University, Iran, with a total load of daily 3 kWh. They used HOMER software to optimize the size of the system, and results suggested that a PV-battery system with 1.2 kW PV arrays and 6 units of 3 kW batteries is the most economical solution. The net present cost of the system is \$8173, and the cost of energy is 0.546 \$/kWh. A rooftop PV system for a residential house in East Azerbaijan province, Iran, is another example analyzed by Mirzaei Darian et al. [10]. Using RETScreen Expert software, they suggested the designed system comprises 15 320 watts PV panels and 5 kW inverter can produce 8373 kWh/year. They projected the experimental results in this study and proved that the payback period for the system is 5.3 years. Aminy et al. [11] designed a grid-connected PV-battery system for a rural house in Meshkin-Dasht, Karaj, Iran. In this study, the system with 11 45 watts PV panels, 2 batteries with a specification of 12 Volts and 120 Ah batteries, and 2, 700W inverters can power a 2.88 kWh daily load.

The most critical part of designing a PV system is analyzing the system's dynamic behaviour to check output parameters. Iqbal et al. [12] designed and analyzed a stand-alone PV system for a rural house in Pakistan. They used HOMER software for system sizing, and the software suggested that a system with 5.8 kW PV panels, 8 batteries of 12 V, 255 Ah, and a 1.4 kW inverter can power a daily 10.28 kWh load. MATLAB/Simulink was used to check the system's dynamic behaviour. Results showed that the system could provide a stable voltage and frequency for the load with the Perturbation and observation (P&O) Maximum Power Point Tracking (MPPT) algorithm. Jayalakshmi et al. [13] simulated a stand-alone PV system for a residential application in MATLAB/Simulink. Their simulation consists of solar energy resource, PV arrays, MPPT controller, battery storage, bi-directional DC-DC converter with controller, PWM inverter with controller, and loads. The designed system can control the voltage and frequency of the load.

In this study, a photovoltaic battery system is designed for powering a rural house equipped with a reverse osmosis water desalination unit in Iran. The major difference of this study with other research in the region is that the PV-battery system can power the house load and RO load simultaneously. Rest of the paper consists of the following major sections:

- (2) Site characteristics such as location specification, solar energy resource, and electrical and water system configuration are described. Moreover, load sizing is determined.
- (3) System sizing is done based on the optimization method with HOMER Pro software to achieve the lowest cost option.

- (4) Dynamic modelling of the small-scale RO unit is described based on the transfer function model to check the response of the desalination unit to input variations.
- (5) The next section proposes system's electrical dynamic simulation in MATLAB/Simulink. Complete system components are designed to check the dynamic behaviour of the PV battery system. Moreover, the MPPT controller, battery Charge controller and PWM inverter controller are explained in this section
- (6) In the last section, results and discussion are presented to check the validity of the simulation. Solar tracking system performance, battery parameters such as SOC, current, and DC voltage, output parameters of the system such as load voltage and current are shown.

3.2 Site Specifications and System Configuration

3.2.1 Site Location

Tehran, the capital of Iran, is in the north of the country. Because of job opportunities, there is a remarkable migration trend to this province, which caused a high amount of air and water pollution. Mainly the rural migrated population prefers to stay in small towns or rural areas around Tehran city, which is more affordable. The selected site in this project is a rural house, depicted in Figure 3.1, located in the Sinak village in Lavasanat District, Shemiranat County, Tehran Province, Iran, with a latitude $35^{\circ}51'06.1''$ N and longitude $51^{\circ}41'14.3''$ E. Four people live in this village house, and their water source is well water for all purposes. They use pumps and tank to store the well water as are shown in Figure 3.2. Moreover, like most rural areas in Iran, the house electrical system is isolated powered by a fossil fuel generator. Heating and cooking are based on oil and natural gas

because of their availability and low price. As a result, a small PV system can power the house because a small electrical load for this house mainly consists of lighting, electricity for appliances, and water pumping.



Figure 3.1. Different views of the selected house in Sinak village



Figure 3.2. Well water system elements in the house

3.2.2 Solar Energy Source

The selected Site in Sinak village has a remarkable irradiance because of its elevation. According to the database from NASA's prediction of worldwide energy resources, the annual average radiation is $4.89 \text{ kWh/m}^2/\text{day}$ with a maximum and minimum of $7.35 \text{ kWh/m}^2/\text{day}$ and $2.38 \text{ kWh/m}^2/\text{day}$, respectively. Temperature data of the site is another parameter is affecting the efficiency of the PV system. The data from the NASA database indicates the annual average temperature for the selected site is $12.63 \text{ }^\circ\text{C}$ with a maximum of $23.88 \text{ }^\circ\text{C}$ and a minimum of $0.58 \text{ }^\circ\text{C}$. The monthly radiation and temperature, and clearness index are shown in Figure 3.3.

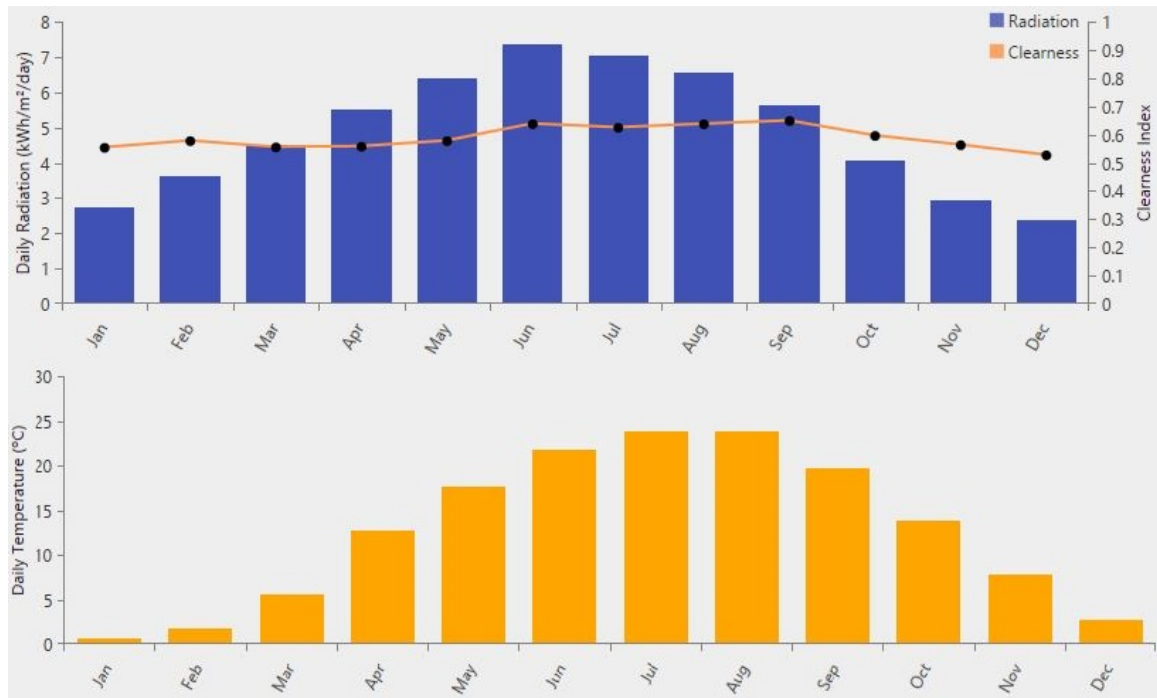


Figure 3.3. Monthly solar radiation, temperature, and clearness index in Sinak village

3.2.3 Water System Configuration and RO Load

A reverse osmosis water desalination system design is mainly based on the characteristic of brackish source water and desalinated output water. The current water system configuration on the house consists of a submersible pump located in the well at a depth of 25 meters from the ground and can pump water up to 38 meters. Pumped water from the well will be stored in the atmospheric tank at the height of 3 meters above ground with a capacity of 1000 litres. Finally, a jet pump pressurizes the water in the tank and supplies the house. The concept of adding an RO unit to the house is to provide desalinated water only for drinking and cooking in this research, not to design a unit for all purposes. The benefit of this system is less power consumption, which is doable regarding the

existing water system configuration. The proposed water system configuration is depicted in Figure 3.4. According to this configuration, an average daily 1500 liters water consumption will be passed through the jet pump for washing and cleaning and daily 100 liters desalinated water pass through pressure pump, RO membrane, and pressure tank for cooking and drinking.

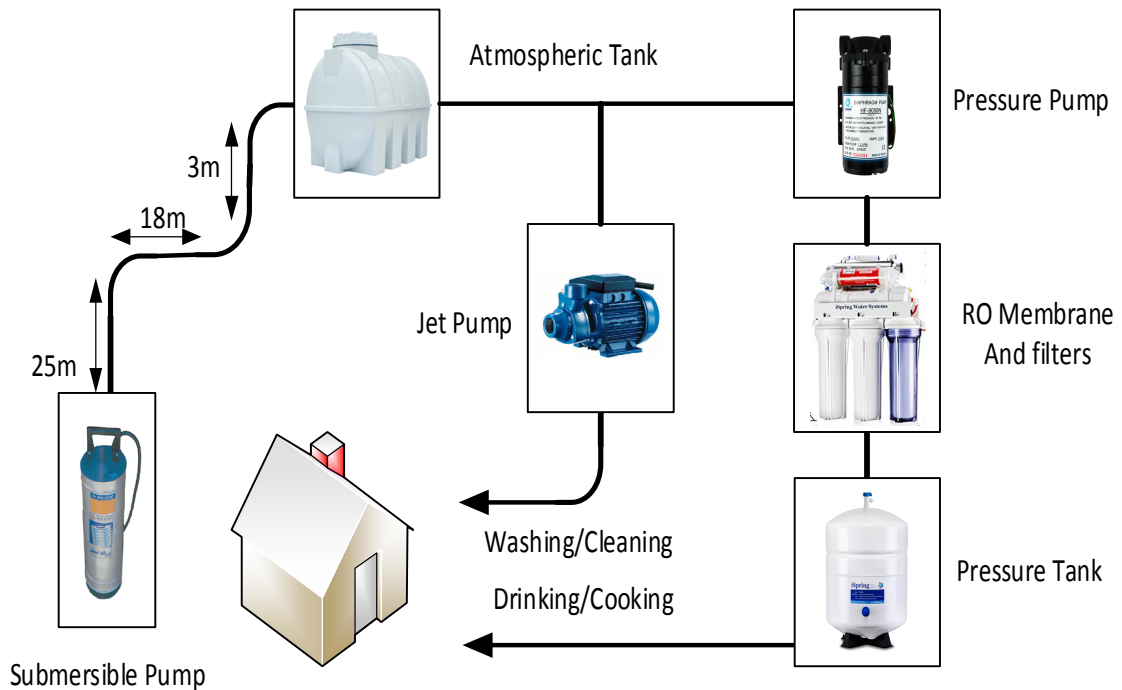


Figure 3.4. The proposed water system configuration for selected site

ISpring RCC7P-AK is the multiple-stage filtration RO unit selected for this research with 75 gallons desalinated water capacity per day [14]. The pressure pump is 60 watts PMP5 Booster pump with the specification of 24V and 2.5A input power. Reverse osmosis membrane, GAC filter, and CTO filter can remove different chemicals, and in the last

stage, T32M 3.2 gallon pressure tank increase the output water pressure for better performance.

To calculate electrical RO load, all electrical elements in the water system considered as the RO load. This assumption will let to model the RO load as the deferrable load. The deferrable load requires a certain amount of power, but the exact timing is not restricted. In other words, the deferrable load can be powered when surplus energy exist in the system. As a result, the daily energy requirement of the submersible pump, jet pump, and pressure pump should be calculated. Based on the specification of the submersible pump, for pumping 1500 litter water, it needs to operate 30 minutes per day. The pump power rate is 1100 watts, and subsequently, the daily energy for this pump is 0.55 kWh. The jet pump needs to operate one hour per day to provide high-pressure water for washing and cleaning, and as its power rate is 470 watts, daily energy consumption is 0.47 kWh. The pressure pump's daily energy requirement should be calculated to provide 110 litters (10% margin) desalinated water. Pressure pump wattage is 60 watts, and RO capacity is 75 GPD. The energy can be calculated by Equation 3.1.

$$\begin{aligned} \text{Pressure pump daily energy consumption} &= \text{daily GPD} \times \text{time for 1 GPD} \times \\ \text{pump wattage} & \end{aligned} \tag{3.1}$$

$$= \left(\frac{110}{3.785} \right) \left(\frac{24}{75} \right) 60 \cong 0.55 \text{ kWh}$$

Finally, the total daily deferrable RO load is:

$$E_{ro} = 0.55 + 0.47 + 0.55 = 1.57 \text{ kWh / day} \tag{3.2}$$

3.2.4 Electrical system configuration and the house load

The electrical system describes various elements and control units involved in transferring energy in solar radiation form to the electrical loads. The system configuration in a typical hybrid power system mainly consists of photovoltaic panels, DC/DC converter, storage element, DC loads, DC/AC converter, and AC loads. The proposed PV system in this study is a stand-alone hybrid PV battery system. The battery storage system can increase the system's reliability without adequate PV power production for the loads. There are no DC loads, and there are two types of AC loads in the electrical system. Control units in the electrical modelling of the system are as crucial as the power stage of the system because they can monitor and maintain important parameters in the system. Output parameters control of the PV, storage element control, and output parameters control of the system are the main control parts of hybrid power systems.

Like most rural houses in Iran, there is no metering system in the house, and the best solution for calculating the house load is listing various appliances in the house with their daily used time. Table 3.1 is prepared based on the site survey and shows the daily energy consumption of each appliance. The results indicate that the house load is approximately 5.42 kWh per day.

Table 3.1. Daily energy consumption of various appliances in the house

Household appliances	Rated watts (watt)	Timed used (hour)	Daily energy consumption (kWh)
Refrigerator	150	8	1.2
Wall-mounted gas boiler	140	6	0.84
Light bulb - Common*2	200	3	0.6
Light Bulb - LED*38	266	2	0.532
Laptop	50	8	0.4
TV 42" LCD	120	3	0.36
Extractor Fan*2	40	8	0.32
Microwave	900	0.3	0.27
Home internet router	10	24	0.24
Vacuum cleaner	900	0.2	0.18
Home phone	6	24	0.144
Light bulb - LED*6	72	2	0.144
Washing machine	200	0.3	0.06
Cooker hood	140	0.4	0.056
Blender	400	0.1	0.04
Electric meat grinder	350	0.1	0.035
Electric shaver	15	0.2	0.003

3.3 Optimum Sizing of the PVRO System in HOMER Pro

Various factors affect the designing of a hybrid power system, such as renewable resources in the selected site, system configuration, size of the components, type of the loads, the life cycle of the system, environmental factors, efficiency and reliability of the designed system. Moreover, cost aspects of the system such as overall cost of the system, net present cost, and maintenance cost are important. Hybrid Optimization of Multiple Energy Resources (HOMER) software is used in this research for system sizing. HOWER

Pro software offers the appropriate configuration based on the optimization method and considering cost analysis of the system, environmental factors, and maximum renewable fraction. The software mainly calculates the hourly cost of energy production and compares various configurations to select the cost-effective optimized system [15]. The designed PVRO system in HOMER software is depicted in Figure 3.5, mainly consisting of PV panels, battery storage, inverter, house load, and deferrable load.

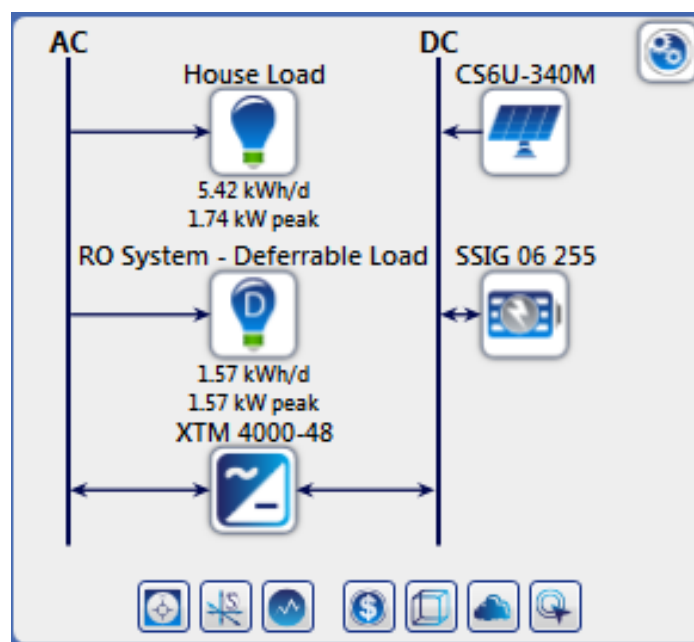


Figure 3.5. PV-battery-RO system in HOMER Pro

The selected PV panel for this study is CS6U-340M from the CanadianSolar manufacturer, with 340 watts power rating and 17.49% efficiency. The storage is the lead-acid Trojan battery, SSIG-06-255, with a maximum capacity of 255 Ah under the nominal voltage of 6 volts. Based on the calculation, the daily average of house load is 5.42 kWh/day with a peak of 1.74 kW, and the deferrable RO load is 1.57 kWh/day. Moreover, a 4 kW inverter is considered to connect the DC bus to the AC bus. It is noticeable that the rated power is 20% more than the peak loads' total wattage. Cost details of each component

are imported to extract the most effective optimized results from the software. Figure 3.6 illustrates the electrical specifications and size of the proposed system by HOMER software simulation.

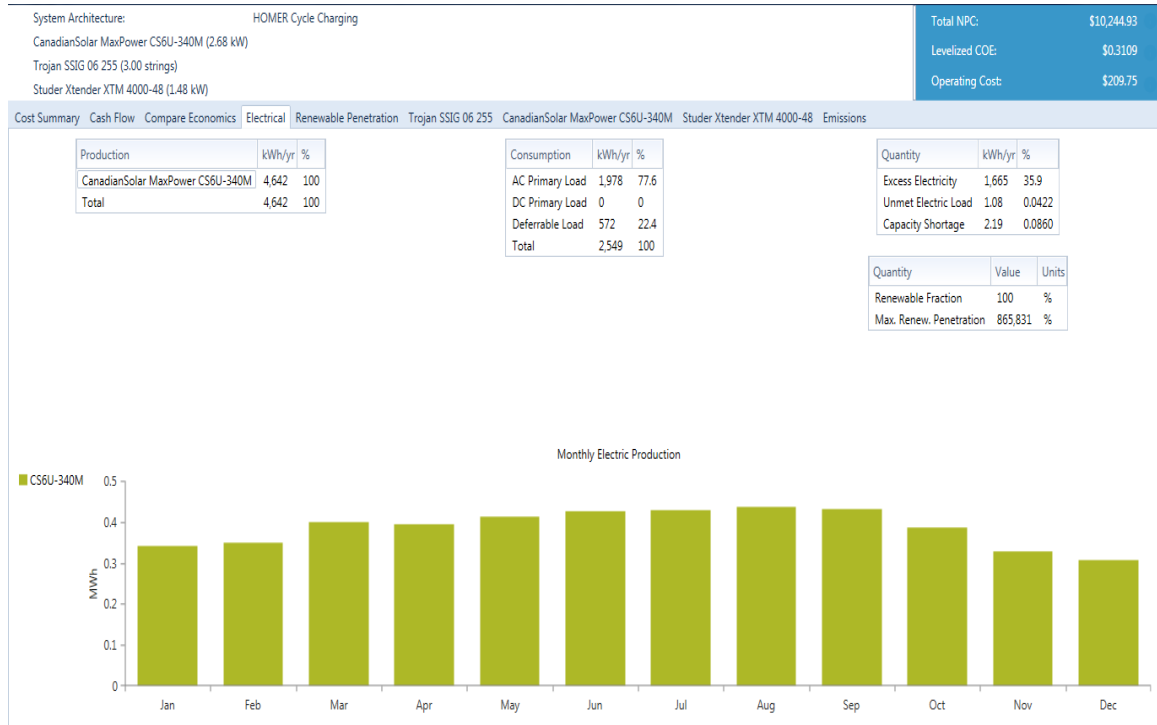


Figure 3.6. Electrical specifications and size of the proposed system by HOMER Pro

According to the results, the HOMER software suggests 2.68 kW of 340 watts solar panels, 8 panels in real system installation with yearly 4,642 kW energy production. 24 6-volts, 255 Ah Trojan battery in 3 strings are connected to the 48 volts DC bus to reduce the DC current. The battery system's total capacity and the annual throughput are 765 Ah are 1,579 kWh, respectively. Moreover, the battery system autonomy is 100 hours, and as a result, the system can power the loads for more than 4 days without renewable resources. A converter of 1.48 kW will be enough to meet the load, and the dispatch control strategy is cycle charging in this system. The system has a 100% renewable fraction, which means the system is environmentally friendly with zero carbon emissions. Based on HOMER

software calculation, the total yearly load of the system is 2,549 kWh, which the shares of house load and deferrable RO load are 77.6% and 22.4%, respectively. Moreover, excess electricity and unmet loads are 1,665 and 1.08 kWh, 35.9% and 0.042%, respectively. The unmet load percentage indicates that the system is designed and sized efficiently. Finally, the software shows that total net present cost, Levelized cost of energy, and operating and maintenance cost are 10,244.93 US\$, 0.3109 US\$, and 209.75 US\$, respectively.

3.4 Dynamic Modelling of Small-scale RO unit

3.4.1 RO Unit Modelling (Transfer Function-Based)

Water desalination in reverse osmosis unit is based on the process in which pressure pump increases water pressure to a point greater than the osmotic pressure of water. The desalination process in the RO method is energy-intensive, and a good control method of the unit will decrease water production cost and increase system efficiency and availability. As a result, arranging linear dynamic modelling of the RO unit is essential due to applying control techniques to the system model [16]. RO Unit is a multi-input multi-output (MIMO) system in which various output parameters can be affected by different inputs. Figure 3.7 depicts a general diagram of the reverse osmosis plant in conjunction with inputs/outputs of the system [17]. As the diagram shows, the pre-treatment filter, high-pressure pump, membrane assembly, and post-treatment filter are the main parts of the RO unit. Moreover, feed water PH (PH), feed water pressure (P) are input parameters of the dynamic model, and output water flow rate (F) and conductivity (C) are the output parameters of the model.

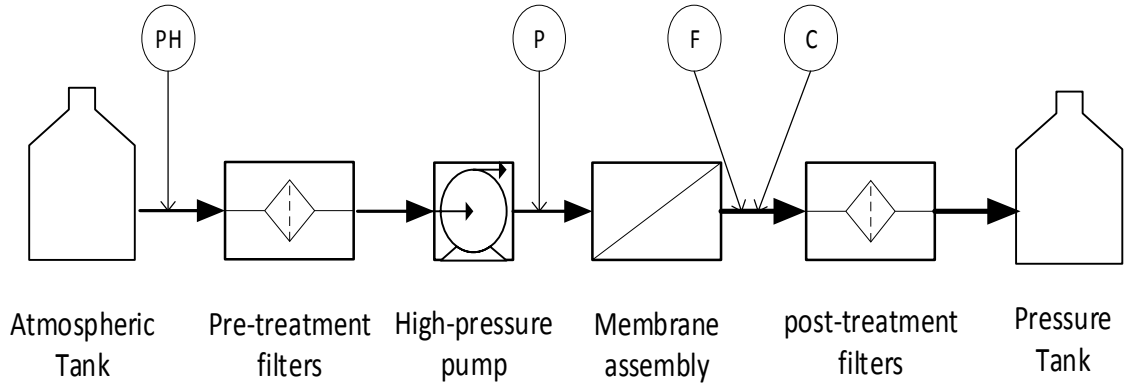


Figure 3.7. General diagram of a reverse osmosis plant

In industrial plants, the system's model obtains by identifying a time-discrete model in z-domain and transformation to s-domain. A transfer function matrix can model the RO unit as there are two inputs and two outputs in the system. As Equation 3.3 shows, each output parameters of the system, which are flow rate and conductivity, are a function of feed water pressure and PH, and the system is generally open-loop stable because each subsystem of the model is stable. Based on the linear models in research, each transfer function in the matrix can be achieved by fitting a second-order transfer function in the form of Equation 3.4 [18]. The transfer function-based model selected for this study is presented in Equation 3.5 according to the model in [19].

$$\begin{bmatrix} F \\ C \end{bmatrix} = \begin{bmatrix} G_{11} & G_{12} \\ G_{21} & G_{22} \end{bmatrix} \times \begin{bmatrix} P \\ PH \end{bmatrix} \quad (3.3)$$

$$G_{ij}(s) = \frac{K_{ij}(\tau_{ij}s + 1)}{\tau_{ij}^2 s^2 + 2\zeta_{ij}\tau_{ij}s + 1} \quad (3.4)$$

$$\begin{bmatrix} F \\ C \end{bmatrix} = \begin{bmatrix} \frac{0.007(0.056s+1)}{0.213s^2+0.7s+1} & 0 \\ \frac{-7.3(0.35s+1)}{0.213s^2+0.7s+1} & \frac{-57(0.32s+1)}{0.6s^2+1.8s+1} \end{bmatrix} \times \begin{bmatrix} P \\ PH \end{bmatrix} \quad (3.5)$$

In this research, the output flow rate is the desired output to analyze. On the other hand, for the selected site, water PH is close to 7 and stable. Therefore, while modelling the RO unit, PH is not considered a variable, and only G11 can describe the relationship between feed water pressure (psi) and output flow rate (GPM). Mentioned transfer function in Equation 3.5 is based on the specific range of input and output of a plant. By some modification related to the RO unit in this study, Equation 3.6 describes the transfer function.

$$G_{11} = \frac{F}{P} = \frac{0.000392s + 0.0007}{0.213s^2 + 0.7s + 1} \quad (3.6)$$

3.4.2 Simulation and Result

Transfer function model of the RO unit defined in MATLAB to check the validity of the proposed model. The selected RO unit in this research is a 75 GPD unit with sufficient input pressure of 30-70 psi pressure. In other words, the unit can process feed water with a maximum pressure of 70 psi to produce maximum desalinated water with a 0.052 GPM flow rate. Decreasing the input pressure by changing the switch on the pressure pump can decrease the output flow rate, which means less water production or more working hours for a certain amount of output water. Different amounts of input pressure applied to the transfer function model of the system and output flow rates are depicted in the Figure 3.8. The results indicate that the transfer function precisely models the dynamic of the RO unit.

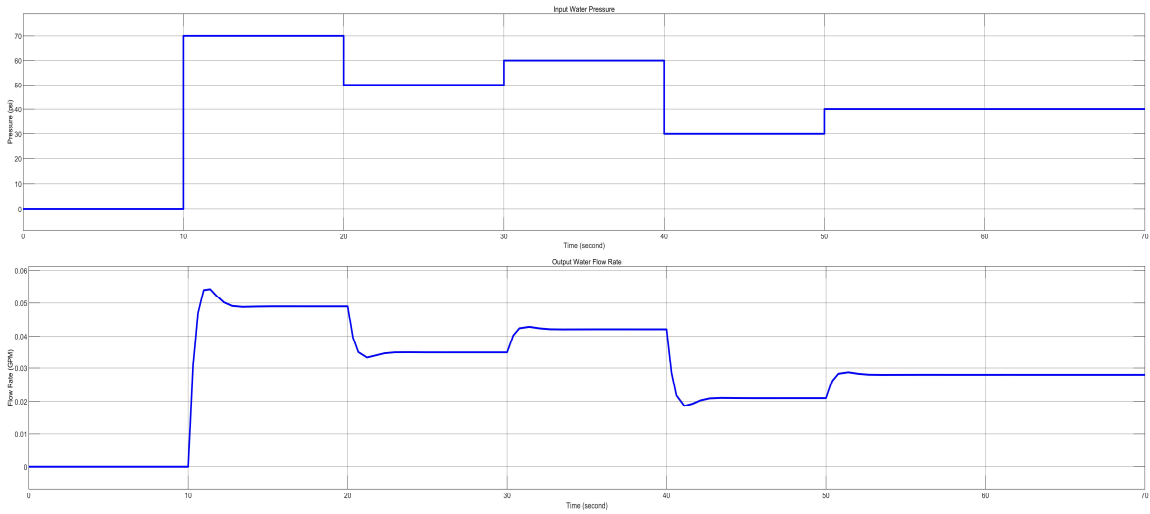


Figure 3.8. RO unit parameters: (a) input pressure (b) output flow rate

3.5 Electrical Dynamic Modelling and Simulation of the Proposed PV System in MATLAB/Simulink

Electrical dynamic modelling of the PV hybrid system is necessary because a well-designed model can simulate the system's behaviour to any changes in input parameters. Moreover, the model can predict the response of the system to any external turbulences. Figure 3.9 shows the overall block diagram of the proposed PV battery system. The block diagram shows that the electrical system mainly consists of photovoltaic panels and a non-Inverting buck boost converter to transfer solar energy to the DC bus in designed DC voltage. Battery storage can store extra energy or deliver stored energy to the system. PWM inverter and step-up transformer convert and adjust DC power for the loads in proper AC voltage and frequency. There are three control units in this research: (1) MPPT controller helps the system to extract maximum power from PV panels (2) CCCV charge controller is responsible for controlling DC bus voltage and check the battery charging procedure. (3)

Inverter controller regulates PWM inverter output voltage and frequency. Moreover, there are two different RO and house loads in the system. In the following, each subsystem is described in detail, and the overall system is simulated in MATLAB/Simulink based on the system sizing results in previous sections.

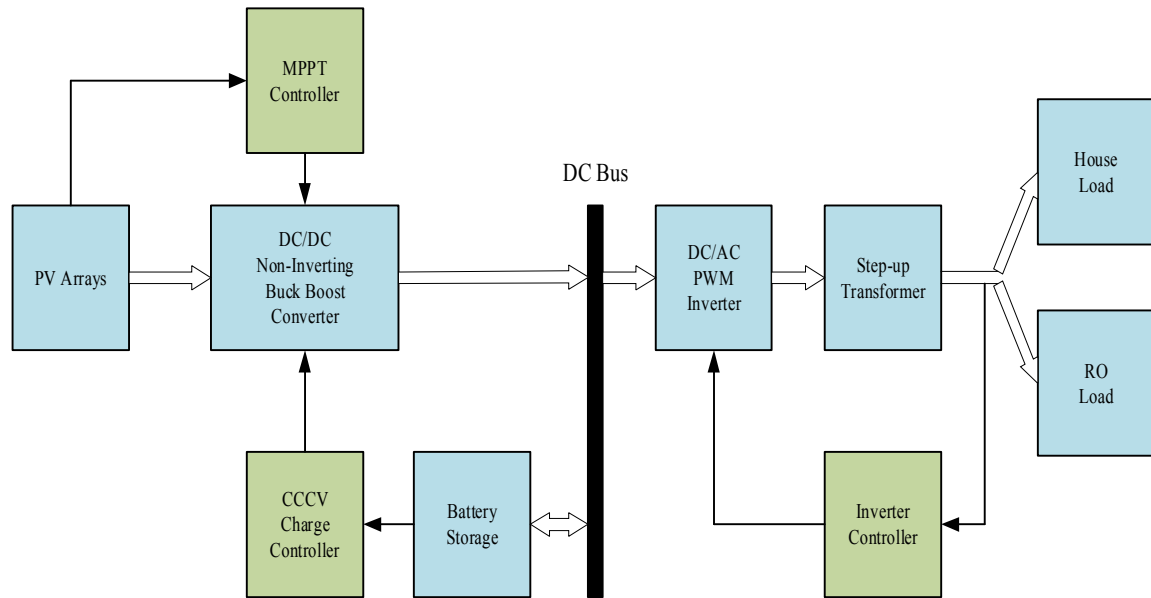


Figure 3.9. General block diagram of the proposed PV battery system

3.5.1 PV Arrays

PV modules are a fundamental component in a PV system, which converts solar radiation to electricity directly by absorbing photons of light and releasing electron charges. PV modules have nonlinear output parameters affected by environmental factors such as irradiance and temperature. PV arrays consist of several modules connecting in series and parallel and every module consists of series PV cells, a PN junction diode with a reverse direction current. A PV module model can be a single diode or two diode model, and a

single diode is selected for this research as depicted in Figure 3.10 [20]. This model comprises a current source, a diode, shunt resistance R_{sh} , and series resistance R_s .

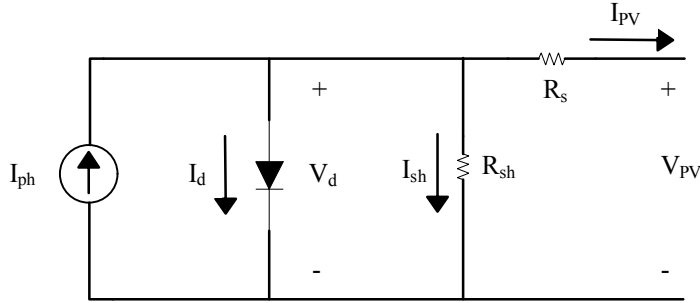


Figure 3.10. Single diode model of a PV module

The output mathematical expression of the module is projected in Equations 3.7 to 3.10 [21]. In these equations, I_{ph} is the light-generated current, I_d is the diode current, I_0 is the diode saturation current, V_d is the diode voltage, V_T is thermal voltage equivalent, A is the diode ideality factor, K is the Boltzman constant equal to 1.3806×10^{-23} J/K, T is the cell temperature, q is the electron charge equal to 1.602×10^{-19} C, and N_{cell} is the number of cells connected in series in a module. Moreover, V_{pv} and I_{pv} are module voltage and current, respectively.

$$I_d = I_0 \left[\exp\left(\frac{V_d}{V_T}\right) - 1 \right] \quad (3.7)$$

$$V_T = \frac{KT}{q} \times A \times N_{cell} \quad (3.8)$$

$$V_d = V_{pv} + R_s I_{pv} \quad (3.9)$$

$$I_{PV} = I_{ph} - I_d - \frac{V_d}{R_{sh}} \quad (3.10)$$

As the equations show, all the output parameters of a PV module, like the voltage, current, and power, vary by irradiance and temperature variations. In this research, based on the results of the HOMER software, the PV arrays consist of 4 strings of Canadian Solar CS6U-340M panel in parallel with 2 series panels in each string. Output power is $4 \times 2 \times 0.34 = 2.72$ kW, and the output voltage at maximum power point is $2 \times 37.9 = 75.8$ V.

3.5.2 Non-Inverting Buck-Boost Converter

Stabilizing the output of a PV panel to deliver maximum power of the panel in various temperatures and irradiance is a major concern in hybrid PV systems. On the other hand, an appropriate battery charger is needed to store excess energy in the battery system in stand-alone systems. In this study, a non-inverting buck-boost (NIBB) DC-DC converter feeds the inverter and charges the battery system in fix and stable 48 volts DC bus. Numerous topologies can be used for DC-DC converters, such as buck converter and inverting buck-boost converter. They have drawbacks like having pulsation in input current and output opposite polarity, respectively. In addition to maintaining the polarity of output voltage, NIBB can operate as a boost converter to step up or buck converter to step down the voltage level of the PV, which makes it a great option for a renewable hybrid system. Because of the low complexity, fewer components, low voltage stress, high reliability, switch and inductor low losses, and low cost of the topology, the NIBB (cascaded buck-boost) converter has become popular for PV applications. Figure 3.11 shows NIBB topology [22].

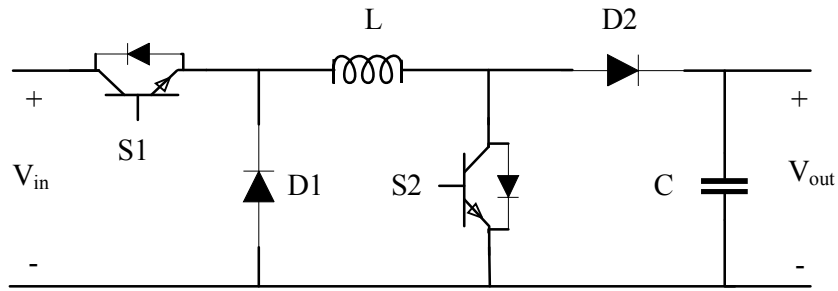


Figure 3.11. Non-inverting buck boost converter topology

As the topology shows, two PWM switches, S1 and S2, control the non-inverting buck-boost converter. According to any combination of switches' status, different operation modes of the converter can be achieved. Table 3.2 describes the converter operation modes: (1) NIBB operates as the buck converter, if S1 switching with D₁ and S2 is off, (2) NIBB operates as boost converter if S1 is on and D₁ is equal to 1 and S2 switching with D₂, (3) NIBB operates as buck-boost converter if S1 and S2 switching with D₁ and D₂, respectively [23].

Table 3.2. NIBB converter operation modes

Operation Mode	S1	S2
Buck	D1	D2=0
Boost	D1=1	D2
Buck Boost	D1	D2

The output voltage of the converter is given by Equation 3.11 [23]. It is noted that the following guidelines need to be considered for designing the control signals: Both PWM signals should have the same frequency, D₂ should be always smaller than D₁, PWM signal

of S1 must be enabled before PWM signal of S2, and PWM signal of S1 must be disabled after PWM signal of S2 [22].

$$V_{out} = \frac{D_1}{1 - D_2} V_{in} \quad (3.11)$$

NIBB converter is mainly used as a battery charger in most research and applications while the same PWM signal is fed to the switches. For instance, in [24], the authors designed a battery charger based on the NIBB converter for a PV system controlled by a two-stage voltage and current control. They claimed that the charger could work in either buck mode or boost mode in various environmental conditions for PV panels with different batteries. In [25], a system consists of 10 watts PV panel, NIBB converter, DC load, and a battery is designed, and a prototype approved the results. The most important factor in increasing the efficiency of a PV system is designing an MPPT to extracting maximum power from the panel. In [26], a microcontroller, NIBB converter, a DC load, and lead-acid battery were integrated into a system to show that the selected converter can perform the MPPT technique. In this study, NIBB operates as a battery charger and can deliver maximum power from the panel to the DC bus. In other words, the generated signal from the MPPT algorithm is used to control D_1 , and generated signal from the battery charger algorithm is used to control D_2 . In MATLAB simulation, a filter is added at the converter's final stage to achieve a smaller output voltage ripple.

3.5.3 Battery System

The main drawback of a stand-alone renewable system is the unpredictability feature of the renewable sources. This feature increases the unreliability of renewable systems

because the output power fluctuates according to environmental factor fluctuation. Storage systems, especially battery systems, are introduced to renewable systems to supply unmet loads in the system. The battery bank is a bi-directional element that stores excess energy produced by PV panels in the charging procedure and delivers stored energy to the load in the discharge procedure when the generated power by PV panels cannot supply the load. In this study, the battery is not simulated separately, and the battery block from Simulink is selected. The generic dynamic model that governs lead-acid batteries in MATLAB is based on two Equations 3.12 and 3.13. In this model, E_0 is constant voltage (V), K is polarization constant (V/Ah), Q is maximum battery capacity (Ah), it is extracted capacity (Ah), i^* is low frequency current dynamics (A), i is battery current (A), A is exponential voltage (V), and B is exponential capacity (1/Ah) [27].

$$E_{discharge} = E_0 - K_{batt} \cdot \frac{Q}{Q-it} \cdot i^* - K_{batt} \cdot \frac{Q}{Q-it} \cdot it + Laplace^{-1} \left(\frac{Exp(s)}{Sel(s)} \cdot 0 \right) \quad (3.12)$$

$$E_{charge} = E_0 - K_{batt} \cdot \frac{Q}{it + 0.1 \cdot Q} \cdot i^* - K_{batt} \cdot \frac{Q}{Q-it} \cdot it + Laplace^{-1} \left(\frac{Exp(s)}{Sel(s)} \cdot \frac{1}{s} \right) \quad (3.13)$$

$$\frac{Exp(s)}{Sel(s)} = \frac{A}{1/(B \cdot i(t) \cdot s + 1)} \quad (3.14)$$

The selected battery for this research is a lead-acid Trojan SSIG-06-255 battery, and based on the HOMER results, 24 batteries can fulfill the system backup task. Nominal DC voltage is designed to be 48 volts, and each battery is 6 volts; as a result, 3 strings of batteries and 8 series batteries in each string are required. The total capacity of the battery bank is $3 \times 255 = 765$ Ah, which is defined in the MATLAB model.

3.5.4 MPPT Controller

PV array's P-V and I-V curves are affected by environmental factors such as temperature and irradiance continuously, and subsequently, output parameters of the panel would be affected. PV has a maximum power point (MPP), which is important for the panel to work at this operating point. Maximum power point tracking (MPPT) is a process in which an algorithm forces the panel to work on its optimum operating point to extract maximum power. There are numerous MPPT techniques, such as perturb and observe (P&O) method or incremental conductance method, but in this research, the P&O method is selected due to its simplicity. This method is based on the perturbation of the power by continuously increasing or decreasing the panel's voltage. The P-V curve in Figure 3.12 describes the P&O technique. There are two types of operation points (OP) in this graph. For any OP like point 1 on the left side of the MPP, the voltage should be increased, and for any OP like point 2, the voltage should be decreased [28].

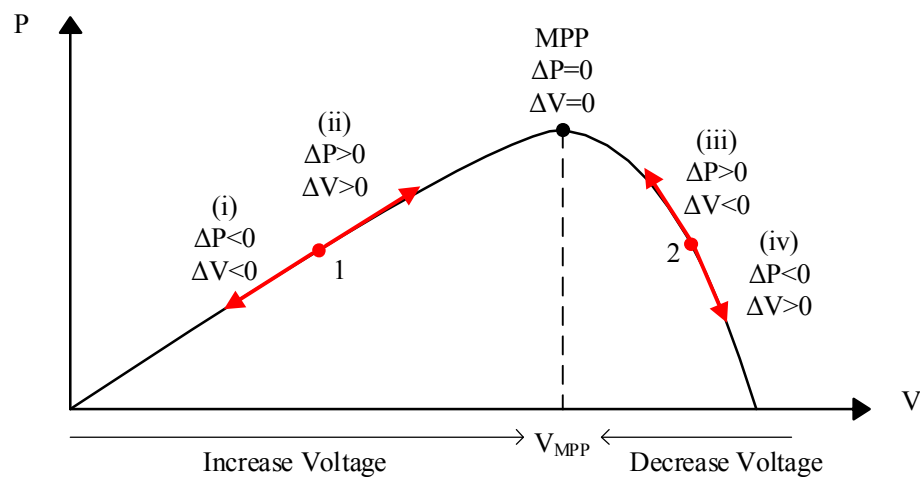


Figure 3.12. P&O MPPT technique principle

To implementing the P&O method in MATLAB, a code-based function is defined according to the flowchart in Figure 3.13. Inputs of the MPPT are voltage and current of the PV measured by the sensors, and the algorithm's output is the duty cycle. The duty cycle will be used to generate a PWM signal applying to the buck switch in the NIBB converter to control the voltage. Any change in the duty cycle means changing the panel's output voltage and, subsequently, changing the output power. Based on the flowchart, a small perturbation on the duty cycle changes the output power in the first step, and MPPT calculates the panel's output power. As a result of this perturbation, ΔP and ΔV determine the next step of the algorithm. If ΔP is zero, the system is working on the MPP, and no other changes are required. If ΔP and ΔV both have the same sign (positive or negative), the MPPT will increase the voltage by adding ΔD to the duty cycle and again, it will check the parameters. If ΔP and ΔV have different signs (positive and negative), the MPPT will decrease the voltage by deducting ΔD from the duty cycle. The process will be repeated until the MPPT controller reaches the maximum power point.

3.5.5 CCCV Battery Charge Controller

As the battery storage is added to the PV system to increase reliability, a battery charge controller should be considered to control the battery charging process. Normally, the constant current constant voltage (CCCV) method is used in small applications due to its simplicity and easy implementation, as it is selected in this research. This study's designed CCCV battery charge controller consists of three main sections: voltage controller, current

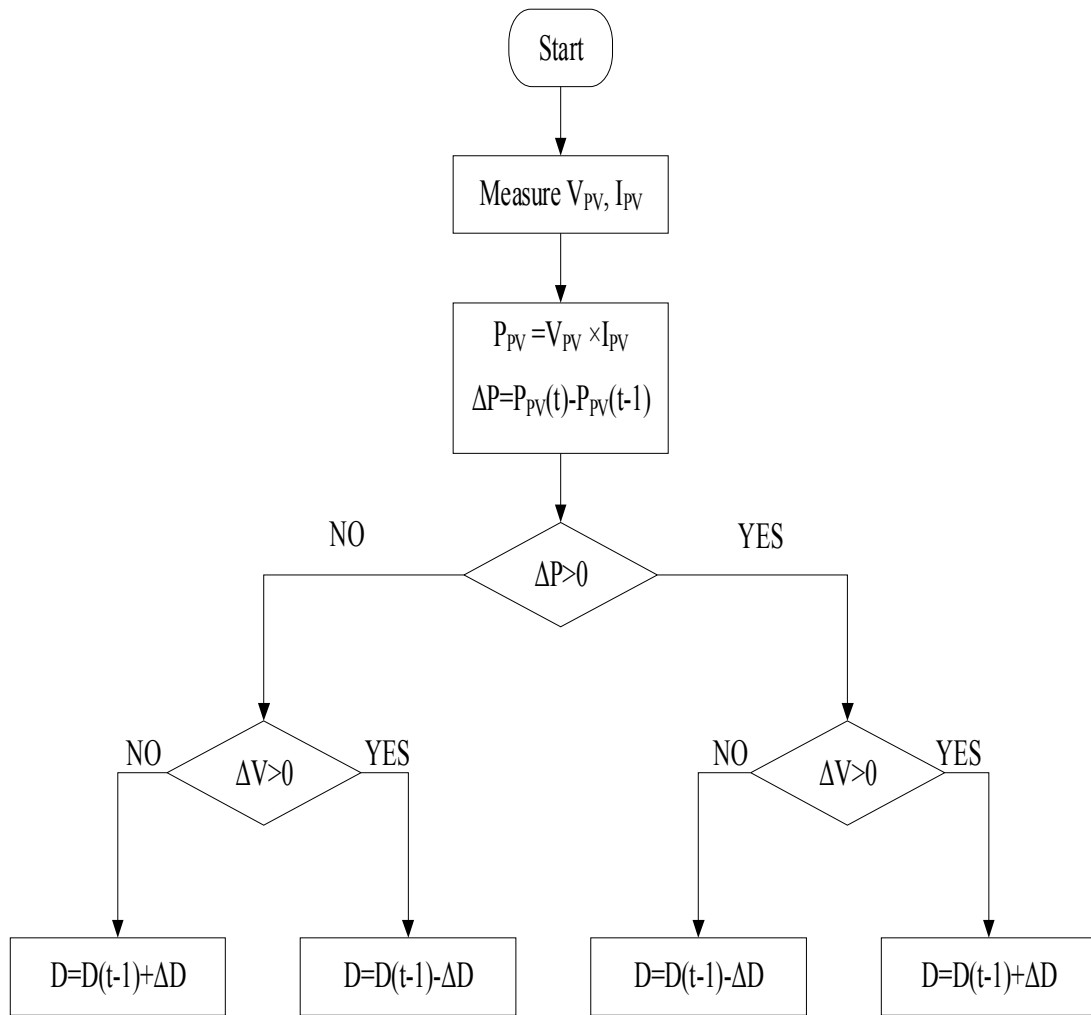


Figure 3.13. P&O method flowchart

controller, and CCCV code-based function to perform the algorithm. Figure 3.14 illustrates the battery charging profile. Based on this graph, the charging process in the CCCV method has two stages. At the initial stage, which is the constant current (CC) zone or bulk stage, CCCV charges the battery in constant current, referred to as bulk current, while voltage increases. The controller charges the battery until approximately 80% of the state of charge (SOC), where the battery reaches its open-circuit voltage. After this point, the battery voltage will be constant, and the current starts to decrease. The second stage is the constant

voltage (CV) or abortion stage, and the battery current drops until float current [29]. Based on this principles and charging curves, the MATLAB code in this project is designed to receive battery parameters like voltage and current and generates reference signals to decide the stage of the operation for the CCCV battery controller.

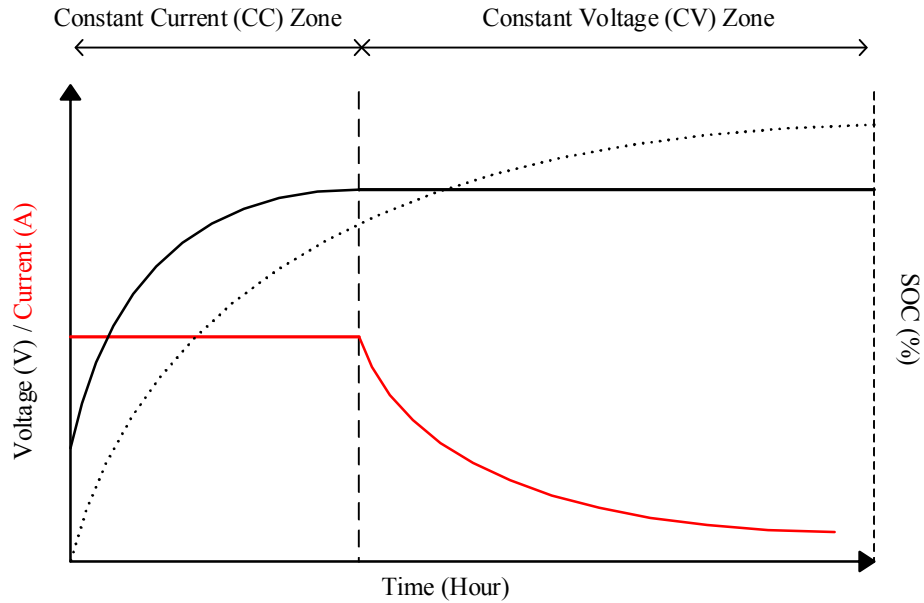


Figure 3.14. Lead-acid battery charging profile in CCCV charging method

The other two parts of the CCCV charge controller, the voltage controller and current controller, are designed to convert reference signals to appropriate PWM signals based on selected batteries for the boost switch in the NIBB converter. According to Figure 3.15, both voltage and current controllers have the same structure to generate PWM signals. In the current controller, the reference signal will be compared with the maximum charge current, which is 13% of the maximum capacity of the selected battery based on the datasheet. In the voltage controller, the reference signal will be compared with the

absorption voltage of the PV array, which is $4 \times 14.7 = 58.8$ volts, according to the datasheet [30]. The results of both comparisons go to the PI controller, and in the final step, a PWM generator will generate the switch signal [31].

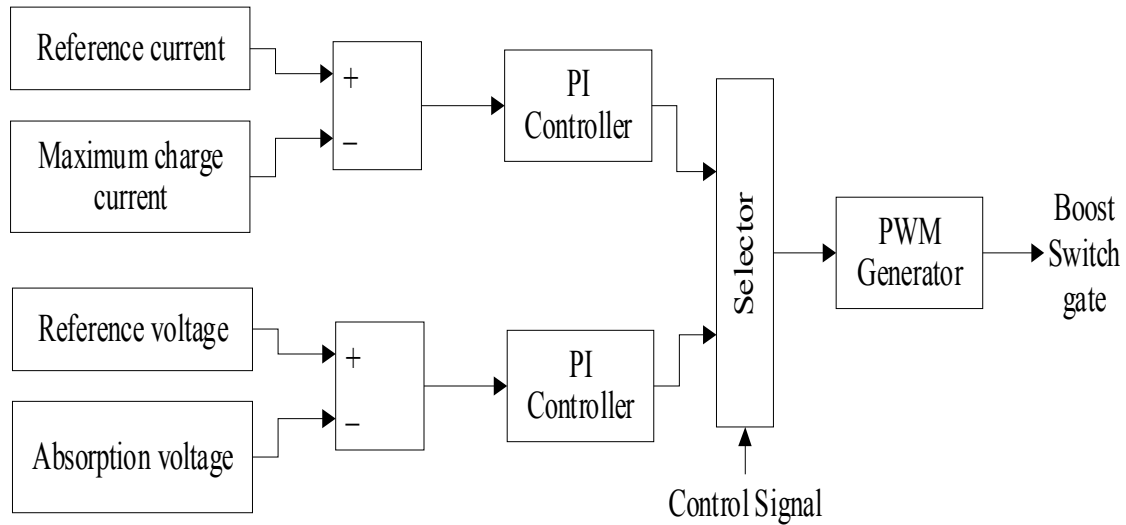


Figure 3.15. Voltage and current controller in CCCV charging method

3.5.6 Inverter

An inverter converts the output DC voltage of the NIBB converter to a single-phase AC voltage with appropriate magnitude and frequency. The inverter in this study is an H-bridge inverter with a symmetrical output, and its name is from the specific graphic of the circuit, which is depicted in Figure 3.16. The single-phase voltage source inverter comprises two similar legs with two isolated gate bipolar transistors (IGBTs) and two diodes in each leg. As the DC bus voltage is 48 volts, the inverter output is designed to have a 48 volts magnitude and 50 Hz frequency. Sinusoidal pulse width modulation (SPWM) switching technique controls the gate of four switches S1, S2, S3, and S4, by

generating four signals G1, G2, G3, and G4. When the switches S1 and S4 are closed, and S2 and S3 are open, $+V_{dc}$ appears across the load. By closing S2 and S3 switches and opening S1 and S4, $-V_{dc}$ appears across the load. Two switches in one leg of a full-bridge inverter should not be closed simultaneously due to the short circuit across the input source [32]. Table 3.3 describes the switching modes and output voltage of the inverter.

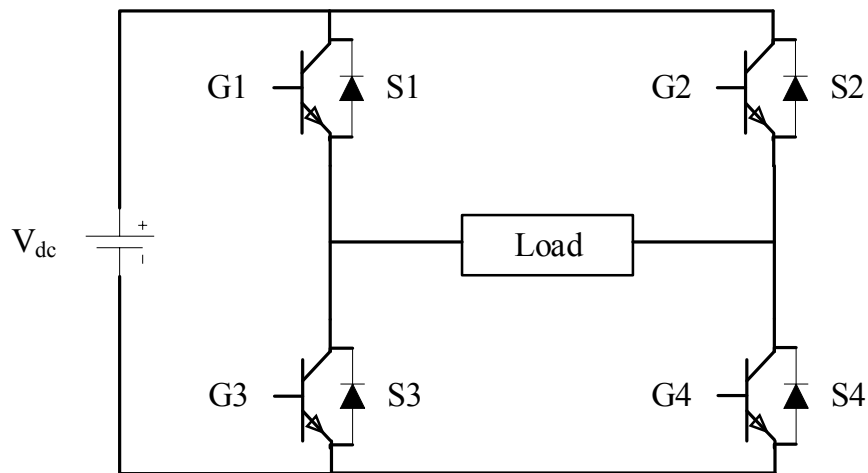


Figure 3.16. Single-phase H-bridge inverter topology

Table 3.3. Switching modes and output voltage in the inverter

Switches Mode	Voltage Level
S1, S4 ON / S2, S3 OFF	$+V_{dc}$
S2, S3 ON / S1, S4 OFF	$-V_{dc}$

3.5.7 Inverter Voltage Controller

One of the main purposes of the single-phase inverter is to fix the amplitude and frequency of the output voltage because the output parameters of the inverter can be easily

affected by changes in input voltage. A closed-loop voltage controller is designed in this project to control the output voltage of the system. As depicted in Figure 3.17, the inverter controller has two connected parts: voltage regulator and SPWM generator. The regulator maintains the RMS of the system's output voltage in constant value, 220 volts in this study. The system's output voltage goes to an RMS block, and the result will be compared with reference RMS voltage to generate an error. The error is fed to a PI controller to produce DC quantity. This DC signal will be used as a DC carrier for the next part [33].

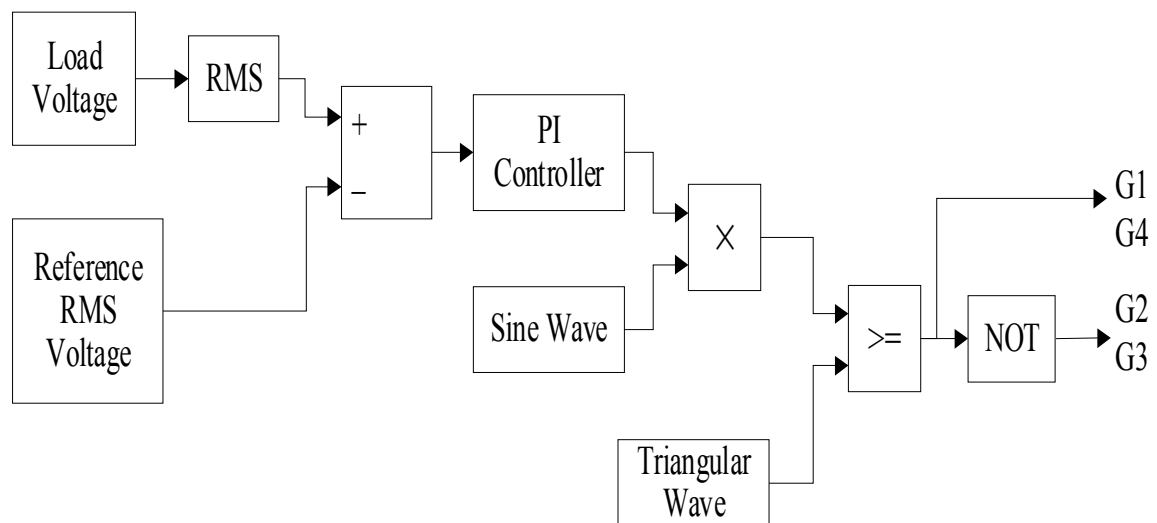


Figure 3.17. Inverter voltage controller

SPWM generator is responsible for creating appropriate signals for inverter switch's gates. Different type of SPWM methods exists like bipolar switching method and unipolar switching method, and bipolar switching method is selected due to its simplicity. In this method, the DC carrier multiplies by a sinusoidal wave known as the reference signal. In the final stage, the sine wave is compared with a triangular wave signal, and the output

signal goes to switches S1 and S4. Simultaneously, this signal passes through a NOT gate to control switches S2 and S3. In the SPWM technique, there are two important factors in designing the system: amplitude modulation index and frequency modulation index. These two factors are defined in Equations 3.15 and 3.16. The frequency of the inverter output voltage fundamental component is equal to the sine wave signal frequency (f_0), and its amplitude is $m_a \times V_{dc}$. It is noted that the first harmonic frequency of output voltage is equal to $m_f \times f_0$ [34].

$$m_a = \frac{V_{m,reference}}{V_{m,carrier}} \quad (3.15)$$

$$m_f = \frac{f_{carrier}}{f_{reference}} \quad (3.16)$$

3.5.8 Transformer

To deliver converted power at the inverter's output terminals to the AC house load and RO load, the magnitude of the inverter output voltage should be increased at the same frequency. In this research, a single-phase step-up transformer increases the 48 volts output voltage of the inverter to 220 volts RMS voltage with 60 Hz frequency. A transformer is an electrical device with two windings, which can either increase or decrease the voltage level connected to the primary side by changing the magnetic field. The windings are separated by a magnetic core that provides electrical isolation between primary and secondary sides [35]. In an ideal transformer, the exact power applied to the primary side will be transferred to the secondary side. As the Equation 3.17 indicates, by increasing the voltage level of the primary side in constant power, the output current in the secondary side

will be decreased [27]. Nominal power for the transformer block in MATLAB is selected equal to the maximum output power of the PV arrays, which is $8 \times 340 = 2720$ watts.

$$\frac{N_p}{N_s} = \frac{V_p}{V_s} = \frac{I_s}{I_p} \quad (3.17)$$

3.5.9 Load Model

As described and modelled in previous chapters, there are two different loads in this study: regular house load and deferrable RO load. A regular house is a load that exists all the time, and the designed hybrid PV system is responsible for powering it. This load mainly consists of appliances' power usages listed in the Table 1.1. Although not all the appliances are running simultaneously, an average of 1000 watts resistive load is considered the house load to check the system's response. On the other hand, the deferrable RO load is a type of load that the system is responsible for supplying whenever extra generated energy exists. In other words, the system's priority is to serve the house load and then deferrable RO load. Based on the RO load sizing, 1100 watts resistive load is selected as deferrable RO load. A breaker added to the load model to model the loads and priority concept, as depicted in Figure 3.18. This breaker is open when generated power by the PV arrays is less than the house load, and the breaker will be closed if the PV power generates excess energy.

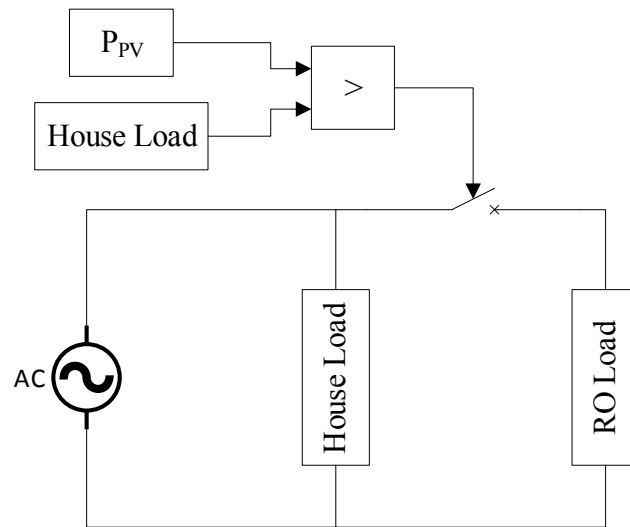


Figure 3.18. Load model for the PVRO system in MATLAB/Simulink

3.6 Simulation Results and Discussion

Dynamic modelling of the proposed hybrid PV-battery-RO system simulated in MATLAB and complete Simulink model is depicted in Figure 3.19. All the subsystems modelled in the previous chapter separately are included in one uniform model to check the behaviour of the different parameters of the system to various conditions. Figures 3.20 and 3.21 show the solar data applied to the system, including the irradiance (W/m^2) and the temperature ($^{\circ}\text{C}$). Figure 3.22 and 3.23 depict the output voltage and current of the PV arrays based on the designed solar data. Figure 3.24 shows output PV power, and Figure 3.25 depicts the DC link voltage. Figures 3.26 and 3.27 illustrate the output AC voltage and current (load parameters) of the system. Finally, Figures 3.28, 3.29, and 3.30 show the state of charge (SOC), battery current, and voltage, respectively. According to the graphs, results can be categorized in four different conditions as stated in the following.

Condition 1: In this condition, which is between 0 to 0.5 seconds, the solar irradiance and the temperature are 400 W/m^2 and $25 \text{ }^\circ\text{C}$, and the system is working in normal conditions. The output voltage of the PV is approximately 75.8 volts, and the PV current is 14.5 A. The output PV power precisely follows the MPP around 1100 watts, which means the P&O algorithm is working well, and the DC voltage link is close to 48 volts, as expected. Output load voltage RMS is acceptable around 220 voltage with 60 Hz frequency, which means the inverter voltage controller operates perfectly. The load current is close to 9.5 A, and because PV power is more than house load power, the load switch is closed, and the system supply both house and RO load. In this condition, the battery is discharging as SOC decreases, battery current is positive around 21 A, and the battery voltage decreases.

Condition 2: This condition, which is between 0.5 to 1 second, mimics situations in which there is no irradiance like nighttime or cloudy day. As Figure 20 shows, the irradiance is zero, and subsequently, the output voltage, current, and power are zero. DC voltage is close to 48 volts, and load voltage is 220 volts RMS with 60 Hz frequency. In this scenario, the load tends to discharge the battery with more current in the absence of the PV generation, but the load switch will disconnect the RO load the total system load decreases from 2100 watts to 1000 watts. This load changing causes the battery discharge current to be similar to the previous condition, close to 20 A.

Condition 3: Between 1 to 3 seconds, which is the third condition, the system experience zero to maximum irradiance and will work in this condition for a period. During a short period, Output PV voltage returns to 75.8, and the DC voltage is around 48 volts.

As the irradiance increases, the PV arrays' output current increases from zero to approximately 36 A, and the output PV power reaches its maximum, which is 2.72 kW. Figure 3.24 shows the MPPT system follow the power curve. Around 1.3 seconds, the PV power generation is more than the house load, and the load switch connects the RO load, and the total load current will be increased from 4.5 A to 9.5 A. In this time, the battery current, which was started to be decreased, will be increased again. Approximately in time 1.85 seconds, the battery current crosses the zero point, which means the battery charger starts charging the battery. The charger operates in CC mode, and the voltage will be increased. At the end of this condition, the battery current is negative 8.5 A.

Condition 4: In this condition, between 3 to 5 seconds, the PV arrays experience a net-zero energy condition. Firstly, the irradiance will be reduced to 900 W/m^2 , and then the temperature will be increased to $50 \text{ }^\circ\text{C}$. As expected, the output PV voltage drops to 68.5 volts and the output power will be decreased. PV current, DC voltage, load voltage, and currents are the same as the previous condition. At time 4.5 seconds, as the Figure 29 shows, the battery current is approximately zero, which means all PV arrays generation will power the house-RO load. The SOC and battery voltage are constant, and the system experience a net-zero energy condition.

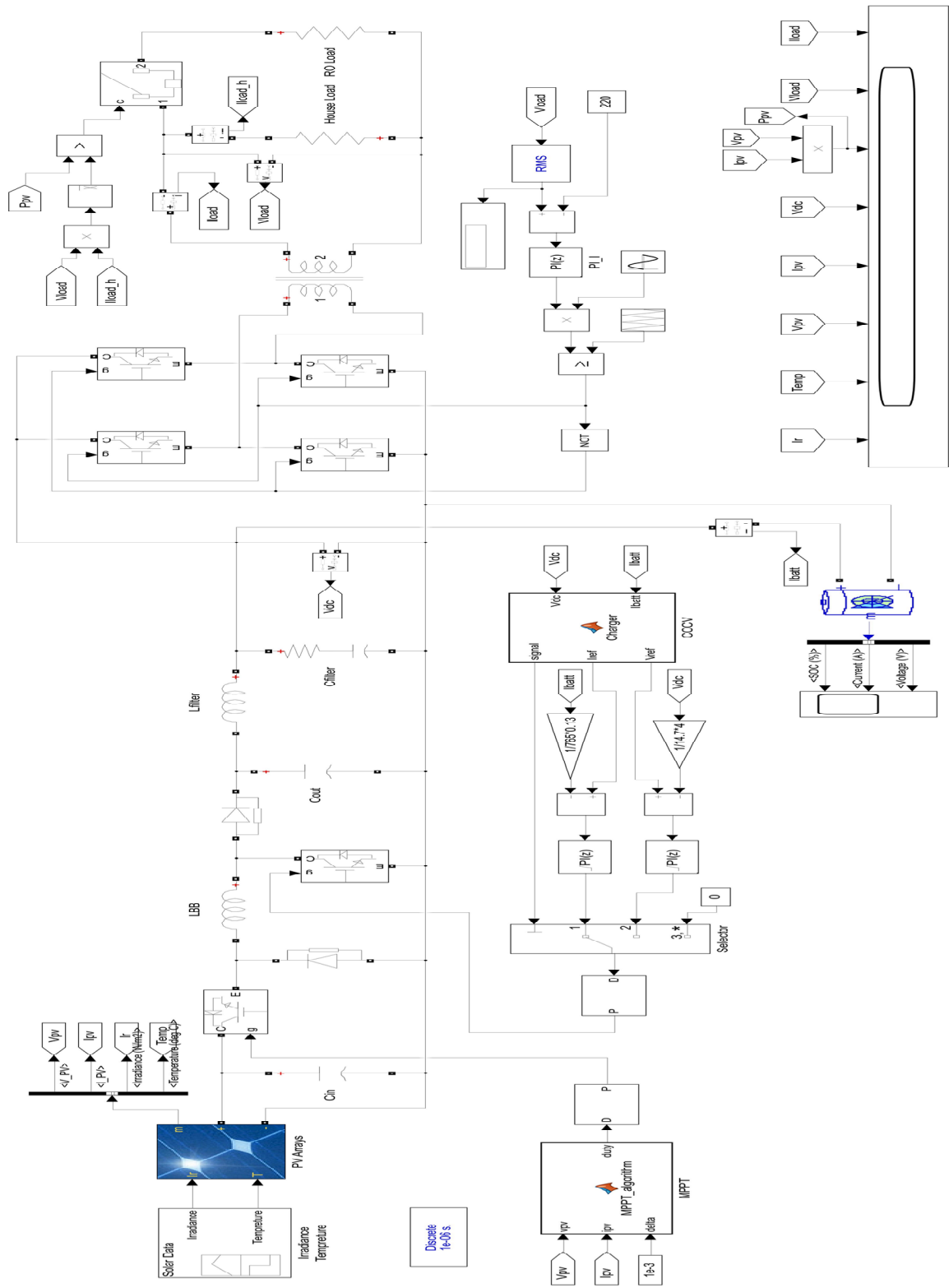


Figure 3.19. MATLAB/Simulink model for the proposed PV-battery system

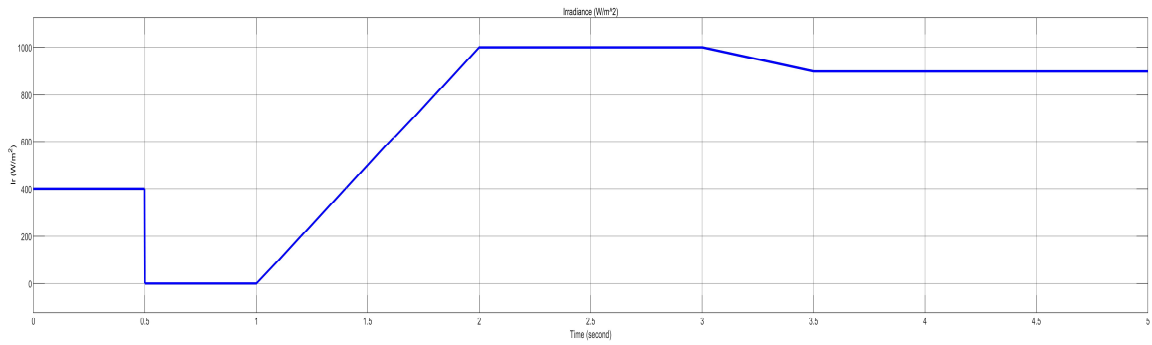


Figure 3.20. Solar Irradiance applied to PV arrays (w/m2)

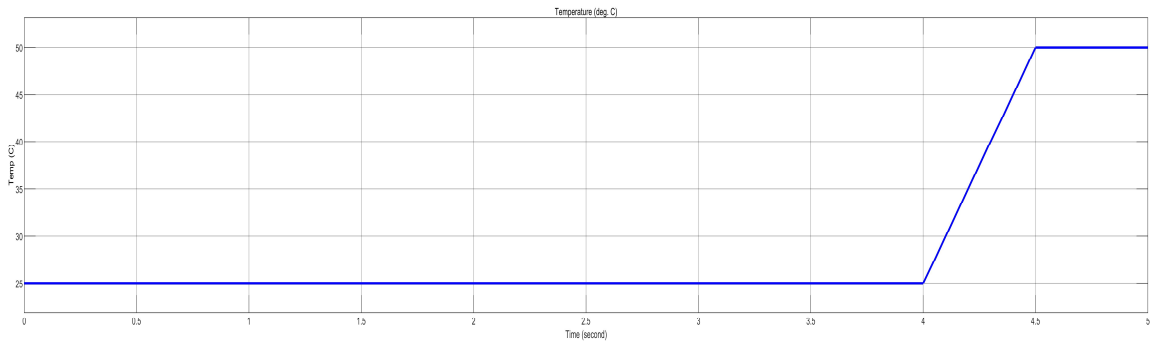


Figure 3.21. Temperature applied to the PV arrays (°C)

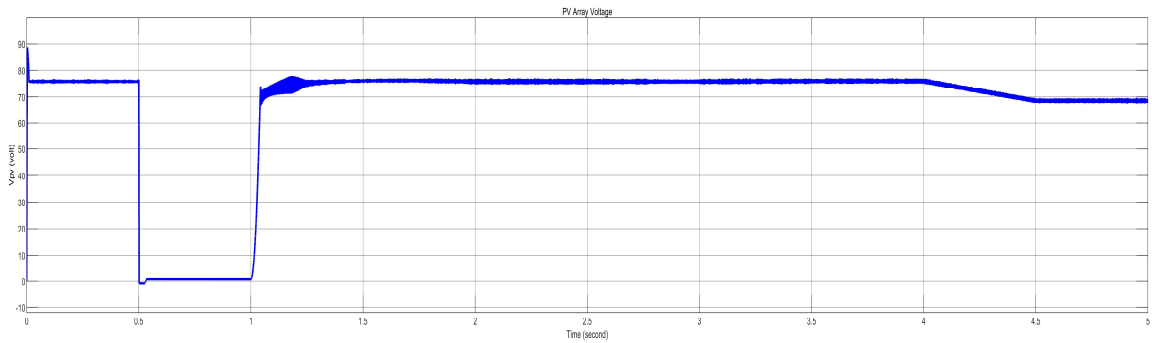


Figure 3.22. PV arrays output voltage

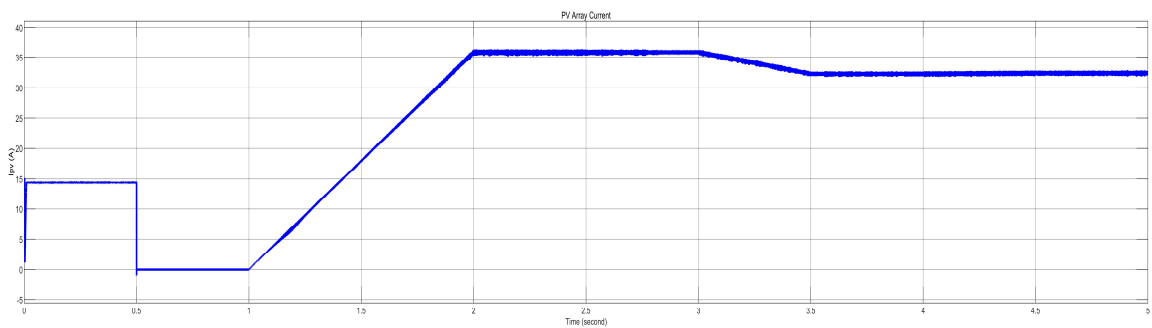


Figure 3.23. PV arrays output current

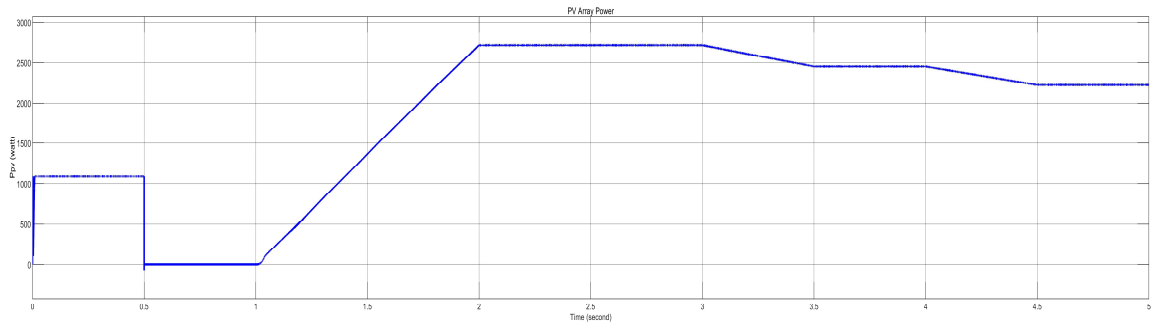


Figure 3.24. PV arrays output power

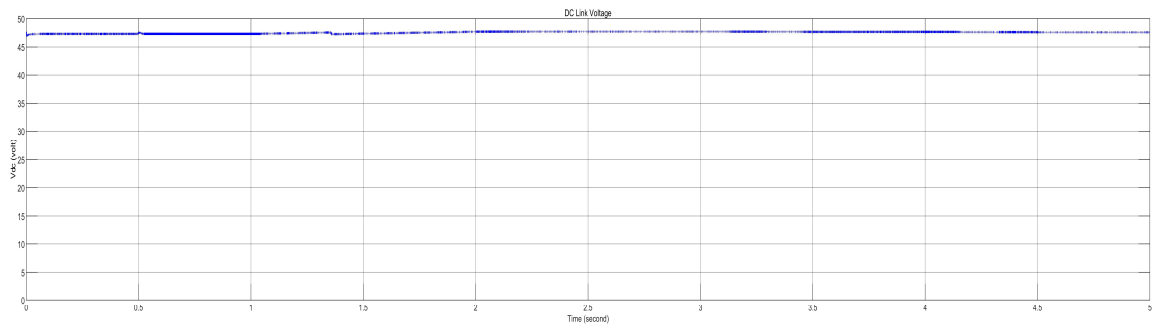


Figure 3.25. DC link voltage

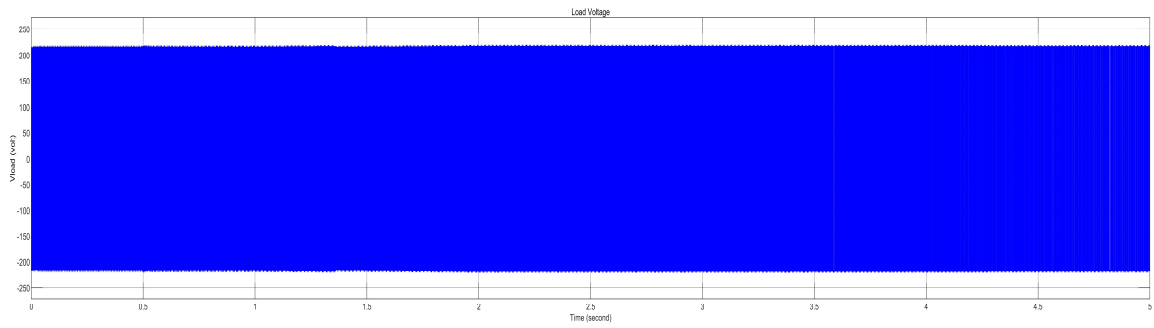


Figure 3.26. Output AC voltage

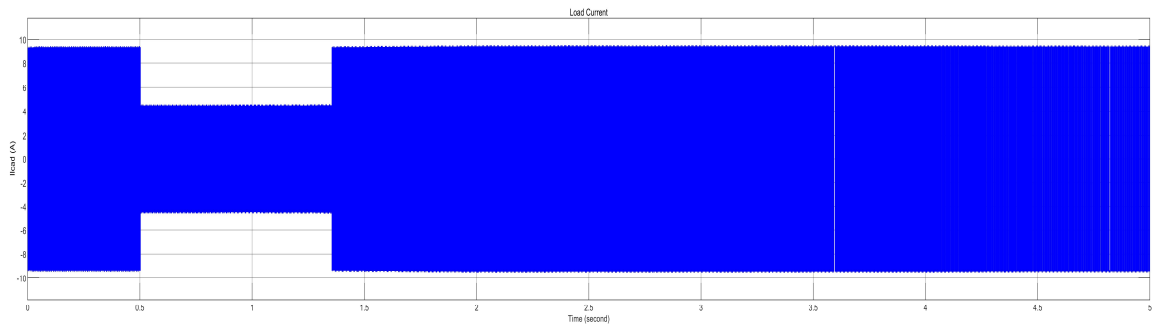


Figure 3.27. Output AC current

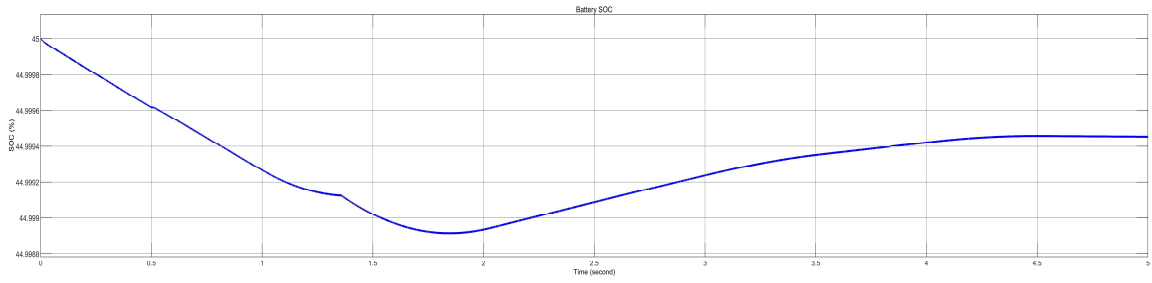


Figure 3.20. Battery bank state of charge (SOC)

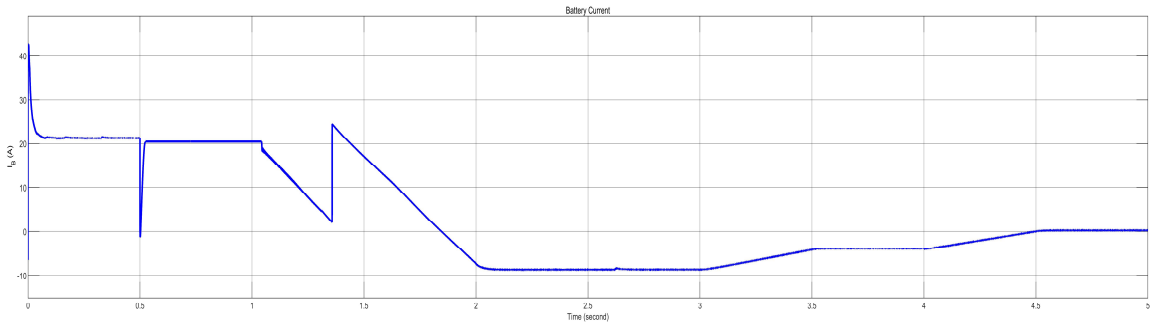


Figure 3.21. Battery bank current

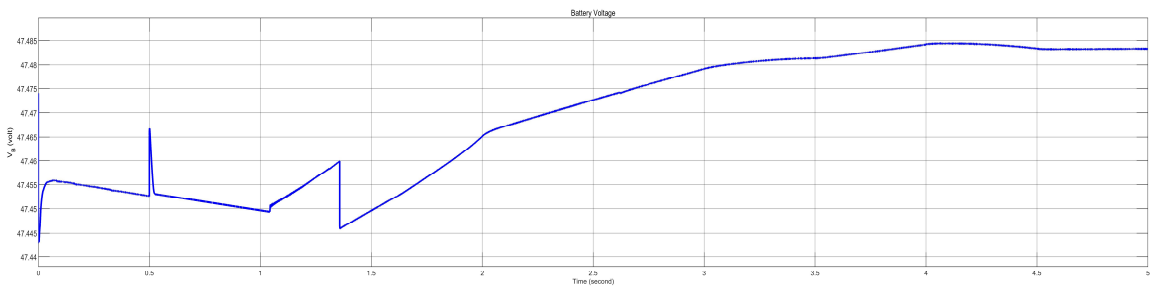


Figure 3.22. Battery bank voltage

3.7 Conclusion

As a novel design for PVRO systems, a hybrid PV-battery system for a rural house in Sinak village, Tehran, Iran, is presented in this paper to power the house and the reverse osmosis water desalination system simultaneously. The selected site is located in a high elevation location and has an average of 4.89 kWh/m²/day radiation, making it an appropriate option for designing a PV system. Two different types of loads have been introduced, which are regular house load and deferrable RO load. The water system configuration comprises a submersible pump, atmospheric tank, jet pump, pressure pump, RO membrane, and pressure tank, and the entire system needs daily 1.57 kWh energy. On the other hand, the house load has been calculated based on the appliances' energy summation, which is 5.42 kWh/day.

Optimization of the proposed system in HOMER pro software was done to extract electrical system sizing, which is a lowest cost solution, by defining exact detailed components in the software. The techno-economic analysis results suggested 8,340 watts CanadianSolar panels and 24, 6-volts, 255 Ah Trojan battery in 3 strings for the system. It is reported that the battery system's total capacity and autonomy are 765 Ah and 100 hours, while the renewable fraction is 100 hours. Dynamic modelling in this research consists of two major parts that were done in MATLAB/Simulink software. In the first part, transfer function-based dynamic modelling has been conducted to check the behaviour of the small-scale reverse osmosis unit. It stated that two feed water PH and pressure (P) are inputs of the system and water flow rate (F) and conductivity (C) are outputs of the system. The model proves that the output flow rate is a function of input water pressure as the 75 GPD

unit with input pressure of 70 psi can produce maximum desalinated water with a 0.052 GPM flow rate. Moreover, the simulation shows that the output flow rate of the suggested model can follow any variations in the input pressure.

Electrical dynamic simulation models the system to check the behaviour of the electrical system in various conditions. The introduced system comprises the PV arrays, non-inverting buck-boost converter, battery system, MPPT controller, CCCV battery charger, inverter, inverter voltage controller, transformer, and the load model. Four different conditions have been considered in this research. In the first condition, the normal condition, the hybrid PV battery system properly supplies the loads in fixed and stable load voltage of 220 volts RMS and 60 Hz frequency. Moreover, the MPPT system precisely follows the PV array's maximum power point, and the battery will experience discharging cycle. In the second condition, the system can operate properly in the absence of solar irradiance, while RO load is disconnected from the system. In the third condition, the system receives the maximum solar irradiance, and the load switch connects the RO load. In this condition, the battery current crossing zero, and the battery charger starts to charge the battery in constant current mode. In the final condition, it is depicted that the solar voltage and power production will be dropped by increasing the temperature.

Acknowledgement

This research was partially funded by Elecomp Fadak Security Systems Company. The authors would like to acknowledge all the support and help from friends, family, and Memorial University of Newfoundland.

References

- [1] S. Z. Baykara, “Hydrogen: A brief overview on its sources, production and environmental impact,” *International Journal of Hydrogen Energy*, vol. 43, no. 23, pp. 10605–10614, Jun. 2018, doi: 10.1016/j.ijhydene.2018.02.022.
- [2] C. Ammari, D. Belatrache, B. Touhami, and S. Makhloufi, “Sizing, optimization, control and energy management of hybrid renewable energy system—A review,” *Energy and Built Environment*, p. S2666123321000301, May 2021, doi: 10.1016/j.enbenv.2021.04.002.
- [3] M. A. M. Khan, S. Rehman, and F. A. Al-Sulaiman, “A hybrid renewable energy system as a potential energy source for water desalination using reverse osmosis: A review,” *Renewable and Sustainable Energy Reviews*, vol. 97, pp. 456–477, Dec. 2018, doi: 10.1016/j.rser.2018.08.049.
- [4] M. A. Alghoul et al., “Design and experimental performance of brackish water reverse osmosis desalination unit powered by 2 kW photovoltaic system,” *Renewable Energy*, vol. 93, pp. 101–114, Aug. 2016, doi: 10.1016/j.renene.2016.02.015.
- [5] G. Najafi, B. Ghobadian, R. Mamat, T. Yusaf, and W. H. Azmi, “Solar energy in Iran: Current state and outlook,” *Renewable and Sustainable Energy Reviews*, vol. 49, pp. 931–942, Sep. 2015, doi: 10.1016/j.rser.2015.04.056.
- [6] U. Caldera, D. Bogdanov, M. Fasihi, A. Aghahosseini, and C. Breyer, “Securing future water supply for Iran through 100% renewable energy powered desalination,” *IJSEPM*, vol. 23, pp. 39-54, Sep. 2019, doi: <https://doi.org/10.5278/ijsepm.3305>.

- [7] F. Banat, H. Qiblawey, and Q. A.- Nasser, "Design and Operation of Small-Scale Photovoltaic-Driven Reverse Osmosis (PV-RO) Desalination Plant for Water Supply in Rural Areas," *CWEEE*, vol. 01, no. 03, pp. 31–36, 2012, doi: 10.4236/cweee.2012.13004.
- [8] A. Mostafaeipour, M. Qolipour, M. Rezaei, and E. Babae-Tirkolae, "Investigation of off-grid photovoltaic systems for a reverse osmosis desalination system: A case study," *Desalination*, vol. 454, pp. 91–103, Mar. 2019, doi: 10.1016/j.desal.2018.03.007.
- [9] M. Haratian, P. Tabibi, M. Sadeghi, B. Vaseghi, and A. Poustdouz, "A renewable energy solution for stand-alone power generation: A case study of KhshU Site-Iran," *Renewable Energy*, vol. 125, pp. 926–935, Sep. 2018, doi: 10.1016/j.renene.2018.02.078.
- [10] M. M. Mirzaei Darian, A. M. Ghorreshi, and M. J. Hajatzadeh, "Evaluation of Photovoltaic System Performance: A Case Study in East Azerbaijan, Iran," *Iranian (Iranica) Journal of Energy & Environment*, vol. 11, Issue 1, pp. 75-78, Feb 2020, doi: 10.5829/ijee.2020.11.01.12.
- [11] M. Aminy, N. Barhemmati, A. Hadadian and F. Vali, "Design of a photovoltaic system for a rural house," 2012 Second Iranian Conference on Renewable Energy and Distributed Generation, 2012, pp. 18-22, doi: 10.1109/ICREDG.2012.6190460.
- [12] A. Iqbal and M. T. Iqbal, "Design and Analysis of a Stand-Alone PV System for a Rural House in Pakistan," *International Journal of Photoenergy*, vol. 2019, pp. 1–8, Apr. 2019, doi: 10.1155/2019/4967148.

- [13] N. S. Jayalakshmi, D. N. Gaonkar, A. Balan, P. Patil and S. A. Raza, "Dynamic modeling and performance study of a stand-alone photovoltaic system with battery supplying dynamic load," *International Journal of Renewable Energy Research*, vol. 4, Issue 3, 2014, pp. 635-640.
- [14] iSpring RCC7P-AK Under Sink 6-Stage Reverse Osmosis Drinking Filtration System and Water Softener with Alkaline Remineralization, and Pump. [Online]. Available: <https://www.123filter.com/ac/ispring-6-stage-superb-taste-boosted-performance-under-sink-reverse-osmosis-drinking-water-filtration-with-alkaline-remineralization-rcc7p-ak>. [Accessed: 17-Sep-2021].
- [15] A. Singh, P. Baredar, and B. Gupta, "Computational Simulation & Optimization of a Solar, Fuel Cell and Biomass Hybrid Energy System Using HOMER Pro Software," *Procedia Engineering*, vol. 127, pp. 743–750, 2015, doi: 10.1016/j.proeng.2015.11.408.
- [16] A. Gambier, A. Krasnik and E. Badreddin, "Dynamic Modeling of a Simple Reverse Osmosis Desalination Plant for Advanced Control Purposes," *2007 American Control Conference*, 2007, pp. 4854-4859, doi: 10.1109/ACC.2007.4283019.
- [17] K. Chithra, A. Srinivasan, V. Vijayalakshmi and A. Asuntha, "PID Controller Tuning in Reverse Osmosis System based on Particle Swarm Optimization," *International Journal for Research in Applied Science and Engineering Technology (IJRASET)*, vol. 3, Issue 5, pp. 351-358, 2015.
- [18] C. Riverol and V. Pilipovik, "Mathematical Modeling of Perfect Decoupled Control System and Its Application: A Reverse Osmosis Desalination Industrial-Scale

- Unit,” *Journal of Automated Methods and Management in Chemistry*, vol. 2005, no. 2, pp. 50–54, 2005, doi: 10.1155/JAMMC.2005.50.
- [19] S. Sobana and R. C. Panda, “Review on modelling and control of desalination system using reverse osmosis,” *Reviews in Environmental Science and Bio/Technolog*, vol. 10, no. 2, pp. 139–150, Jun. 2011, doi: 10.1007/s11157-011-9233-z.
- [20] V. Tamrakar, G. S.C, and Y. Sawle, “Single-Diode and Two-Diode Pv Cell Modeling Using Matlab For Studying Characteristics Of Solar Cell Under Varying Conditions,” *Electrical & Computer Engineering: An International Journal (ECIJ)*, vol. 4, no. 2, pp. 67–77, Jun. 2015, doi: 10.14810/ecij.2015.4207.
- [21] B. Jiang and M. T. Iqbal, “Dynamic Modeling and Simulation of an Isolated Hybrid Power System in a Rural Area of China,” *Journal of Solar Energy*, vol. 2018, pp. 1–13, Jun. 2018, doi: 10.1155/2018/5409069.
- [22] A. Srilatha, M. Kondalu and S. Ananthasai, “Non-Inverting Buck–Boost Converter for Charging Lithium-Ion Battery using Solar Array,” *International Journal of Scientific Engineering and Technology Research (IJSETR)*, vol. 3, Issue 11, pp. 2364-2369, Jun 2014.
- [23] R. Dowlatabadi, M. Monfared, S. Golestan and A. Hassanzadeh, "Modelling and controller design for a non-inverting buck-boost chopper," *Proceedings of the 2011 International Conference on Electrical Engineering and Informatics*, 2011, pp. 1-4, doi: 10.1109/ICEEI.2011.6021735.
- [24] D. Rezzak, A. Sitayeb, Y. Houam, K. Touafek and N. Boudjerda, "A New Design of Lead-Acid Battery Charger Based on Non-Inverting Buck-Boost Converter for the

- Photovoltaic Application," 2018 6th International Renewable and Sustainable Energy Conference (IRSEC), 2018, pp. 1-7, doi: 10.1109/IRSEC.2018.8703034.
- [25] K. A. Ogudo and P. Umenne, "Design of a PV Based Power Supply with a NonInverting Buck-Boost Converter," 2019 IEEE PES/IAS PowerAfrica, 2019, pp. 545-549, doi: 10.1109/PowerAfrica.2019.8928656.
- [26] S. M. Çınar and E. Akarslan, "On the Design of an Intelligent Battery Charge Controller for PV Panels," Journal of Engineering Science and Technology Review (JESTR), vol. 5, no. 4, pp. 30–34, Dec. 2012, doi: 10.25103/jestr.054.06.
- [27] MathWorks Inc. "Simscape™ Electrical™ Reference (Specialized Power Systems)". Mathworks.com. 2021. [Online]. Available: https://www.mathworks.com/help/pdf_doc/phymod/sps/powersys_ref.pdf. [Accessed: 17- Sep- 2021].
- [28] H. M. Abd Alhussain and N. Yasin, "Modeling and simulation of solar PV module for comparison of two MPPT algorithms (P&O & INC) in MATLAB/Simulink," IJEECS, vol. 18, no. 2, p. 666, May 2020, doi: 10.11591/ijeeecs.v18.i2.pp666-677.
- [29] Y. Gao, X. Zhang, Q. Cheng, B. Guo and J. Yang, "Classification and Review of the Charging Strategies for Commercial Lithium-Ion Batteries," in IEEE Access, vol. 7, pp. 43511-43524, 2019, doi: 10.1109/ACCESS.2019.2906117.
- [30] Trojanbattery.com, "Solar SSIG 06 225 Datasheet". 2021. [Online]. Available: https://www.trojanbattery.com/pdf/datasheets/SSIG_06_255_DS.pdf. [Accessed: 17- Sep- 2021].

- [31] A. Nasir, M. S. Hamad and A. K. Elshenawy, “Design and Development of a Constant Current Constant Voltage Fast Battery Charger for Electric Vehicles,” 4th International Conference on Modern Research in Science, Engineering and Technology, 2021, pp. 13-55.
- [32] Smt. S. Bhutada, and Dr. S. R. Nigam, “Single Phase PV Inverter Applying a Dual Boost Technology,” IJSET, vol. 4, no. 6, pp. 356–360, Jun. 2015, doi: 10.17950/ijset/v4s6/603.
- [33] N. Upadhyay, V. K. Singh and S. Urooj, “ Closed Loop Voltage Control Design For Photovoltaic Inverter,” 3rd IEEE Conference Nanotechnology for Instrumentation and Measurement Workshop, 2017.
- [34] J. Soomro, T. D. Memon and M. A. Shah, "Design and analysis of single phase voltage source inverter using Unipolar and Bipolar pulse width modulation techniques," 2016 International Conference on Advances in Electrical, Electronic and Systems Engineering (ICAEES), 2016, pp. 277-282, doi: 10.1109/ICAEES.2016.7888052.
- [35] L. O. Aghenta and M. T. Iqbal, “Design and Dynamic Modelling of a Hybrid Power System for a House in Nigeria,” International Journal of Photoenergy, vol. 2019, pp. 1–13, Apr. 2019, doi: 10.1155/2019/6501785.

Chapter 4.
MPPT Techniques Comparison for a Small-Scale PVRO
System in Iran

Mohammad Mousavi¹, M. Tariq Iqbal²

^{1,2}Electrical and Computer Engineering Department, Faculty of Engineering and Applied
Science, Memorial University of Newfoundland, St. John's, Canada

A version of the manuscript in this chapter has been accepted and presented as a conference paper in the 2021 IEEE 12th Annual Information Technology, Electronics and Mobile Communication Conference (IEEE IEMCON). As the primary author in this paper, Mohammad Mousavi carried out the research under the supervision of M. Tariq Iqbal as the co-author. The MEng candidate performed the literature review and was involved in technique selection, designs, calculations, simulation, and data analysis. Moreover, he prepared the first draft of the paper. The co-author supervised the research by actualization the research ideas, reviewing and correcting the manuscript.

Abstract

Energy crisis and water scarcity are among major concerns in which addressing them in one solution is a trend. Renewable energy systems, especially PV systems, can be used to power a Reverse Osmosis (RO) water desalination system. On the other hand, increasing the efficiency of the PV systems is important to achieve the best performance of the system. In this paper, a PVRO system is designed, and different Maximum Power Point Tracking (MPPT) techniques are provided to increase the efficiency and find the best response. In the first part, PVRO system configuration, including load sizing, system sizing by HOMER Pro software, system components, and system diagram, has been discussed. Perturb and Observe (P&O), Incremental Conductance (InC), and Fuzzy Logic (FL) MPPT techniques are introduced and implemented separately in MATLAB/Simulink. In the last part, a comparison of these three controllers is made. It is shown that the FL controller has better results in rise time, average efficiency, ability to track sudden changes, and oscillations.

Keywords — PVRO system, MPPT control, Perturb & Observe, Incremental Conductance, Fuzzy Logic Controller

4.1 Introduction

Greenhouse gas emissions (GHG) and global warming, which are unavoidable consequences of burning fossil fuel-driven resources, are increasing nowadays, and governments are attempting to find an appropriate replacement for these energies. Renewable energy systems (RES), which can introduce sustainable energies, are an excellent solution. A renewable system, mainly a stand-alone or grid-connected photovoltaic panel or wind turbine, has various advantages like cost reduction over time, stability, and being environmentally friendly. The predictions state that they generate 25% of electricity in 2040 [1]. On the other hand, the potable water crisis is a major concern in the modern world because of the increasing global warming and population. The best method to address this problem is water desalination. Water desalination is the process of removing unhealthy ingredient from brackish water. As desalination is an energy-consuming process and Iran has appropriate solar energy, the photovoltaic Reverse Osmosis (PVRO) system is widely accepted in small-scale applications because of low energy consumption and cheaper technology [2].

Although the PV system use the energy source that is free, generated electricity is costly due to the panel's low efficiency. Moreover, PV panel output highly varies by input irradiance and temperature variation. As a result, it is important to design a control system known as a maximum power point tracker (MPPT) to force the panel to work in maximum power point. MPPT techniques can be classified into two general categories: (1) traditional algorithms such as perturb and observation (P&O), fractional short circuit current, fractional open-circuit voltage, sliding mode control, and incremental conductance (InC).

(2) Artificial intelligence algorithms like fuzzy logic controller (FLC), neural networks, and particle swarm optimization method [3]. As the former methods provide the simplest techniques, the latter ones offer more accurate techniques. Various MPPT control methods designing for a specific PV system help find a more efficient algorithm and compare the results with other algorithms. Narendiran et al. [3] first has designed a P&O method for a PV system and boost converter and then checked the system with FLC MPPT techniques. They claim that the FLC controller provides better response time, less initial oscillation, and a more accurate tracking system. A P&O-based fuzzy logic controller has been presented in [4] by M. Sadek et al. to feed a combined DC-AC load. They state that the FLC controller operates faster with less fluctuation in comparison with the traditional P&O method. Al-Gizi et al. [5] made a more comprehensive comparison between MPPT methods by designing P&O, Incremental Conductance (InC), and FLC controller. They suggested that the InC method has a better steady-state response and less oscillation in comparison with the P&O method, while the FLC controller offers better responses than the two other methods.

This paper briefly describes the PVRO system configuration in section II by discussing the system diagram, load sizing, PV sizing, and non-inverting buck-boost converter (NIBB). Sections III to V introduces three different MPPT controller method for the designed PVRO system including perturb and observation, Incremental Conductance, and fuzzy logic controller. The concepts and flowcharts are discussed in each section, and then MATLAB/Simulink models are presented. In Section VI, results and discussion regarding the different methods are presented, and a comparison is made.

4.2 PVRO System Configuration

A renewable resources-driven water desalination system can be a large plant to feed the required water for a region, or it can be a small-scale plant to provide water for a small group of people. In this research, in a different approach, the PV system is designed to power a rural house and a small-scale RO unit simultaneously. The selected site is a house with four people, located in Sinak village in Lavasanat District, Shemiranat County, Tehran Province, Iran (35°51'06.1"N 51°41'14.3"E) and has favourable solar irradiance.

4.2.1 Load and System Sizing

In this study, there is a combined load consist of a regular house load and deferrable RO load. The regular house load is a base load, which should be powered by the PV system all the time. As there is not a metering system in the house, like most of the rural houses, the best approach is doing a site survey and listing appliances in the house. By considering the daily used time of every appliance in the house, the daily energy consumption is achievable, which is 5.42 kWh per day.

Water system configuration in the house consists of a submersible pump, atmospheric tank, jet pump, pressure pump, RO membrane, and pressure tank. Because of the different tanks in the system, the pumps can be considered as deferrable load. A deferrable load is a type of load, which can be served when excess energy exists in the system. For pumping 1500 litres of water, the submersible pumps need to work for 30 minutes. As the power rating of the pump is 1100 watts, the daily energy consumption of the pump (E_{sp}) is 0.55

kWh. On the other hand, the jet pump, which is considered to provide water for only washing and cleaning, should work 1 hour to meet the water requirement. The power rating of the pump is 470 watts, and the daily energy consumption of the jet pump (E_{jp}) is 0.47 kWh. In order to calculate the daily energy consumption of the pressure pump (E_{pp}), it is noticeable that the RO unit should provide 110 liters of water for cooking and drinking, the RO unit capacity is 75 GPD, and the pressure pump rated power is 60 watts. Equation 4.1 presents the calculation for E_{pp} , and Equation 4.2 shows the daily energy required for the RO system (E_{ro}), which is 1.57 kWh per day.

$$E_{pp} = \frac{110 \times 24 \times 60}{3.785 \times 75} \cong 0.55 kWh \quad (4.1)$$

$$E_{ro} = E_{sp} + E_{jp} + E_{pp} = 1.57 kWh / day \quad (4.2)$$

System sizing in a renewable system can be achieved by exact calculation or using optimization software. In the calculation method, the system is normally oversized because of natural resources unpredictability, especially when a storage element like a battery exists in the system. In this study, Hybrid Optimization of Multiple Energy Resources (HOMER) software is used for PV panel and battery sizing. The HOMER software offers the most cost-effective, environmentally friendly and system with less renewable fraction. The imported PV panel is CS6U-340M, with 340 watts power rating and 17.49% efficiency. The battery is the lead-acid Trojan, SSIG-06-255, with a maximum capacity of 255 Ah with 6 volts nominal voltage. Moreover, the DC bus voltage is 48 volts. Figure 4.1 depicts the designed system in HOMER software.

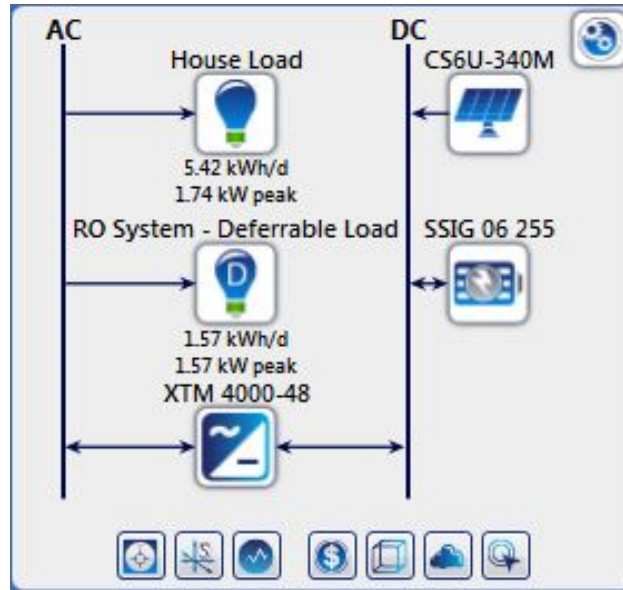


Figure 4.1. PVRO system schematic in HOMER Pro

Figure 4.2 shows the software optimization's results. Based on this result, 2.68 kW PV panels, which is 8, 340 watts panels in real installation, and 24 Trojan batteries in 3 strings are connected to 48 volts DC bus with a total capacity of 765 Ahr. Moreover, the total net present cost, levelized cost of energy, and operating and maintenance cost are 10,244.93 US\$, 0.3109 US\$, and 209.75 US\$, respectively.

System Architecture:		HOMER Cycle Charging		Total NPC:	\$10,244.93
CanadianSolar MaxPower CS6U-340M (2.68 kW)				Levelized COE:	\$0.3109
Trojan SSIG 06 255 (3.00 strings)				Operating Cost:	\$209.75
Studer Xtender XTM 4000-48 (1.48 kW)					
Cost Summary Cash Flow Compare Economics Electrical Renewable Penetration Trojan SSIG 06 255 CanadianSolar MaxPower CS6U-340M Studer Xtender XTM 4000-48 Emissions					
Production		Consumption		Quantity	
kWh/yr	%	kWh/yr	%	kWh/yr	%
CanadianSolar MaxPower CS6U-340M	4,642	100	AC Primary Load	1,978	77.6
Total	4,642	100	DC Primary Load	0	0
			Deferrable Load	572	22.4
			Total	2,549	100
				Excess Electricity	1,665 35.9
				Unmet Electric Load	1.08 0.0422
				Capacity Shortage	2.19 0.0860
Quantity		Value	Units		
Renewable Fraction	100	%			
Max. Renew. Penetration	865,831	%			

Figure 4.2. System sizing and electrical specification for the PVRO system proposed by HOMER Pro

4.2.2 Non-Inverting Buck-Boost Converter

DC-DC converter in this study performs two major tasks: (1) delivering maximum power of the PV panels to the loads in order to stabilizing output of the panels; (2) operates as a battery charger to store extra energy in the system. Non-inverting buck-boost converter (NIBB) or cascaded buck-boost can be used for this study because of fewer components, less complexity, low losses and cost. As it is depicted in Figure 4.3, NIBB converter comprises two main switches including S1 and S2 which are controlled by D_1 and D_2 respectively. With different combination of the switches, different operation modes are achievable: when S1 is on and S2 is off, NIBB operates as Buck converter, when D_1 is equal to 1 and S2 is on, it operate as boost converter and when S1 and S2 are both on, operation mode is buck-boost. The output voltage of the NIBB converter is given by Equation 4.3 [6].

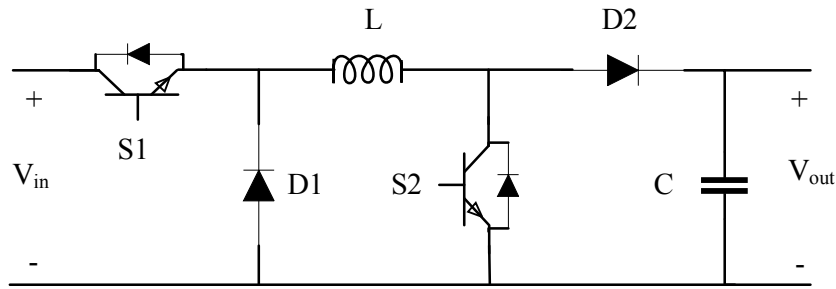


Figure 4.3. Non-inverting buck-boost (NIBB) converter topology

$$V_{NIBB} = \frac{D_1}{1 - D_2} V_{pv} \quad (4.3)$$

Controlling NIBB, as a double-task converter in this study, requires two various signals; the first signal is S1, which is the output of the MPPT controller, and the second one is S2, which is generated by a charge controller. It is noticeable that, for designing PWM signals, both should have the same frequency. Moreover, S1 should always be greater than S2, PWM signal of S2 must be enabled after PWM signal of S1, and must be disabled before PWM signal of S1 [7].

4.2.3 System Diagram

Electrical dynamic simulation helps to check the behaviour of the system in response to variations in system inputs or internal changes. The suggested model for the PVRO system in this study is designed to deliver solar power to AC load with appropriate voltage and frequency. The system is simulated in MATLAB/Simulink with the following components, as it is shown in Figure 4.4: photovoltaic panels, non-inverting buck-boost converter, single-phase PWM inverter, Battery storage, step-up transformer, load model and load control unit, maximum power point tracker controller, charge controller, and inverter voltage controller. Load controller is defined to control when the RO load should be connected to the system. The inverter voltage controller is added to control the output AC voltage and frequency of the system. The battery charger is working based on the constant-current constant-voltage battery charger method to manage the charging and discharging regime of the battery. Finally, the MPPT controller extracts the maximum power of the panels and delivers it to the NIBB converter. In the rest of this paper, three different MPPT techniques will be defined to check the response of the system.

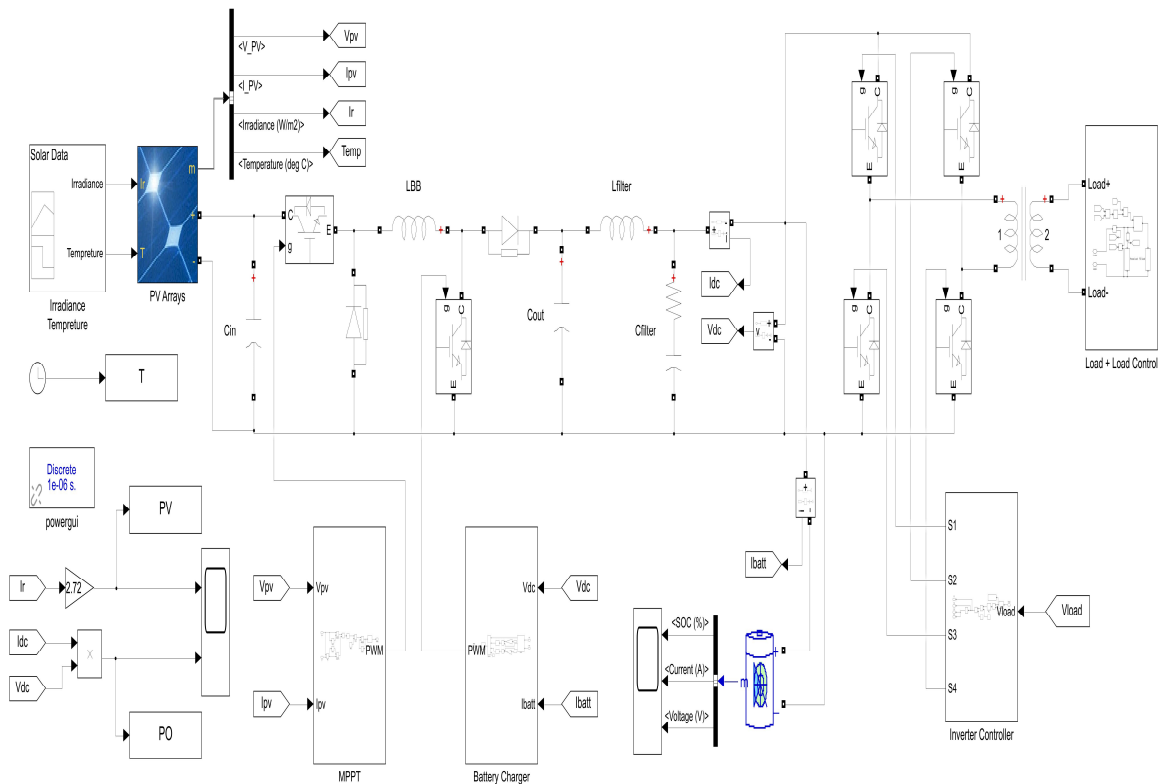


Figure 4.4. Proposed PV system diagram implemented in MATLAB/Simulink

4.3 Perturb and Observe (P&O) Method

Temperature and irradiance are two environmental factors, which affect the panel's output power, voltage, and current. Figure 4.5 depicts the typical P-V curve of a PV panel. Based on the figure, it is important to force the panel to work on maximum power point (MPP) to have maximum efficiency. The concept of every MPPT controller is to change the applied duty cycle to the DC-DC converter in order to change the output voltage positively or negatively and subsequently reaching to the V_{MPP} . For any point like A, the voltage should be increased, and for any point like B, the voltage should be decreased.

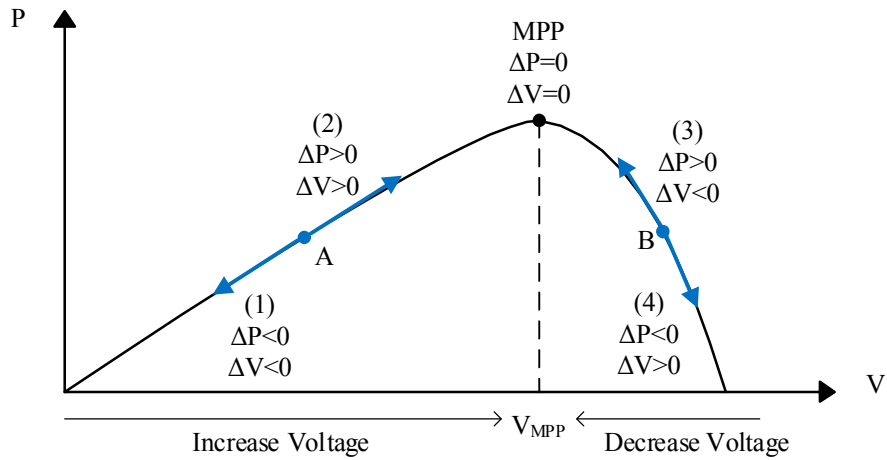


Figure 4.5. Typical P-V curve of a PV panel with MPP and various regions

Perturb and observe method, which is known as the hill-climbing method, is the oldest and most commonly used technique due to simplicity, being not expensive and requiring fewer sensors. In this method, a small perturbation will be applied to the voltage and changes in power will be checked. If ΔP is positive, the operation point is in region 2 or 3, which means the perturbation moved the operation point to MPP and the next perturbation is in the same direction. If ΔP is negative, regions 1 and 4 are the ones in which the operating point is working, which means perturbation moved the operation point away from MPP. As a result, the next perturbation is in the opposite direction. According to this analysis, a flowchart in Fig. 6 describes the P&O algorithm [8].

In order to simulate the P&O method in Simulink, two sensors can be used to measure the voltage and current of the PV panel. Based on the flowchart, signs of the ΔV and ΔP are determining the voltage changes. If ΔV and ΔP have the same signs, the sign detector will pass (+1), and the duty cycle will be decreased. If ΔV and ΔP have opposite signs, (-

1) will be passed, and the duty cycle will be increased. Finally, the duty cycle will pass through a PWM generator to generate a signal for the switch [9]. Figure 4.7 illustrates the perturb and observe method simulation in MATLAB/Simulink.

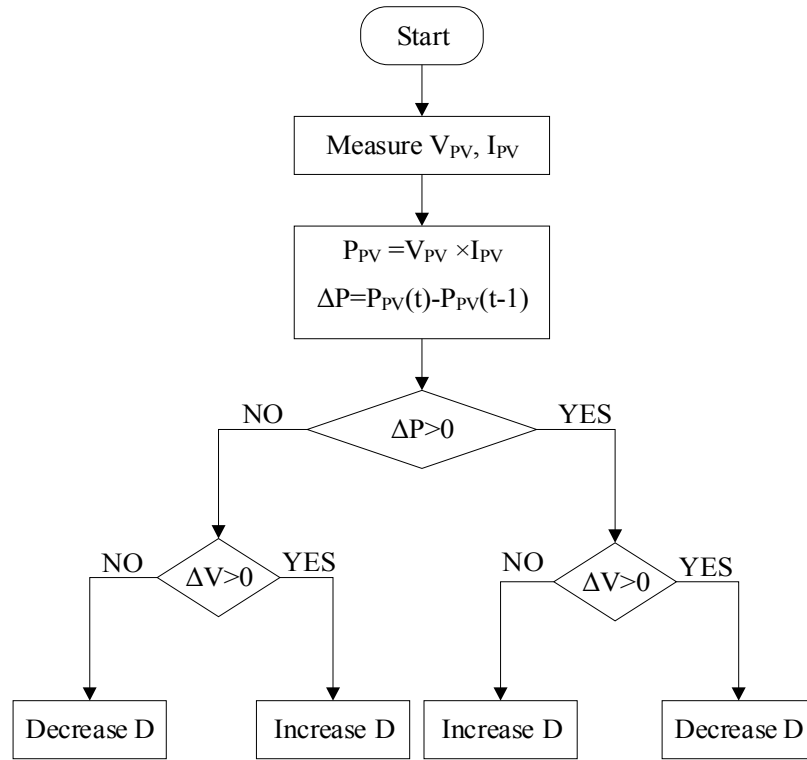


Figure 4.6. Perturb and Observe (P&O) MPPT controller flowchart

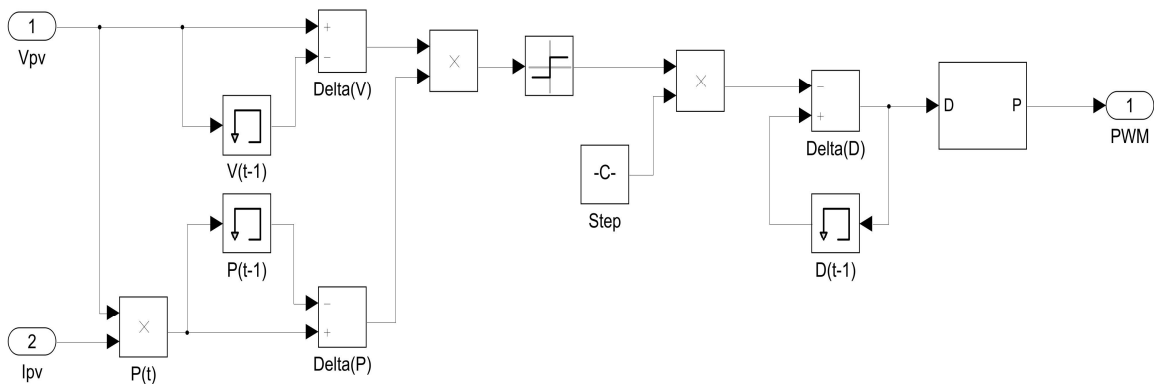


Figure 4.7. Perturb and Observe (P&O) MPPT controller in Simulink

4.4 Incremental Conductance (InC) Method

The incremental conductance (InC) method is introduced to solve the major issues in the P&O method. As stated in the P&O method, the controller perturbs the voltage all the time to check the changes in the ΔP . In other words, the operation point will always oscillate around the MPP even if the controller detects it. The InC method is based on the conductance definition, which is I/V . As shown in Figure 4.5, in MPP dP/dV is equal to zero, which means the slope of the power curve is zero. Subsequently, for any operation point like A, the slope of the power curve is positive, and for any point like B, the slope of the power curve is negative. Equations 4.4 to 4.7 describe the InC method and help to design the flowchart.

$$\frac{dP}{dV} = \frac{d(IV)}{dV} = I + V \frac{dI}{dV} \cong I + V \frac{\Delta I}{\Delta V} \quad (4.4)$$

$$I + V \frac{\Delta I}{\Delta V} = 0 \Rightarrow \frac{\Delta I}{\Delta V} = -\frac{I}{V} \Rightarrow MPP \quad (4.5)$$

$$I + V \frac{\Delta I}{\Delta V} > 0 \Rightarrow \frac{\Delta I}{\Delta V} > -\frac{I}{V} \Rightarrow V \uparrow \Rightarrow D \downarrow \quad (4.6)$$

$$I + V \frac{\Delta I}{\Delta V} < 0 \Rightarrow \frac{\Delta I}{\Delta V} < -\frac{I}{V} \Rightarrow V \downarrow \Rightarrow D \uparrow \quad (4.7)$$

Equation 4.6 describes when the slope of the power curve is positive, the incremental conductance is greater than the negative conductance, and the voltage should be increased. Equation 4.7 shows that when the incremental conductance is less than negative

conductance, the voltage should be decreased. Figure 4.8 shows the incremental conductance MPPT technique [10].

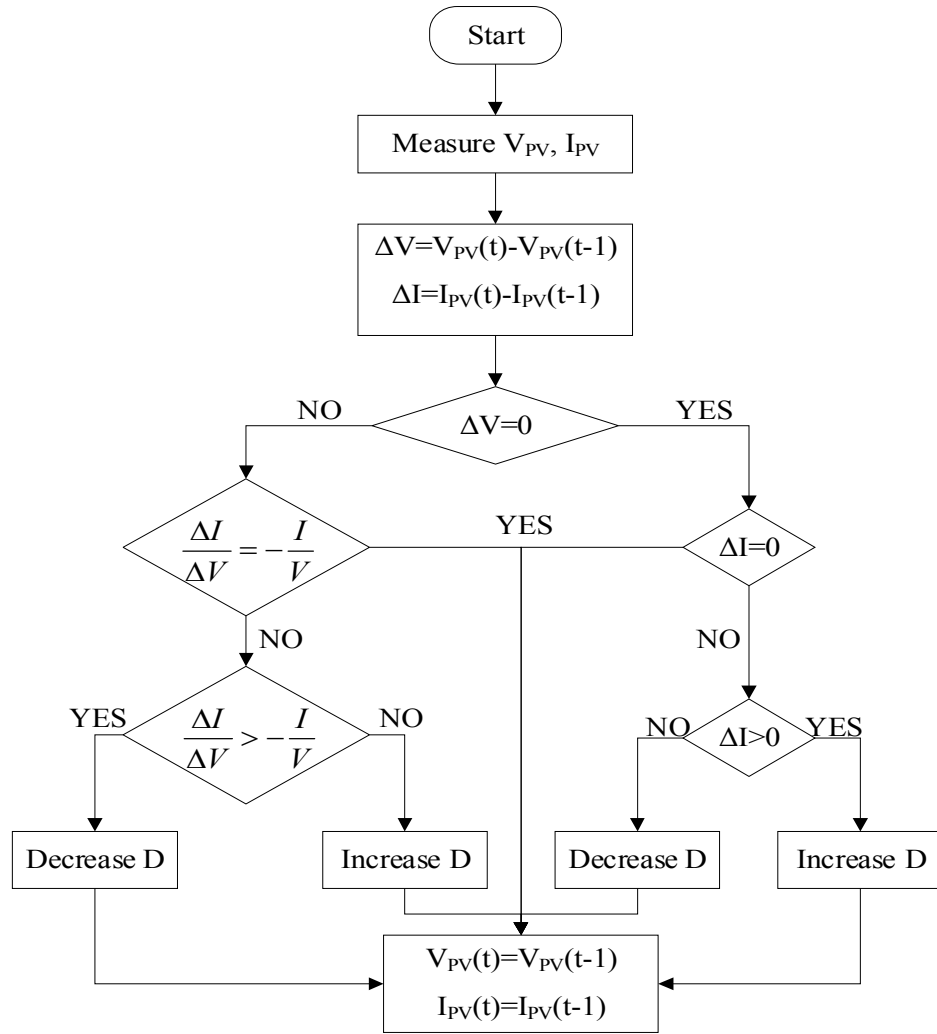


Figure 4.8. Incremental Conductance (InC) MPPT controller flowchart

In order to simulate the incremental conductance method in MATLAB/Simulink, it is necessary to follow the flowchart step by step. Firstly, two sensors should measure voltage and current and ΔV , ΔI , instantaneous conductance, and incremental conductance will be

calculated. Afterward, two branches of the flowchart will be designed to check the sign of the $(\Delta I/\Delta V + I/V)$ and (ΔI) by help of four different switches. Then the results will be connected to the last switches to complete the flowchart. Finally, the result create required changes in duty cycle and will pass through a PWM generator to make appropriate control signal for DC-DC converter. Figure 4.9 depicts simulated incremental conductance MPPT technique simulated in Simulink [11].

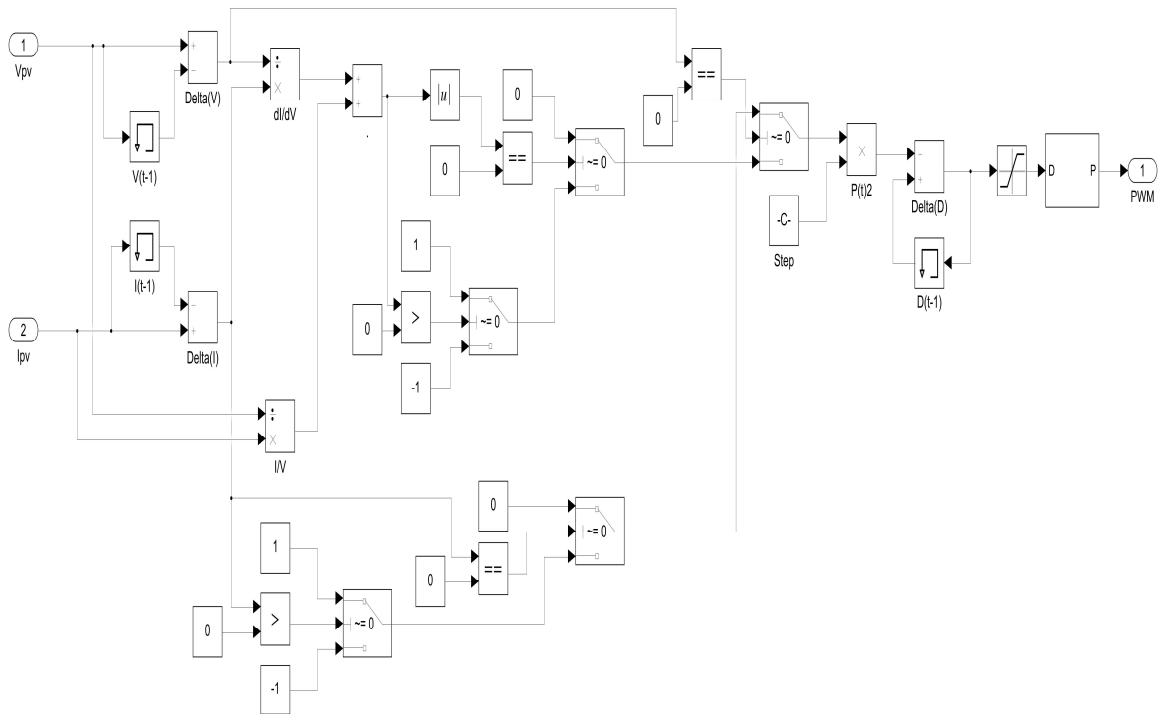


Figure 4.9. Incremental Conductance (InC) MPPT controller in Simulink

4.5 Fuzzy Logic (FL) Method

Fuzzy logic (FL) controller, has become popular for solar MPPT during the last decade because of numerous advantages over conventional methods. Fuzzy logic MPPT or multi-rules base MPPT can work in nonlinear conditions with imprecise inputs, and an accurate

mathematical model is not required [11]. The key disadvantage of the FL method is the complexity of implementation, and it will be increased in an adaptive FL MPPT controller. For designing a fuzzy logic MPPT controller, the flowchart comprises two main parts: one part relates to preparing the inputs for the FL controller and appropriate PWM output from the controller, and the other part is designing the FL controller. Equations 4.8 and 4.9 describe inputs of the controller, and Figure 4.10 shows the fuzzy logic controller flowchart [12].

$$E(k) = \frac{\Delta P}{\Delta V} = \frac{P(k) - P(k-1)}{V(k) - V(k-1)} \quad (4.8)$$

$$\Delta E(k) = E(k) - E(k-1) \quad (4.2)$$

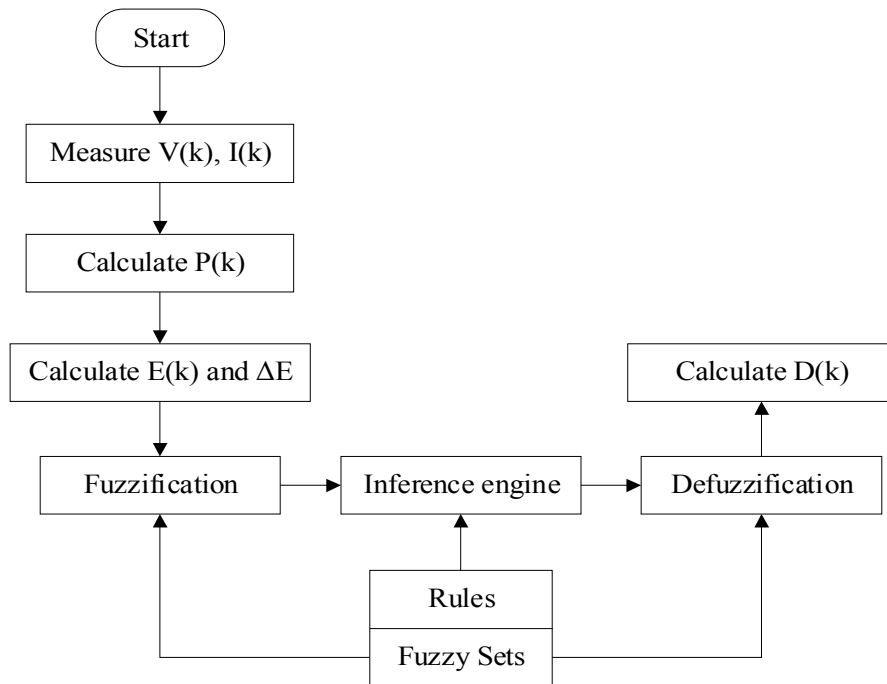


Figure 4.10. Fuzzy Logic (FL) MPPT controller flowchart

According to the flowchart, fuzzy logic controller consists of three major parts: fuzzification, rule-based inference engine, and defuzzification. Each part is explained and designed in MATLAB separately.

4.5.1 Fuzzification

The fuzzy logic controller is a precise method because it defines a fuzzy space for inputs and output. In other words, the logic for decision-making belongs to a space, not several quantities. As a result, the first stage of the FLC is fuzzification, which converts inputs and output to linguistic variables with the help of fuzzy membership functions. In this study, every inputs and output will be expressed in five linguistic fuzzy sets, based on practical and intuitive reasons, including negative big (NB), negative small (NS), zero (ZO), positive small (PS), and positive big (PB). The ranges for input E , ΔE and output ΔD are (-10:10), (-100:100), and (-0.1:0.1), respectively, and they are depicted in Figure 4.11.

4.5.2 Rule-based Inference Engine

The next step in a fuzzy logic controller is defining certain rules to specify fuzzy output sets to a combination of fuzzy input sets. As an if-then statement, the inference engine is working based on the Mamdani fuzzy inference method in this study. Every two inputs in this study have five fuzzy sets, and 25 rules should be defined as stated in Table 4.1 [13].

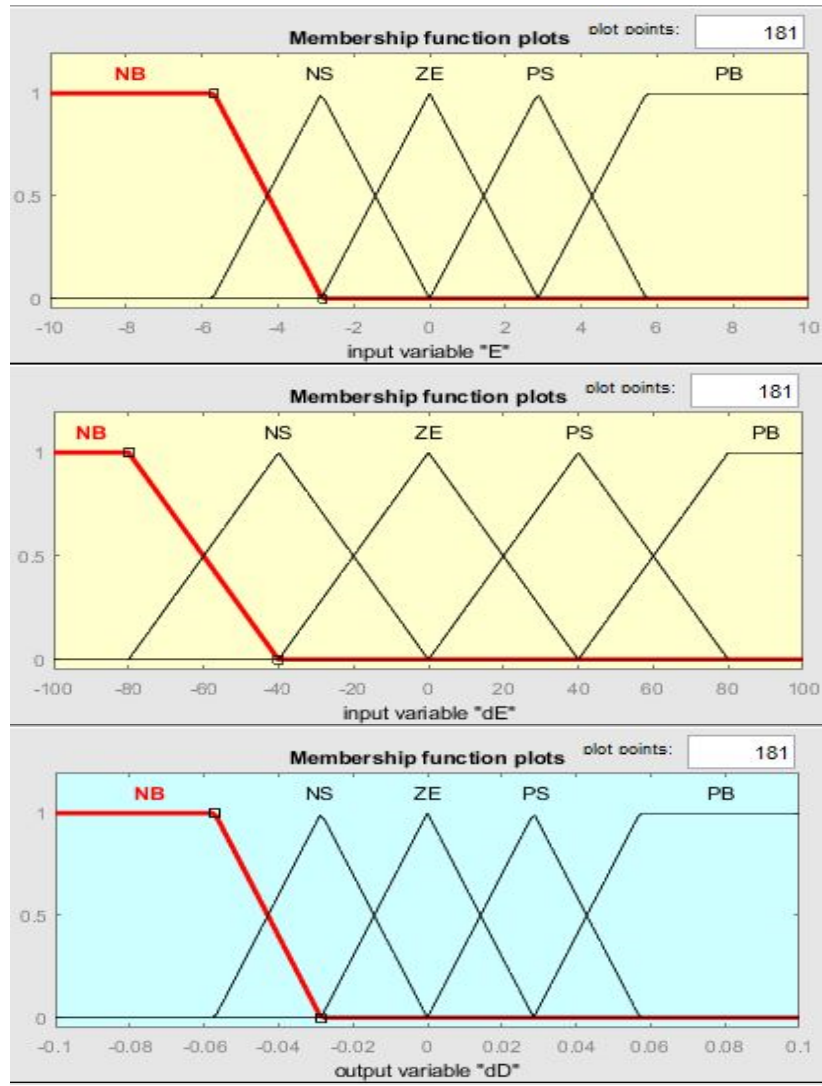


Figure 4.11. Membership functions for inputs E and ΔE , and output ΔD in FL controller

Table 4.1. FL Controller Rule Table

E	ΔE				
	NB	NS	ZE	PS	PB
NB	ZE	ZE	NB	NB	NB
NS	ZE	ZE	NS	NS	NS
ZE	NS	ZE	ZE	ZE	PS
PS	PS	PS	PS	ZE	ZE
PB	PB	PB	PB	ZE	ZE

Rules in Table 4.1 are designed to move the operation point in the P-V curve to MPP. According to the definition of input E, it is the slope of the P-V curve and input ΔE is the displacement of this point. In other words, Positive E means any point on the left side of the curve and negative E means any point on the right side of the curve. As an example: if E is NB and ΔE is ZE, then ΔD is NB. This rule means that if the slope is negative big and the displacement of E is zero, the operation point is far away from the MPP on the right side without significant changes; if so, D should be greatly decreased. Rule surface is illustrated in Figure 4.12.

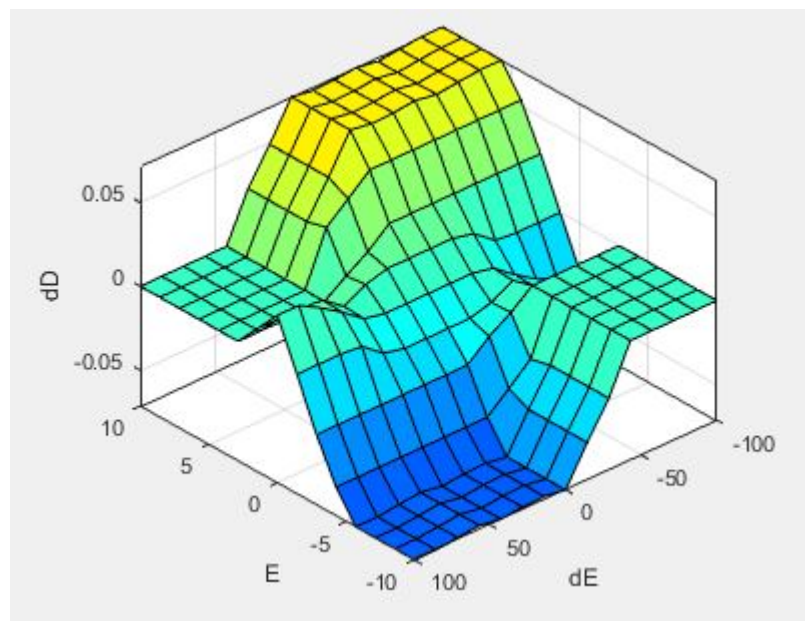


Figure 4.14. FL Controller Rule Surface

4.5.3 Defuzzification

As in previous section stated, the output of the inference engine is a fuzzy set with linguistic variables. At the same time, the NIBB converter needs a precise control signal of

D to control the switch gate. Defuzzification is the process of transferring out fuzzy sets to deterministic information or actual mathematical numbers. The center of area (COA) algorithm is used for the defuzzification of output in this study.

Finally, based on the proposed flowchart, the output of the FLC is used to create the duty cycle, and it will pass through a PWM generator. Simulated fuzzy logic MPPT controller in Simulink is depicted in Figure 4.13.

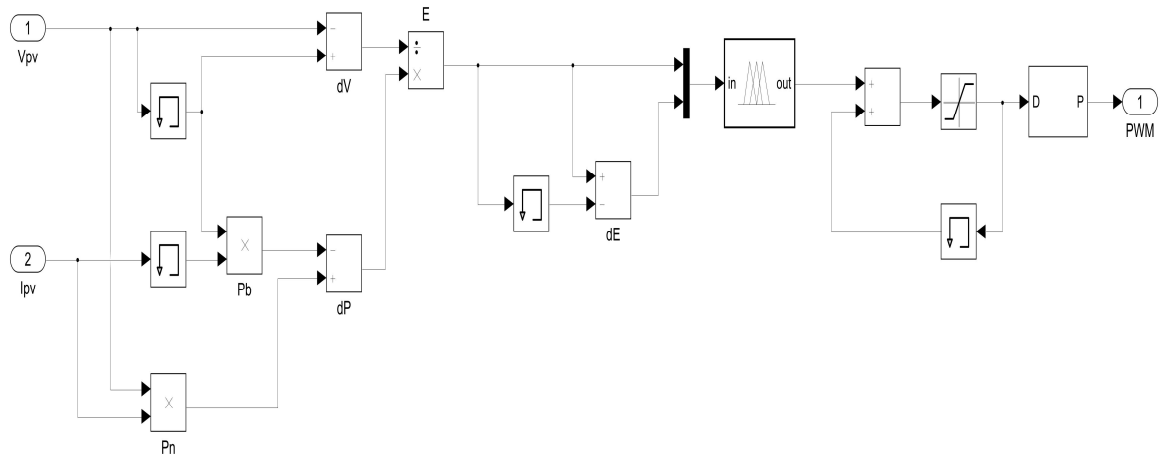


Figure 4.15. Fuzzy Logic (FL) MPPT controller in Simulink

4.6 Results and Discussion

The PVRO system dynamic simulation has been completed in MATLAB/Simulink, depicted in Figure 4.4. To achieve the best results from the system, three different MPPT controllers have been designed and tested separately to compare. The most difficult part of designing in this research is that the proposed system is a complex, uniform interconnected system with different components and control units, and every small change will affect the other results. Three solar irradiance levels are selected to check the results: 400 W/m², 1000

W/m², and 100 W/m². The maximum output powers of the PV arrays regarding these irradiances are 1088 watts, 2720 watts, and 272 watts, respectively, which are known as ideal powers. It is noticeable that maximum power is achievable in Simulink when maximum irradiance of 1000 W/m² apply to the panels. As a result, the ideal power will be the product of irradiance and 2.72 (340*8/1000) in this study. The tests are done at a constant temperature of 25 °C. Simulation results are exported separately for each technique, and they are depicted in Figure 4.14 altogether.

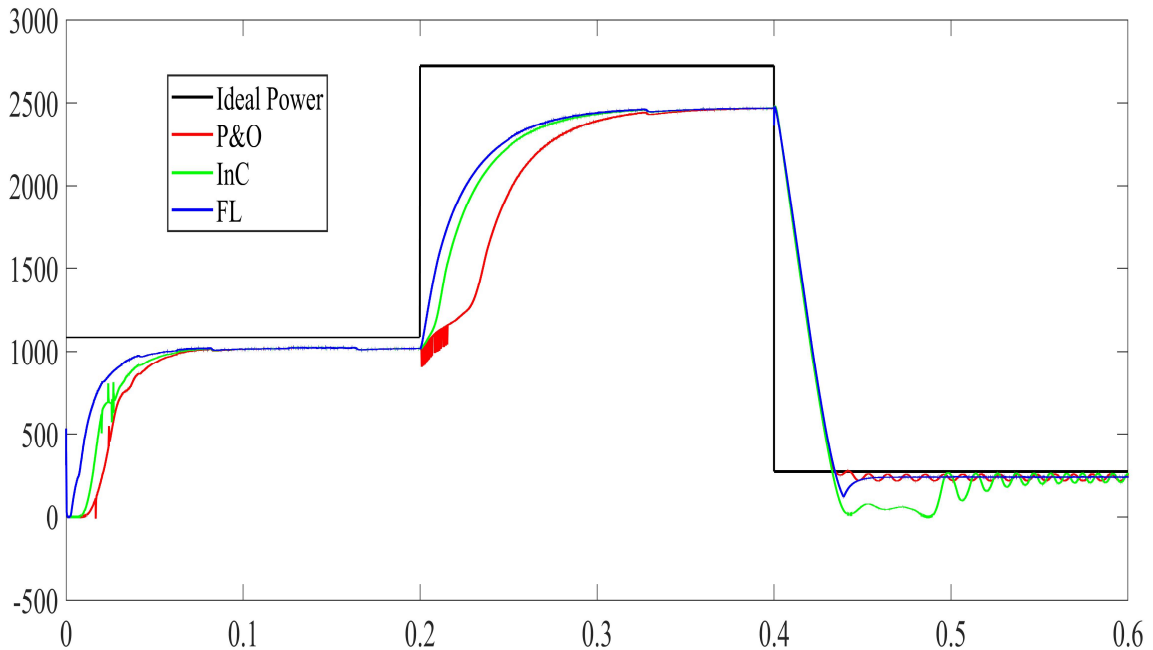


Figure 4.16. Simulation results for P&O, InC, and FL MPPT controller

Based on the results in Figure 3.14, four differences between the techniques are remarkable. Firstly, the major drawback of the P&O and InC methods is that they cannot track sudden changes in irradiance. In other words, conventional methods cannot track the

changes in cases like cloud shadows or running the system in high irradiance conditions. On the other hand, the fuzzy logic controller operates in this condition precisely as it can be seen between times 0.4 to 0.6 seconds when the irradiance drops from 1000 W/m^2 to 100 W/m^2 . Moreover, FL can extract maximum power when the system runs with an irradiance of more than 600 W/m^2 .

The other difference is oscillation. As the figure shows, especially between times 0.4 to 0.6 seconds, P&O and InC methods have many oscillations as expected. But the fuzzy logic controller has fewer oscillations with minimum undershoot. The FL technique is appropriate and because, like traditional techniques, it will not oscillate on MPP when it reaches it.

Average delivered power is the average of power that is achievable in each specific irradiances at DC bus. The average efficiency equals the average delivered power in each irradiance divided by ideal power based on this average power. Table 4.2 depicts average powers and efficiencies for the three techniques at two different irradiances. According to these results, fuzzy logic can deliver more power to the DC bus in both irradiances and has better average efficiency. Average delivered power by FL MPPT in 400 W/m^2 and 1000 W/m^2 are 942 watts and 2294 watts, respectively. Moreover, the average efficiencies are 86.5% and 84.3%.

Finally, a remarkable difference between techniques is about transient behaviours such as rise time. The most important benefit of the fuzzy logic MPPT controller is providing a fast response. The rise time is a time taken by the controller to reach from 10% to 90% of

the target power. Table 4.3 shows time details for all proposed techniques in transient from 400 W/m² to 1000 W/m². Based on the results, the FL MPPT controller has the fastest response. It reaches 10% and 90% of the maximum power, 2720 watts in 0.203 seconds and 0.257 seconds, respectively. Moreover, the rise time for the FL controller is 0.054 seconds.

Table 4.2. Average Power and Power Efficiency of MPPT Techniques

Technique	Average Power @ 400 W/m ²	Average Efficiency (%)	Average Power @ 1000 W/m ²	Average Efficiency (%)
Ideal Power	1088 W	100%	2720 W	100%
P&O	870 W	79.90%	2121 W	77.90%
InC	899 W	82.60%	2252 W	82.70%
FL	942 W	86.50%	2294 W	84.30%

Table 4.3. Time Details for Proposed MPPT techniques

Technique	Time reached to 10% (s)	Time reached to 90% (s)	Rise time (s)
P&O	0.218	0.285	0.067
InC	0.208	0.264	0.056
FL	0.203	0.257	0.054

4.7 Conclusion

A rural PVRO system can simultaneously meet the electrical demands of a house and small-scale desalination unit, and an appropriate control method increases the system's efficiency. Load sizing and system sizing indicated that 8, 340 W PV panels are required. Non-inverting buck-boost converter (NIBB) is selected as the DC-DC converter in this study. Two traditional MPPT techniques, including perturb and observe (P&O) and

incremental conductance (InC), and one artificial intelligence technique, which is fuzzy logic (FL) controller, were discussed in three different sections. In each section, the technique was first described by a flowchart and then simulated in MATLAB/Simulink. Although P&O is a simple method and InC can solve the oscillation issue in P&O, the FL controller has higher overall performances. The comparison results have shown that the FL controller: (1) can precisely track sudden irradiance changes, especially in the system running in high irradiance conditions; (2) has less oscillation, overshoot, and undershoot; (3) has higher average efficiency, around 86.5% and 84.3% in 400 W/m² and 1000 W/m², respectively; (4) has a faster rise time close to 0.054 seconds.

Acknowledgement

The authors would like to thank Elecomp Fadak Company for partially sponsoring this research.

References

- [1] C. Ammari, D. Belatrache, B. Touhami, and S. Makhloufi, "Sizing, optimization, control and energy management of hybrid renewable energy system—A review," *Energy and Built Environment*, p. S2666123321000301, May 2021, doi: 10.1016/j.enbenv.2021.04.002.
- [2] U. Caldera, D. Bogdanov, M. Fasihi, A. Aghahosseini, and C. Breyer, "Securing future water supply for Iran through 100% renewable energy powered desalination," *IJSEPM*, vol. 23, pp. 39-54, Sep. 2019, doi: <https://doi.org/10.5278/ijsepm.3305>.

- [3] S. Narendiran, S. K. Sahoo, R. Das and A. K. Sahoo, "Fuzzy logic controller based maximum power point tracking for PV system," 2016 3rd International Conference on Electrical Energy Systems (ICEES), 2016, pp. 29-34, doi: 10.1109/ICEES.2016.7510590.
- [4] S. M. Sadek, F. H. Fahmy, A. E.-S. A. Nafeh, and M. A. El-Magd, "Fuzzy P & O Maximum Power Point Tracking Algorithm for a Stand-Alone Photovoltaic System Feeding Hybrid Loads," SGRE, vol. 05, no. 02, pp. 19–30, 2014, doi: 10.4236/sgre.2014.52003.
- [5] A. G. Al-Gizi and S. J. Al-Chlahawi, "Study of FLC based MPPT in comparison with P&O and InC for PV systems," in 2016 International Symposium on Fundamentals of Electrical Engineering (ISFEE), Bucharest, Romania, Jun. 2016, pp. 1–6. doi: 10.1109/ISFEE.2016.7803187.
- [6] R. Dowlatabadi, M. Monfared, S. Golestan and A. Hassanzadeh, "Modelling and controller design for a non-inverting buck-boost chopper," Proceedings of the 2011 International Conference on Electrical Engineering and Informatics, 2011, pp. 1-4, doi: 10.1109/ICEEI.2011.6021735.
- [7] A. Srilatha, M. Kondalu and S. Ananthasai, "Non-Inverting Buck–Boost Converter for Charging Lithium-Ion Battery using Solar Array," International Journal of Scientific Engineering and Technology Research (IJSETR), vol. 3, Issue 11, pp. 2364-2369, Jun 2014.
- [8] A. M. Othman, M. M. M. El-arini, A. Ghitas, and A. Fathy, "Realworld maximum power point tracking simulation of PV system based on Fuzzy Logic control," NRIAG

- Journal of Astronomy and Geophysics, vol. 1, no. 2, pp. 186–194, Dec. 2012, doi: 10.1016/j.nrjag.2012.12.016.
- [9] O. Bel Hadj Brahim Kechiche, B. Barkaoui, M. Hamza and H. Sammouda, "Simulation and comparison of P&O and fuzzy logic MPPT techniques at different irradiation conditions," 2017 International Conference on Green Energy Conversion Systems (GECS), 2017, pp. 1-7, doi: 10.1109/GECS.2017.8066266.
- [10] M. C. Argyrou, P. Christodoulides and S. A. Kalogirou, "Modeling of a photovoltaic system with different MPPT techniques using MATLAB/Simulink," 2018 IEEE International Energy Conference (ENERGYCON), 2018, pp. 1-6, doi: 10.1109/ENERGYCON.2018.8398734.
- [11] N. Hussein Selman, "Comparison Between Perturb & Observe, Incremental Conductance and Fuzzy Logic MPPT Techniques at Different Weather Conditions," IJRSET, vol. 5, no. 7, pp. 12556–12569, Jul. 2016, doi: 10.15680/IJRSET.2016.0507069.
- [12] Carlos Robles Algarín, John Taborda Giraldo, and Omar Rodríguez Álvarez, "Fuzzy Logic Based MPPT Controller for a PV System," Energies, vol. 10, no. 12, p. 2036, Dec. 2017, doi: 10.3390/en10122036.
- [13] B. Bendib, F. Krim, H. Belmili, M. F. Almi, and S. Boulouma, "Advanced Fuzzy MPPT Controller for a Stand-alone PV System," Energy Procedia, vol. 50, pp. 383–392, 2014, doi: 10.1016/j.egypro.2014.06.046.

Chapter 5. Conclusions and Future Works

5.1 Conclusions

Hybrid renewable energy systems (HRES) are great replacements for conventional fossil fuel resources, and they generate green power that reduces greenhouse gas (GHG) emissions. Although governments have a tremendous interest in building large renewable stations like solar plants or offshore wind turbines, small-scale renewable generations have become popular during the last decades. Small-scale PV systems are widespread nowadays because they can generate and store electricity in isolated configurations, are relatively cheap, and are more stable. An HRES system not only does power the regular loads with electrical components and different storage systems, but also it can power a water desalination system. Water desalination systems are required as freshwater reservoirs' levels have dangerously declined in the past century. A reverse osmosis (RO) system is a wonderful option in small-scale applications because it can be easily commissioned and combined with exciting water systems.

There are two major issues in the rural areas: lack of electricity and potable water. People globally solve these problems with frustrating approaches, spending remarkable money and generating emissions. A stand-alone or grid-connected PV-powered system is a well-known solution to generate electricity for a house. On the other hand, the number of PV-powered RO water desalination systems for medium to community-size applications is increasing. In this study, a small-scale stand-alone PV system was designed to power a rural house and a small-scale RO system simultaneously in an innovative approach.

Firstly, a comprehensive literature review was conducted regarding renewable resources in Iran, renewable system components and configurations, water resources in Iran, and water desalination methods. Based on this review, although oil and natural gas are highly cheap in Iran, the country has good potential for renewable resources, especially wind and solar energy. In recent years there has been an interest in small-scale PV systems among people as they are experiencing many electricity blackouts. The presented statistics showed that Iran suffers from water stress conditions and various locations have a freshwater accessibility issue. A small-scale RO unit is suggested in the review, as they are the most available and cost-effective solution for remote areas.

The selected site in Sinak village, Tehran, Iran, was surveyed completely as a remote house supplied with well water. The water system configuration in the house comprised a submersible pump, atmospheric tank, and jet pump. After designing a RO system for the house, a pressure pump, RO membrane, and pressure tank were added. Two different loads were defined in the system: firstly, a deferrable RO load was considered to model the water system components energy requirements; secondly, a regular house load is defined as daily energy consumption for the house.

After load-sizing, a renewable system design had been started with component selection and system optimization. HOMER Pro software was chosen in this study for system and cost analysis. Two scenarios were designed in this research: (1) Photovoltaic system with battery storage, and (2) Photovoltaic system with battery storage and natural gas generator. The results showed that although the system with a small-scale natural gas generator has less initial capital cost and net present cost, this scenario use LF dispatch strategy and

consumes yearly 399m³ natural gas. On the other hand, the PV battery RO system is environmentally friendly with zero carbon emission. This system has fewer O&M costs, more autonomy, less control complexity due to the CC dispatch strategy and fewer components in the system. Moreover, sensitivity analysis conducted in this research has proved that the PV battery system is less sensitive because of fewer sensitivity variables than other systems.

The next step after system optimization and sizing was dynamic modelling of the proposed PV battery system and small-scale RO unit. Dynamic models helped the authors to check the behaviours of the systems with different inputs and conditions. The simulation was designed in MATLAB/Simulink for both PV system and RO system separately. A transfer function-based model was presented for the desalination unit while two feedwater PH and pressure (P) are inputs of the system, and water flow rate (F) and conductivity (C) are outputs of the system. It is shown that the output flow rate of the suggested model can follow any changes in the input pressure. For instance, the selected 75 GPD unit can desalinate brackish water with a 0.052 GPM flow rate when the input pressure is 70 psi.

The electrical dynamic modelling of the PV battery system with deferrable RO load was simulated completely in MATLAB/Simulink. The proposed model consisted of PV arrays, non-inverting buck-boost converter, battery system, MPPT controller, CCCV battery charger, inverter, inverter voltage controller, transformer, and the load model. Four different conditions were designed in this research to observe the system's response. In the first condition, the PV arrays powered both loads perfectly while the inverter controller delivered power in fixed and stable voltage and frequency. Moreover, the MPPT controller

followed radiation variations, and the battery charge controller worked precisely. The second condition proved that the system could work in the absence of solar irradiance while the load control algorithm disconnected the RO load. In the third condition, PV panels received the maximum power, load switch connected the RO load, and the battery charger charged the battery bank. The last condition, known as zero energy condition, battery state of charge was constant and generated energy by PV panels was equal to loads requirements.

The purpose of the last phase in this thesis was to enhance system efficiency by checking the system's performance in the presence of other control techniques. The maximum power point tracking system delivered the maximum received energy through the NIBB converter to the loads in PV systems. Two traditional MPPT techniques, including perturb and observe (P&O) and incremental conductance (InC), and one artificial intelligence technique, which is fuzzy logic (FL) controller, were introduced, designed, and implemented in MATLAB/Simulink. P&O techniques offered the simplest method, and the InC method could solve the ripple problem in P&O. However, the fuzzy logic MPPT controller offered the following advantages for the system: (1) the technique precisely tracked sudden irradiance changes, especially when the system was running with high irradiance; (2) the system response had less oscillation, overshoot, and undershoot; (3) It had higher average efficiency, around 86.5% and 84.3% in 400 W/m² and 1000 W/m², respectively; (4) this algorithm has a faster rise time.

Finally, contributions of this thesis are listed below:

- Water system configuration in a rural house re-designed after load sizing to combine reverse osmosis (RO) water desalination system into the house.
- Optimization was conducted for different hybrid PV topologies in HOMER software for cost and performance analysis.
- A transfer function-based model was offered for the small-scale RO system.
- Dynamic behaviour analysis was performed in MATLAB/Simulink for the system comprises PV, NIBB converter, battery charger, inverter, and various controllers
- MPPT techniques comparison in MATLAB/Simulink for the PVRO-battery system suggested fuzzy logic MPPT controller increases the efficiency.

5.2 Future Works

The research presented in this thesis has provided a new approach to small-scale PVRO systems by designing a double-purpose PV power system. However, several design gaps and research and experimental works can be addressed. A list of future works is recommended in the following:

- A whole house reverse osmosis system can be designed to supply the house for all purposes. There are basic elements in the current house's configuration, like pumps and tanks. This solution is doable if the exact cost and energy analysis have been conducted and compared with this system.

- As the selected site in this research is located in the elevated mountain areas, adding a small-scale wind turbine to the proposed systems will offer a system with fewer PV panels and batteries and more renewable penetration.
- Designing a dynamic model for a PV-battery-natural gas generator in MATLAB/Simulink helps researchers check the effects of adding a conventional generator to the behaviour of the renewable system.
- The electric grid is expanding day in day out in rural areas in Iran. Designing a grid-connected version of the proposed PVRO system will keep the door open for maintaining the system with few changes.
- A low-cost internet of things (IoT) – based power metering system can be designed for the house by Arduino or ESP32 boards. This implementation helps the residents to check their power consumption remotely and help the system to log the power consumption for protection or future designs.
- Designing a SCADA system for the proposed RO system is another future work. Such a system will measure and monitor the reverse osmosis system's parameters like water PH, pressure, or flow rate.
- Last but not least, for further increasing the efficiency and improving the system performance, more sophisticated MPPT techniques can be designed for the PV system, such as neuro-fuzzy logic or artificial neural network MPPT controllers.

5.3 List of Publications

1. M. Mousavi and M. T. Iqbal, “Optimum Sizing Comparison of Stand-alone Hybrid PV Systems for a Rural House in Iran Equipped with a RO Water Desalination System,” accepted for publication in the Jordan Journal of Electrical Engineering, April 2021.
2. M. Mousavi and M. T. Iqbal, “Design and Dynamic Modelling of a Hybrid PV-Battery System for a House with an RO Water Desalination Unit in Iran,” accepted for publication in the European Journal of Electrical Engineering and Computer Science, October 2021.
3. M. Mousavi and M. T. Iqbal, “MPPT Techniques Comparison for a Small-Scale PVRO System in Iran,” accepted and presented at the 12th Annual IEEE IEMCON conference, Vancouver, October 2021.
4. R. Sundararajan, M. Mousavi, H. Hassanien and M. T. Iqbal, “Dynamic simulation of an isolated solar-powered charging facility for 20 electric vehicles in St. John’s, Newfoundland,” presented at the 29th Annual IEEE NECEC conference St. John's, November 19th, 2020.